

Mélissa José

Biological contaminant detection in industrial microalgal cultures



UNIVERSIDADE DO ALGARVE

Faculdade de Ciências e Tecnologia

2023

Mélissa José

Biological contaminant detection in industrial microalgal cultures

Mestrado em Biologia Molecular e Microbiana

Supervisor:

Prof. Dr. João Varela – CCMAR, GreenCoLab

Co-supervisor:

Dr. Lisa Schüler – GreenCoLab



UNIVERSIDADE DO ALGARVE

Faculdade de Ciências e Tecnologia

2023

Biological contaminant detection in industrial microalgal cultures

Declaração de autoria de trabalho

Declaro ser a autora deste trabalho, que é original e inédito. Autores e trabalhos consultados estão devidamente citados no texto e constam da listagem de referências incluído.

(Mélissa José)

«Copyright» - Méliça José

“A Universidade do Algarve reserva para si o direito, em conformidade com o disposto no Código do Direito de Autor e dos Direitos Conexos, de arquivar. Reproduzir e publicar a obra. Independentemente do meio utilizado. Bem como de a divulgar através de repositórios científicos e de admitir a sua cópia e distribuição para fins meramente educacionais ou de investigação e não comerciais. Conquanto seja dado o devido crédito ao autor e editor respetivos”.

Agradecimentos

Gostaria de agradecer ao Professor João Varela, por todas as oportunidades e apoio que me deu, desde as aulas na licenciatura até à orientação na tese de mestrado. Ao Hugo Pereira, pela oportunidade e confiança de fazer parte da equipa GreenColab.

Um grande agradecimento à Lisa Schueler, por ser uma excelente orientadora, e por ter ajudado tanto no desenvolvimento desta tese. À Cristina Paulino, por todos os bons conselhos e a paciência no laboratório. A todos os membros do GreenColab, por me terem acolhido tão bem e por todos os bons momentos passados.

Por fim, quero agradecer especialmente à minha família, namorado e amigos, por terem sempre acreditado em mim e por me terem apoiado tanto. Não teria sido possível sem vocês.

Abstract

Biological contamination is one of the greatest limitations in the industrial cultivation microalgae, since the productivity is reduced within a few hours upon detection. The determination and quantification of different biological contaminants is a difficult task, and techniques have been developed aiming to control or eliminate them. Molecular approaches are the most specific/sensitive, allowing for their detection at an early stage. Once the contaminant is detected, mitigation strategies involving the manipulation of environmental/abiotic factors, such as the addition of chemical compounds, are used.

In this thesis, molecular methods were developed and used to identify harmful biological contaminants in industrial microalgal cultures focusing on eukaryotic taxa. Samples from contaminated cultures of *T. lutea* and *P. triornutum* were taken to extract DNA and sequenced using NGS technology. The data obtained was analysed using bioinformatic and phylogenetic tools to identify the possible contaminants collapsing the cultures.

For the contaminated cultures of *T. lutea*, the most likely candidate causing the culture collapse was the "golden alga" *Paraphysomonas* (Chrysophyceae). One primer pair was designed and optimized, and the limit of detection (LOD) was tested, corresponding to an LOD = 0.0049% relative abundance. The *Paraphysomonas* life cycle was studied, and several mitigation strategies were tested. Salinity of 60 ppt and GeO₂ at 1 mg/L showed to be promising, with the ability to control the development of this chrysophyte without harming *T. lutea*. Concerning the contaminated cultures of *P. triornutum*, the Heterolobosea contaminant (Excavata) showed to be the main cause of the culture collapse. Three robust primer pairs were designed with promising results under standard PCR conditions. The life cycle of Heterolobosea contaminant was studied, and only one mitigation strategy was tested (pH at 10). However, the treatment did not show the ability to control the development of this heterolobosean contaminant, and no further mitigations were tested.

Keywords: *Tisochrysis lutea*, *Phaeodactylum triornutum*, industrial microalgal cultures, biological contaminants, molecular methods.

Resumo

As microalgas são um grupo de organismos microscópicos unicelulares, que se podem organizar em colónias ou filamentos, mostrando uma rica biodiversidade. Devido à sua composição de macro- e micronutrientes, as suas aplicações são versáteis, desde alimentos para o consumo humano e animal a produtos nutracêuticos, bioplásticos e biofertilizantes. A produção de microalgas depende de vários fatores de produção, como a luz, água, temperatura, agitação e nutrientes. A contaminação é uma das maiores limitações da produtividade das culturas industriais. Os contaminantes biológicos são capazes de reduzir a concentração celular, causar stress, alterar a biologia celular, degradar a qualidade do produto e até colapsar as culturas de microalgas em poucas horas após a sua deteção. No entanto, nem todos os microrganismos são prejudiciais. Algumas espécies de microalgas são capazes de crescer e produzir biomassas que podem ser utilizadas para fins comerciais com um certo nível de contaminação. Algumas espécies necessitam de macro- e micronutrientes produzidos por outros microrganismos e não sobrevivem em culturas axénicas.

As interações mais comuns das microalgas com outros microrganismos são o mutualismo (afetam positivamente o crescimento, tornando-se essenciais), a competição (por nutrientes e/ou outros fatores ambientais), a predação (por *grazers* de microalgas, que resulta na morte da maioria das células na cultura) e o parasitismo (utilizam as microalgas como seu hospedeiro). Os contaminantes apresentam uma enorme biodiversidade, sendo que “protozoários”, zooplâncton, fungos, bactérias, vírus, outras algas e mesmo insetos podem causar graves perdas económicas, devido ao efeito negativo sobre a produtividade da cultura de microalgas. O principal grupo de contaminantes são os *grazers*, organismos eucarióticos (por exemplo, protozoários, copépodes e rotíferos) geralmente de maior dimensão que as microalgas. Este grupo é o mais difícil de prevenir e controlar, devido à sua capacidade de afetar rapidamente a cultura e a colapsar em poucas horas. Alguns *grazers* podem formar formas de dormência de elevada resiliência (por exemplo, cistos e esporos) que representam uma grande ameaça nos sistemas abertos, pois espalham-se por correntes de vento, e nos sistemas fechados, são retidos na forma de sedimentos e biofilmes, mantendo-se viáveis durante anos.

A determinação e quantificação de diferentes contaminantes em culturas de microalgas é uma tarefa difícil. Quando uma cultura está altamente contaminada, os efeitos são visíveis a olho nu. No entanto, neste estágio avançado de contaminação, é muitas vezes demasiado tarde para aplicar estratégias de mitigação para controlar o contaminante e salvar a cultura. Por isso,

nos últimos anos têm sido desenvolvidas várias técnicas destinadas para controlar a contaminação biológica das culturas industriais de microalgas como, por exemplo, a microscopia, a contagem de colónias em placas de agar, a citometria de fluxo e os métodos moleculares. Uma vez que o contaminante é detetado, existem várias estratégias de mitigação, que podem ser preventivas, a fim de evitar a entrada de contaminantes; ou corretivas, a fim de controlar ou eliminar o contaminante. As estratégias de mitigação corretivas mais usadas são a pressão ambiental (fatores abióticos), a separação física dos contaminantes das microalgas, a disruptão física dos tecidos, a adição de compostos químicos e de herbicidas/pesticidas.

Os contaminantes são específicos e a sua classificação taxonómica até ao género ou espécie é muitas vezes desconhecida. Por esta razão, serão desenvolvidos e utilizados métodos moleculares para identificar contaminantes biológicos de culturas industriais de microalgas, em específico, os eucariontes, uma vez que são os principais predadores que causam o colapso das culturas. Foram escolhidos métodos moleculares por serem altamente específicos e sensíveis, além de permitirem a deteção precoce dos contaminantes.

Amostras de diferentes culturas contaminadas de *Tisochrysis lutea* (Necton) e *Phaeodactylum tricornutum* (Almicroalgae) foram recolhidas durante a produção industrial a fim de extrair ADN de alta qualidade e enviadas para serem sequenciadas através da tecnologia de *Next Generation Sequencing* (NGS) com *primers* universais 18S. Os dados obtidos são conhecidos como *zero-radius Operational Taxonomic Unit* (zOTU), tendo sido analisados tendo em conta o número de leituras e que, por definição, cada zOTU identifica uma sequência única capaz de classificar os organismos em grupos, mesmo que sejam evolutivamente próximos. Após a seleção das zOTUs, foram realizadas análises bioinformáticas e filogenéticas, de modo a detetar o contaminante responsável pelo colapso. Culturas contaminadas foram fornecidas por cada empresa de modo a cultivá-las no laboratório com condições controladas, a fim de estudar o ciclo de vida de cada contaminante e testar possíveis mitigações.

Para as culturas contaminadas da *T. lutea*, foram detetadas nove *taxa* diferentes de possíveis contaminantes responsáveis pelo colapso das culturas. As zOTUs mais abundantes foram analisadas, sendo que a “alga dourada” *Paraphysomonas* (*Chrysophyceae*) (zOTU4) foi considerada como a melhor candidata. Foram desenhados vários *primers* após o alinhamento de várias sequências de *Paraphysomonas* e de outras microalgas, através de plataformas bioinformáticas (por exemplo, Qiagen CLC e Geneious), de modo a detetar o contaminante. Os *primers* foram testados através de condições padrão de PCR, sendo que apenas um *primer* teve resultados positivos. O limite de deteção também foi testado, com capacidade de detetar até 0.0049% de abundância relativa de *Paraphysomonas*. O ciclo de vida deste contaminante foi

analisado, e várias estratégias de mitigação de pressão ambiental e compostos químicos foram testadas. A salinidade a 60 ppt e o dióxido de germânio a 1 mg/L mostraram resultados positivos em controlar o desenvolvimento deste predador crisófito, sem afetar as culturas da *T. lutea*.

Relativamente às culturas da *P. tricornutum*, os resultados revelaram seis *taxa* diferentes de possíveis contaminantes responsáveis pelo colapso da cultura. As zOTUs mais abundantes foram analisadas, sendo considerada como a melhor candidata a zOTU2, classificada como pertencente a um contaminante do filo *Heterolobosea* pertencente à clade Discoba do megagrupo Excavata. Foram desenhados vários *primers* após o alinhamento de várias sequências de *Heterolobosea* e de outras microalgas, e testados através de condições padrão de PCR, sendo que três *primers* tiveram resultados positivos com um limite de detecção até 2.2% de abundância relativa do contaminante *Heterolobosea*. O ciclo de vida deste contaminante foi analisado, e apenas uma estratégia de mitigação foi testada. A estratégia de mitigação foi a pressão ambiental a pH = 10, que não mostrou resultados significativos em controlar o contaminante. Contudo, não foram testadas mais estratégias de mitigação.

Para concluir, dois contaminantes das empresas Necton, identificado como *Paraphysomonas*, e Allmicroalgae, identificado como pertencente ao filo *Heterolobosea*, foram detetados em culturas contaminadas de *T. lutea* e *P. tricornutum*, respetivamente. Foram desenhados *primers* específicos para detetar os contaminantes até em baixas concentrações. O ciclo de vida de ambos os contaminantes foram analisados, e foi possível desenvolver duas estratégias de mitigação para o contaminante das culturas da *T. lutea*.

Palavras-chave: *Tisochrysis lutea*, *Phaeodactylum tricornutum*, culturas de microalgas industriais, contaminantes biológicos, métodos moleculares.

Index

Declaração de autoria de trabalho	i
«Copyright» - Méliisa José	ii
Agradecimentos.....	iii
Abstract	iv
Resumo.....	v
1. Introduction	1
1.1. About microalgae	1
1.2. Industrial production	3
1.2.1. Production and cultivation process	3
1.2.2. Large-scale production systems	4
1.2.3. Challenges of microalgal cultivation.....	7
1.3. Biological contaminants	11
1.3.1. Types of contaminants	11
1.3.2. Detection and quantification of contaminants.....	18
1.3.3. Mitigation strategies	22
1.4. Aims and objectives	25
2. Materials and methods	26
2.1. DNA extraction	26
2.2. NGS analysis	26
2.3. Primer design.....	27
2.4. PCR optimization and sequencing	27
2.5. Sampling procedure during the scale-up process	28
2.6. Cultivation and microscopic observations of the contaminants.....	29
2.7. Analysis of growth parameters.....	30
2.8. Mitigation trials	32

2.8.1.	6-well plate screening.....	32
2.8.2.	Lab-scale assays in 100-mL Erlenmeyer flasks	33
2.9.	Statistical analysis	33
3.	Results and Discussion.....	34
3.1.	Biological contaminants of <i>Tisochrysis lutea</i>	34
3.1.1.	NGS analysis	34
3.1.2.	Primer design and optimization.....	41
3.1.3.	Life cycle of contaminant.....	45
3.1.4.	Growth and mitigation trials	48
3.2.	Biological contaminants of <i>Phaeodactylum tricornutum</i>	65
3.2.1.	NGS analysis	65
3.2.2.	Primer design and optimization.....	69
3.2.3.	Life cycle of the heterolobosean contaminant.....	72
3.2.4.	Growth and mitigation trials	74
4.	Conclusion and future expectations	76
	References	77
	Annex	84

Figure index

Figure 1: Production systems: A. Raceway; B. Flat panel; C. Tubular photobioreactor; D. Fermenter (Allmicroalgae®).....	6
Figure 2: Microzooplanktonic grazers: A. <i>Poterioochromonas malhamensis</i> and <i>Chlorella</i> ; B. <i>Nuclearia</i> and <i>Spirulina</i> ; C. <i>Nuclearia</i> and <i>Scenedesmus</i> ; D. <i>Heterolobosean</i> amoebae and <i>Spirulina</i> ; E. <i>Saccamoeba</i> and <i>Nannochloropsis</i> ; F. <i>Frontonia</i> and <i>Spirulina</i> ; G. <i>Colpoda</i> and <i>Chlorella</i> ; H. <i>Euplotes</i> and <i>Nannochloropsis</i> ; I. <i>Sterkiella histriomuscorum</i> and <i>Scenedesmus</i> ; J. <i>Vorticella</i> and <i>Scenedesmus</i> ; K. <i>Lecane inermis</i> and <i>Chlorella</i> ; L. <i>Brachinous plicatilis</i> and <i>Spirulina</i> . Scale bar = 10 µm. [6].	16
Figure 3: Schematic flow diagram on how to analyse microalgal cultures and detect biological contaminants, as well as the advantages (A) and disadvantages (D) of each detection method [24] (www.biorender.com).....	22
Figure 4: Diagram of the scale-up procedure used for both <i>T. lutea</i> and <i>P. tricornutum</i> at Necton and Allmicroalgae, respectively.	28
Figure 5: Abundance of relevant taxa obtained by NGS in inoculum and contaminated samples of <i>T. lutea</i> , namely: 1) Inoculum, 2) ETO3 3/3/21, 3) ETO4 22/7/20, 4) ETO4 22/07/20 and 5) PBR4 22/07/20; with bacteria shown as total number of reads (A) and without bacteria shown as percentage of abundance (B).	35
Figure 6: Distance-based (BioNJ) phylogenetic tree of the Chrysophyceae zOTU4 present in highly contaminated cultures of <i>T. lutea</i> . Several 18S rDNA sequences belonging to the genus <i>Paraphysomonas</i> have been added to determine the root node by means of an outgroup.	38
Figure 7: Distance-based (BioNJ) phylogenetic tree of the ciliate zOTU9 present in highly contaminated cultures of <i>T. lutea</i> . Several 18S rDNA sequences belonging to the genus <i>Euplotes</i> have been added to determine the root node by means of an outgroup.	39
Figure 8: Maximum likelihood (PhyML) phylogenetic tree of the Euglenozoan zOTU28 present in highly contaminated cultures of <i>T. lutea</i> . Several 18S rDNA sequences belonging to the phylum Euglenozoa have been added to determine the root node by means of an outgroup.	40
Figure 9: Optimization steps from amplification products of <i>Paraphysomonas</i> 18S rDNA using the primer pair Chryso_240/Chryso_651 from DNA of different microalgal samples, namely 1) <i>Tetraselmis chui</i> , 2) <i>Chlorella vulgaris</i> , 3) <i>T. lutea</i> and 4) <i>P. tricornutum</i> as well as of <i>T. lutea</i> samples contaminated with <i>Paraphysomonas</i> sp.: 5) ETO3 3/3/21, 6) ETO4 22/7/20, 7) ETO4 22/07/20 and 8) PBR4 22/07/20. Samples of the negative control (NC) and of the 100-bp DNA ladder (L) were also loaded on the gel.	43

Figure 10: Optimization steps from amplification products of *Paraphysomonas* 18S rDNA using the primer pair *Paraphysomonas*_1F/*Paraphysomonas*_1R (A) and the primer pair *Paraphysomonas*_1376F/*Paraphysomonas*_1549R (B, C and D); from DNA of different microalgal samples, namely 1) *Tetraselmis chui*, 2) *Chlorella vulgaris*, 3) *T. lutea* and 4) *P. tricornutum*, as well as of *T. lutea* samples contaminated with *Paraphysomonas* sp.: 5) ETO3 3/3/21, 6) ETO4 22/7/20, 7) ETO4 22/07/20 and 8) PBR4 22/07/20. Samples of the negative control (NC) and of the 100-bp DNA ladder (L) were also loaded on the gel..... 44

Figure 11: Amplification products of *Paraphysomonas* 18S rDNA using the primer pair *Paraphysomonas*_1376F/*Paraphysomonas*_1549R from DNA of different microalgal samples, namely 1) *Tetraselmis chui*, 2) *Chlorella vulgaris*, 3) *T. lutea* and 4) *P. tricornutum*, as well as of *T. lutea* samples contaminated with *Paraphysomonas* sp. (% of relative abundance): 5) ETO3 3/3/21 (0.07), 6) ETO3 3/3/21 (0.0028), 7) ETO3 3/3/21 (0.000112), 8) ETO4 22/07/20 (77), 9) ETO4 22/07/20 (3.08), 10) ETO4 22/07/20 (0.1232), 11) ETO4 22/07/20 (0.004928), 12) ETO4 22/07/20 (0.00019712), negative control (NC) and 100 bp ladder (L). 45

Figure 12: Life stages of the flagellated *Paraphysomonas* sp., feeding on *T. lutea*: small flagellated cells (A); large flagellated amoeba-like cells feeding on microalgae (B, C, D and E); and medium flagellated amoeba-like cells feeding on themselves (F). 46

Figure 13: Growth curve of *T. lutea* cultures without contaminant (Negative control) and inoculated with contaminated cultures: three-week-old (Culture A); two-week-old (Culture B); and one-week-old (Culture C). n=3, mean \pm SD..... 48

Figure 14: 6-well plates trials with *T. lutea* cultures contaminated with *Paraphysomonas*. A) healthy culture, B) culture at its early stages of collapse and C) fully collapsed culture..... 49

Figure 15: Growth curve of *T. lutea* cultures without (negative control) and with contaminant (positive control). Several mitigation agents such as salinity at 50 and 60 ppt, GeO₂ at 2 and 4 mg/L, K₂HPO₄ at 2 and 20 mM, SDS at 20 and 40 mg/L, H₂O₂ at 0.028 and 0.056 mL/L were tested on the cultures of *T. lutea* with *Paraphysomonas* in order to avoid culture collapse. n=3, mean \pm SD..... 50

Figure 16: Growth curve of *T. lutea* cultures without (negative control) and with contaminant (positive control). Several mitigation agents such as salinity at 55 and 60 ppt, GeO₂ at 1 and 2 mg/L, K₂HPO₄ at 10 and 20 mM, SDS at 20 and 40 mg/L, H₂O₂ at 0.028 and 0.056 mL/L were tested on the cultures of *T. lutea* with *Paraphysomonas* in order to avoid culture collapse. n=3, mean \pm SD..... 53

Figure 17: Growth curve of *T. lutea* cultures without (negative control) and with contaminant (positive control). Several mitigation agents such as GeO₂ at 0.25 and 0.5 mg/L, salinity at 45 with GeO₂ at 0.25 and 0.5 mg/L were tested on the cultures of *T. lutea* with *Paraphysomonas* in order to avoid culture collapse. n=3, mean \pm SD. 55

Figure 18: Growth of *T. lutea* (lines) cultures and *Paraphysomonas* contaminant (bars) using cell counts over 14 days of cultivation. Non-contaminated cultures (negative control) and contaminated cultures (positive control) at a standard salinity of 33ppt were compared with treatments at a salinity of 60 ppt. n=3, mean ± SD. 57

Figure 19: Growth curve of *T. lutea* cultures without (negative control) and with contaminant (positive control). Salinity of 60 ppt was applied to the non-contaminated culture of *T. lutea* (Algae), and cultures with *T. lutea* with *Paraphysomonas* (Algae + contaminant). n=3, mean ± SD..... 58

Figure 20: Nitrates measurements of *T. lutea* cultures without (negative control) and with contaminant (positive control). Salinity of 60 ppt was applied to the non-contaminated culture of *T. lutea* (Algae), and cultures of *T. lutea* contaminated with *Paraphysomonas* (Algae + contaminant). n=3, mean ± SD. Different letters over the bars indicate significant differences between samples (p<0.05, ANOVA Tukey). 58

Figure 21: Growth of *T. lutea* (lines) cultures and *Paraphysomonas* contaminant (bars) using cell counts over 7 days of cultivation. Non-contaminated (negative control) and contaminated (positive control) cultures at standard salinity of 33 ppt were compared with treatments at a salinity of 45 ppt and GeO₂ at 0.5 mg/L. n=3, mean ± SD. 60

Figure 22: Growth curve of *T. lutea* cultures without (negative control) and with contaminant (positive control). Salinity of 45 ppt and GeO₂ at 0.5 mg/L were applied to the culture of *T. lutea* only (algae), and cultures with *T. lutea* contaminated with *Paraphysomonas* (algae + contaminant). n=3, mean ± SD..... 60

Figure 23: Nitrates measurements of *T. lutea* cultures without (negative control) and with contaminant (positive control). Salinity of 45 ppt and GeO₂ at 0.5 mg/L were applied to the uncontaminated culture of *T. lutea* (algae), and cultures of *T. lutea* with *Paraphysomonas* (algae + contaminant). n=3, mean ± SD. Different letters over the bars indicate significant differences between samples (p<0.05, ANOVA Tukey). 61

Figure 24: Growth of *T. lutea* (lines) cultures and *Paraphysomonas* contaminant (bars) using cell counts over 14 days of cultivation. GeO₂ at 1 mg/L was applied to the uncontaminated culture of *T. lutea* (Algae), and cultures with *T. lutea* with *Paraphysomonas* (Algae + contaminant). n=3, mean ± SD..... 63

Figure 25: Growth curve of *T. lutea* cultures without (negative control) and with contaminant (positive control). GeO₂ at 1 mg/L was applied to the uncontaminated culture of *T. lutea* (Algae), and cultures with *T. lutea* with *Paraphysomonas* (Algae + contaminant). n=3, mean ± SD..... 63

Figure 26: Nitrates measurements of *T. lutea* cultures without (Negative control) and with contaminant (Positive control). GeO₂ at 1 mg/L was applied on culture of *T. lutea* only (Algae),

and cultures with *T. lutea* contaminated with *Paraphysomonas* (Algae + contaminant). n=3, mean ± SD. Different letters over the bars indicate significant differences between samples (p<0.05, ANOVA Tukey). 64

Figure 27: Abundance of relevant taxa obtained by NGS in inoculum and contaminated samples of *P. tricornutum*, namely: 1) Inoculum, 2) S3 12/3/21, 3) S4 14/3/21, 4) S4 12/3/21 and 5) M5 17/3/21; with (A) and without (B) bacteria being shown as percentage of abundance. 66

Figure 28: Distance-based (BioNJ) phylogenetic tree of the Excavata contaminant (zOTU2) of cultures of *P. tricornutum*. Several 18S rDNA sequences belonging to the clade Discoba have been added to find the tree root by means of an outgroup. 67

Figure 29: Maximum likelihood phylogenetic tree of the Cercozoa contaminant (zOTU8) of cultures of *P. tricornutum*. Several 18S rDNA sequences belonging to the superfamily Sainouroidea have been added to find the tree root by means of an outgroup. 68

Figure 30: Amplification products of Heterolobosea 18S rDNA using the primer pair A) ACA5'/Heterolobosea_3R, B) Heterolo_spec_392F/Heterolo_spec_596R and C) Heterolo_spec_1186F/Heterolo_spec_1620R from DNA of different microalgal samples, namely 1) *Tetraselmis chui*, 2) *Chlorella vulgaris*, 3) *T. lutea* and 4) *P. tricornutum*, as well as of *P. tricornutum* samples contaminated with Heterolobosea: 5) S3 12/3/21, 6) S4 14/3/21, 7) S4 12/3/21, 8) M5 17/3/21. A negative control (NC) and 100 bp ladder (L) were also loaded on the gel. 71

Figure 31: Life stages of the non-flagellated heterolobosean amoeba feeding on *P. tricornutum*: cysts (A); large amoeboid cells feeding on microalgae (B, C, D and E); and even larger amoeboid cells no longer feeding on microalgae, in this case due to cell lysis, with the remnants of the intracellular contents on the right side of the micrograph containing partially digested diatom cells (F). 73

Figure 32: Growth curve of *P. tricornutum* cultures without (negative control) and with (Positive control) contaminant. Alkaline conditions, pH 10, were applied to the uncontaminated culture of *P. tricornutum* (Algae), and cultures with *P. tricornutum* with heterolobosean predator (Algae + contaminant). n=3, mean ± SD. 75

Table index

Table 1: Commercial microalgae.	9
Table 2: Summary of microalgal contaminants detection and mitigation strategies.	13
Table 3: Composition of 1x concentrated MAM.	30
Table 4: Concentrations of the performed mitigation treatments.....	32
Table 5: Samples sequenced by NGS.....	34
Table 6: List of contaminant-specific 18S primers developed for <i>T. lutea</i> contaminant.	41
Table 7: Optimized PCR conditions of the third primer pair.	44
Table 8: Samples sequenced by NGS.....	65
Table 9: List of contaminant-specific 18S primers developed.....	69
Table 10: PCR conditions of the pair primers.	71

1. Introduction

1.1. About microalgae

Microalgae are a group of unicellular organisms that can become organized in the form of colonies. Using the *sensu lato* term, microalgae can be either prokaryotic or eukaryotic microorganisms. Because of their great diversity and ability to survive in harsh environmental conditions, microalgae can be found in almost every habitat. They are mainly found in aquatic environments (seawater, freshwater and wastewater); however, they can also be found in terrestrial (soils and rocks) and extreme environments (desert, ice sheets, hydrothermal vents, ice and hot springs) with broad ranges of pH, temperature and salinity, with the presence of competitors, mutualistic species and/or predators, excessive CO₂, sulphur oxides and nitrogen oxides [1]. Microalgae are one of the oldest and most important organisms at the bottom of the food chain as well as the main producers of oxygen on the planet, contributing to about 40% of the global CO₂ fixation [2].

Microalgae appeared 1.9×10^9 years ago when a eukaryotic host engulfed a photosynthetic cyanobacterium through primary endosymbiosis, giving rise to the lineage Archaeplastida containing the rhodophytes (red algae) and chlorophytes (green algae), among others [3]. Later, several secondary endosymbiotic events took place between a eukaryotic host and another eukaryotic organism, giving rise to different microalgal groups, namely the cryptomonads (e.g., *Rhodomonas*), haptophytes (e.g., *Emiliania huxleyi*), stramenopiles (e.g., diatoms) and alveolates (e.g., dinoflagellates) as well as euglenids such as *Euglena* and chlorarachniophytes, i.e., amoeba-like organisms with filiform pseudopods with green chloroplasts.

These microorganisms are mainly photoautotrophic; however, they are able to grow under heterotrophic and mixotrophic conditions. Under photoautotrophic conditions, microalgae convert light and CO₂ (inorganic carbon source) into oxygen and biomass containing organic components (lipids, proteins and carbohydrates) via photosynthesis. This is the most used and cheapest production technique. However, under heterotrophic growth, microalgae assimilate organic carbon sources (e.g., sugars, acetate or glycerol) synthesised by other organisms in the absence of light through fermentation and respiration.

Nowadays, this technique is being used more frequently as it is easy to scale up, without the requirement of light, leading to higher growth and production rates when compared to photoautotrophic cultivation [4]. However, it consumes more energy than photosynthesis due

to the supply of an organic carbon source. Mixotrophic microalgae grow under both photoautotrophic and heterotrophic conditions simultaneously. They can play a significant role to get maximum biomass formation by joining phototrophic and heterotrophic processes during cultivation [5].

Thousands of years ago, microalgae were served as food in different cultures. However, industrial microalgal biomass production only began in the 1940s using lipids of various microalgae as alternative feedstocks for munition manufacturing during the Second World War. The microalgal biotechnology industry grew significantly in the early 1950's, due to the world's population increase and lack of protein sources as well as for wastewater treatment. Later in the 1970s, due to their ability to accumulate oil in the form of triacylglycerols, microalgae were studied for the production of biofuels [6]. However, microalgae-based biofuel production is not as yet economically viable, still being studied nowadays [7].

In the 2000's, climate change, high demand for energy, food, wastewater treatments and interest in higher value metabolites has led to increased production of microalgal biomass. Finally, due to the great number of synthetic compounds in food, skin care products and pharmaceutical products, there have been emerging health issues such as allergic reaction and hyperactivity, leading to the need for natural products like microalgae [1]. The biocompounds produced by microalgae with various commercial interest are polyunsaturated fatty acids (PUFAs), pigments, carbohydrates, peptides, vitamins and phytosterols, among others, which are used for food, nutraceuticals, pharmaceuticals and cosmeceuticals [2]. However, before microalgal biomass becomes a regular food source and an established crop, it needs to be developed for agricultural scale production. To this end, the nutritional content needs to be evaluated and enhanced, yields optimized, and new traits developed to be appealing to customers in the form of tablets, capsules, liquids or incorporated into pastas, snack foods, candy bars, gums or beverages [8,9].

On the other hand, as photosynthetic organisms, microalgae have been studied to mitigate current environmental issues due to their ability to recycle atmospheric CO₂, minimising the effect of global warming and providing energy. They are also able to integrate carbon from combustion gases as a source of carbon, be grown in wastewater and incorporate pollutants into their metabolism as nutrients. Furthermore, microalgae can be used to produce bioplastics, biofertilizers and biostimulants due to their macro- and micronutrients composition, respectively [2]. Other characteristics of microalgal cultivation is their relatively low demand for nutritional and spatial cultivation requirements. They are able to grow under conditions that are not favourable for terrestrial biomass production (non-arable land), do not need pesticides,

and present higher biomass productivities when compared to those of higher plants [6]. Therefore, microalgae are a good candidate to promote a more circular economy and minimize current environmental issues.

1.2. Industrial production

1.2.1. Production and cultivation process

Microalgal production process depends on the species and on the mode of nutrition (photoautotrophy, heterotrophy or mixotrophy), which defines several production factors, namely water, light, CO₂, temperature, nutrients and cultivation systems. By manipulating these factors, it is possible to improve biomass production and induce the production of specific compounds [9].

Microalgae are often aquatic species that require large amounts of water for survival and cell proliferation. Therefore, water is one of the most important factors for microalgal growth. They can be isolated from seawater, freshwater, brackish water and wastewater and, sometimes, even from soil or rocks. For industrial scale facilities, the water must be free of chemicals and biological contaminants that can affect microalgal growth. There are several water sterilization techniques for microalgae cultivation, including filtration, ozonation, chlorination, hydrogen peroxide treatment and autoclavation [10].

Light is also a crucial environmental factor for microalgal photosynthetic growth since it provides the energy to photosynthesis. To this end, the intensity, wavelengths and utilization of light needs to be appropriate as well as the ratio of light to dark periods. Because of their fast growth rates, microalgae attain high concentrations very quickly, causing shading to other microalgal cells and themselves. Therefore, to improve light absorbance, bioreactors must have a high surface area-to-volume ratio, short light paths and to be continuously agitated in order to the light to reach all cells [11].

The CO₂ concentration in the environment (as a pure gas, in the air, or produced by bacteria and other heterotrophs) is reduced by carbon capture and sequestration by microalgae. When it is assimilated, there is the excretion of OH⁻ into the medium, causing a shift of the equilibrium that results into elevated pH values. Since most microalgae prefer neutral pH, it needs to be maintained by addition of CO₂ in order to keep it in the pH optimum range and to prevent the depletion of carbon from the medium. Nevertheless, different CO₂ concentrations can negatively affect the growth and biochemical compositions of the microalgal species [12].

Temperature affects the metabolism and all molecular activities of microalgae, therefore the optimum range for most species is usually between 20 and 24°C. However, some species tolerate a higher temperature range of 16-27°C. Higher temperatures will accelerate microalgal metabolism while lower temperatures will lead to inhibition of the biochemical reaction rates in cellular compartments [13].

The most important macronutrients during photoautotrophic microalgal growth are inorganic carbon (CO₂), nitrogen (associated with their primary metabolism – some species prefer ammonia instead of nitrate), phosphorus (phosphates), iron and silica (usually only for the cultivation of diatoms). Micronutrients (e.g., K, Mg, Mn and Se) and vitamins (e.g., vitamins B₁, B₇ and B₁₂) are also important factors for effective growth [11]. For heterotrophic growth, microalgae use sugar, acetate or glycerol as their organic carbon source and nitrate, ammonia, urea or peptone as their nitrogen source. Additionally, the same nutrients and vitamins are also used for photoautotrophic growth [14].

The easiest cultivation method is batch culture, in which microalgae are in a closed environment with fixed parameters. All nutrients together with the inoculum are added at the initial time and there is no further addition of nutrients during the process until harvesting of the entire culture. However, the most efficient way of cultivation is the fed batch (semi-continuous) culture. Here the culture medium and the inoculum are added at the beginning of the process. When it reaches the desired biomass concentration, end of the process, part of the culture is discharged and replaced by the same volume of fresh medium. The method with higher product yield, though, is the continuous culture, whereby new medium is introduced until the late exponential growth phase is reached and then the reactor is continuously supplied with culture media with a simultaneous withdrawal of biomass [1].

1.2.2. Large-scale production systems

In large-scale production, cultivation of microalgae involves the interaction of various external and internal factors. There are two main systems used to grow microalgal biomass: open (raceways and thin layer cascades) and closed (vertical/horizontal or flat panel photobioreactors and fermenters) systems [13].

In raceways, the cultures usually flow in a paddlewheel-driven closed loop recirculation channel with a depth of 0.2–0.5 m (**Figure 1A**). The paddlewheel mixes the culture, and the flow is guided around bends by baffles. It is a continuous method with CO₂ and nutrients constantly being added and microalgae removed at the opposite end [1,15]. In thin-layer

cascade systems, cultures are recirculated over a flat surface and operated with a shallow water column characterized by their small depth between 0.5 and 5.0 cm, which maximises light availability, biomass concentration and productivity at the expense of culture volume in the photic region of the reactor. Their use still remains at the laboratory or pilot scale [16].

These open systems are economically advantageous in terms of capital and operational costs; however, they have many disadvantages, such as contamination, no control of the water temperature, evaporation and light fluctuations within a diurnal cycle and season. Their use is also limited to certain robust species that grow under specific conditions like high salinity or alkaline pH, protecting the culture from contaminants (e.g., *Spirulina*, *Dunaliella* and *Nannochloropsis*) [17]. Despite being a promising system for the production of biomass or metabolites, they are only used for low-end applications (e.g., bioremediation of wastewater, nutrient recovery in the form of biomass for feed) and cannot be used for high-end applications (e.g., health supplements, pharmaceuticals or bioactive compounds) [13].

Closed systems are generally used to produce large quantities of microalgal biomass under controlled conditions. Bubble columns or airlifts (vertical photobioreactors [PBRs]) as well as tubular reactors (horizontal PBRs) are usually made of plastic or glass tubes with limited diameter to allow the penetration of light into the cultures and possess a cooling system during daylight hours to decrease the temperature. From an economic point of view, this type of system is more expensive when compared to open systems, especially due to the controlled conditions and materials needed. The production cost can range from 5€/kg for open raceways and 50 €/kg for photobioreactors [1]. Nevertheless, closed systems are the most appropriate cultivation system for high-end use, such as pharmaceutical compounds, since the culture conditions can be controlled, and cultures can be maintained axenic [15].

Vertical photobioreactors are built with cylindrical shaped vessels (height usually twice the diameter) with an air sparger attached at the bottom of the reactor that generates air bubbles (were CO₂ is supplied) to mix the culture and a gas outlet at the top of the reactor. There are two types: bubble columns and airlifts. In bubble columns, the culture is mixed by air bubbles generated at the bottom of the reactor and the light source is supplied externally, which means that only the surface is illuminated. Airlifts are an improved design of the bubble column since air bubbles are generated inside a concentric tube where the light source is supplied and, therefore, the entire culture is illuminated [4].

Tubular photobioreactors are made of long horizontal tubes placed in different variations to form walls, helices or panels. The diameter is smaller than the vertical photobioreactors with high surface area and thus, requires a large area of land. The culture

circulates within the tubes and is recycled back to the reservoir by a pump (**Figure 1C**). Flat panels are another type of horizontal photobioreactors, which have transparent plastic sheets or glass in rectangular forms positioned vertically to receive maximum light (**Figure 1B**). Air bubbles are supplied by an air sparger to mix the culture and provide CO₂. Flat panels have a high surface area to volume ratio and a flexible design for the scale-up process [4].

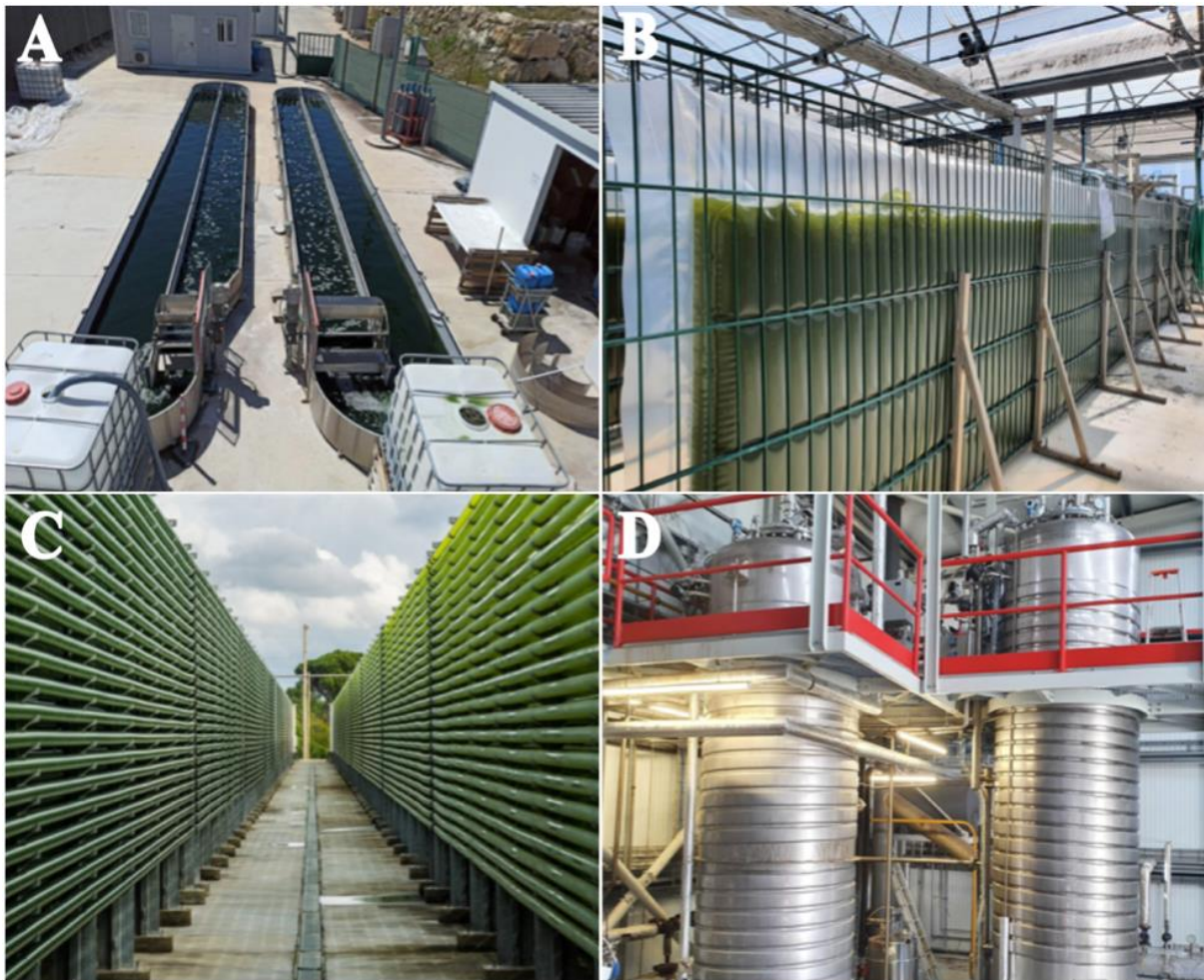


Figure 1: Production systems: A. Raceway; B. Flat panel; C. Tubular photobioreactor; D. Fermenter (Allmicroalgae®).

Fermenters are the only dark systems for cultivation of microalgae under heterotrophic conditions (**Figure 1D**). Besides having no requirement for light, the culture is agitated constantly and a carbon source (e.g., glucose or acetate) is supplied by the culture medium. Because of the greater energy density in the carbon source provided, this type of cultivations has a higher cell mass (~100 g/L) observed compared with photoautotrophic cultivations (2-40 g/L) [4]. In this type of system, microalgae provide mainly high amounts of intracellular lipids with high proportions of polyunsaturated fatty acids (PUFA) and some studies have shown the

concomitant production of pigments [17]. However, protein and carbohydrates contents are usually extracted in low amounts if the right microalga is not selected.

The biomass from heterotrophic cultivation can be used as inoculum for photoautotrophic growth, feed, biofertilizers, biostimulants, biofuels or biogas [18]. Because of the different parameters and conditions of these types of cultivation system, different biomass concentrations can be obtained. For autotrophic cultivation, such as open ponds, cell concentrations range between 2 and 10 g/L; in closed bioreactors, cell concentrations can reach 40 g/L. However, under heterotrophic cultivation in fermenters, cell concentrations in the order of 100 g/L can be achieved. Even though in fermenters higher biomass concentrations than in autotrophic cultivation systems can be reached, instead of fixing CO₂ during growth, it generates CO₂. Therefore, heterotrophic cultivation does not positively contribute to the mitigation of global CO₂ emissions, which is one of the major objectives of microalgae cultivation and production [17]. Thus, a mixed cultivation pipeline has been proposed: heterotrophic cultivation to rapidly produce cultures that can be used to inoculate industrial photobioreactors. For example, *Chlorella vulgaris* cultures grown in industrial fermenters with a productivity of 27.54 ± 5.07 and 31.86 ± 2.87 gL⁻¹d⁻¹ showed a 5-fold and 12-fold decreased in area occupancy and scale-up time, respectively, reaching the standard protein and chlorophyll contents [19].

Currently, around 30,000 microalgal species have been identified and studied; however, just a handful are cultivated for producing commercial products at industrial scale [13]. These species mainly belong to the genera *Chlorella*, *Scenedesmus*, *Chlorococcum*, *Haematococcus*, *Dunaliella*, *Tetraselmis*, *Nannochloropsis*, *Phaeodactylum*, *Tisochrysis* and the cyanobacterium *Arthrospira* commonly known as Spirulina (**Table 1**).

1.2.3. Challenges of microalgal cultivation

Although the above-mentioned species are grown at large scale, the microalgae industry is still facing several challenges. Even if the technology of outdoor systems is relatively simple and operational costs are low, one of the main problems are the meteorological conditions that directly affect the cultures. Especially in open systems, the cultures are usually more vulnerable because the environment cannot be controlled, mixing is usually poor and sterile conditions are not achievable, which leads to a higher contamination risk and impacts the overall growth rate. Therefore, algal cell concentration as well as the productivity are usually low [20].

A possible solution to this is the selection of robust species that are able to adjust their physiology to the changing environment. For example, *Dunaliella* and Spirulina are able to

grow and produce high concentrations of biomass in open systems due to harsh cultivation conditions such as high salinity and pH, respectively [21]. Therefore, to have less expensive cultivation and higher productivities, it is important to select more flexible species able to cope with conditions under which eventual contaminants are not able to thrive. Another way to improve productivity is the rotation of local microalgae throughout the year, physiologically adapted to the seasonal changes [22]. At last, if the microalga is too sensitive and display specific growth conditions, the biological contaminants need to be identified and well-studied in order to find out a way to mitigate them without harming the microalgae [23].

The contaminations that the microalgal cultures suffer from other microorganisms compromise the growth and can in extreme cases collapse the cultures. Thus, besides abiotic factors, biological contaminants are still a major problem for microalgal cultivation in the form of competitors, parasites and predators. The cultures are usually contaminated during the scale-up, when exposed to non-aseptic environments as in the open systems or in contact with non-sterile sites of the closed systems [24].

The source of contaminants is usually the water used or the air, because it is unrealistic to keep sterile conditions in large scale production systems unless fermenters are used. For example, heat sterilization is doable for the stainless steel of the fermenters but not for the glass or plastic from the photobioreactors. Therefore, for photobioreactors, water is processed with bleaching powder and air is filtrated before use for microalgal cultivation to kill or remove most of the contaminants [25]. However, undesired photosynthetic species can outgrow the target species and/or compete for available resources such as nutrients if they are introduced in the cultivation system. This would raise issues in terms of quality control of the harvested biomass, which can only be solved with selection of robust microalgal species or “pest control” [26].

Furthermore, to obtain successfully large quantities of microalgae-based biomolecules from the biomass, the cultivation condition in pilot scale and downstream processing must be appropriate (e.g., harvesting, extraction and purification). Each species of microalgae produces a biomass with different composition of carbohydrates, proteins, lipids, pigments and other compounds. The biocompounds produced may be fragile in low quantities and can be substantially altered during the extraction process. Hence, it is a challenge to extract a single effective compound from microalgal biomass and many methods are being studied [15]. Microalgae harvesting methods involve the process of isolation or removal of microalgal biomass from the growth medium and can be divided into chemical, physical, electrical or biological methods. Because of the high energy demand and capital cost, harvesting makes up 20-30% of the total production cost [1].

Table 1: Commercial microalgae.

Taxon	Microalgae species	Characteristics		Biochemical composition (% of dry weight)			Commercial value		References
		Cell	Growth	Proteins	Lipids	Carbo hydrates	Bio compounds	Application	
Freshwater chlorophytes	<i>Chlorella vulgaris</i>	Spherical	Mixotrophic, tolerate wide environmental conditions	11-58	2-46	12-28	β -glucans, starch, carotenoids, astaxanthin, PUFAs	Medical field, cosmetics, food, colorants, nutraceuticals feed, biodiesel	[4]
	<i>Chlorococcum amblystomatis</i>	Round-shaped, colonies of 2/4 cells	Mixotrophic, wastewater	13-40	8-32	3-40	Lutein, violaxanthin, neoxanthin	Food and biodiesel	[27]
	<i>Haematococcus pluvialis</i>	Spherical	Mixotrophic	29-45	20-25	5-41	Astaxanthin	Cosmetics, food colorant, feed, nutraceutical	[28,29]
	<i>Scenedesmus obliquus</i>	Coenobia of 4 or 8 cells with sharp edges	Mixotrophic, wastewater and inexpensive media	29-47	22-38	22-46	Lipids, triacyl-glycerols	Feed and biodiesel	[30]

Seawater chlorophyte	<i>Dunaliella salina</i>	Egg-shaped or spherical	Mixotrophic, high salinities	2-24	19-53	15-25	β -carotene	Medical field, food, biodiesel	[31]
	<i>Tetraselmis chui</i>	Single cell motile	Mixotrophic	35-40	5-10	30-35	PUFAs	Feed and food, biodiesel	[32]
	<i>Tisochrysis lutea</i>	Small and oval	Mixotrophic	17-36	17-30	14-47	PUFAs, fucoxanthin, chlorophylls	Feed	[33]
SW eustigmatophyte	<i>Nannochloropsis oculata</i>	Smaller, spherical, free-floating	Mixotrophic	12-62	18-55	9-16	β -carotene and PUFA	Nutraceuticals and feed, biodiesel	[4]
SW diatom	<i>Phaeodactylum tricoratum</i>	Pennate	Mixotrophic	<38	<9	<7	PUFAs	Feed and nutraceuticals	[4,34]
SW cyanobacteria	<i>Arthrospira platensis</i>	Multicellular and filamentous	Mixotrophic	55-70	<8	<13	PUFAs and pigments	Nutraceuticals, cosmetics, food, colorant and feed	[35]

The most common harvesting methods are flotation, flocculation, centrifugation and filtration. Flotation uses small bubbles that attach on microalgal cells to promote the floating of cells on the surface of the culture media for easy harvesting. However, additional substances (surfactants) are needed. In the process of flocculation, the microalgal cells aggregate to form a larger particle, using a flocculating agent to remove the surface charge of cells. Two of the disadvantages of flocculation correspond to the difficulty in separating the coagulant from harvested biomass and the requirement of expensive chemicals. Centrifugation separates microalgal cells based on cell density and particle size using centrifugal force. However, there is a risk of cell lysis or cell damage, where sensitive target biocompounds might be lost. Another possible harvesting method is filtration, which utilizes a semipermeable membrane that can retain microalgae, allowing the media to pass through. Nevertheless, there might be the occurrence of membrane clogging, being unsuitable for small species [36].

The drying process of harvested biomass is an important step, as the presence of water in cells can result in the formation of films that hinder solvents from extracting the biocompounds. This step can be accomplished by different drying methods. The most frequently used are spray drying, freeze-drying, drum drying, and sun-drying. The most basic is sun drying. It has lower costs; however, it is a long process (up to 72 h). Spray drying is often used, and the final product is a uniform powder able to be packed directly upon the drying process. Conversely, it has higher energy costs [20].

Microalgae are usually covered with a complex cell wall-like structure that make invasion by bacteria more difficult. However, it also leads to challenges in extraction of intracellular biochemical products. Hence, pre-treatment technology (such as cell disruption) is an essential downstream process that helps to increase the extraction efficiency of microalgae with cell-wall structure [37]. There are four extraction methods, namely mechanical (e.g., shear forces, electrical pulses, or heat to disrupt de cell wall), chemical (e.g., solvents, to extract the intracellular compounds), physical (e.g., microwave and ultrasound operations) and enzymatic lysis (e.g., enzymes to digest the cell wall) [36].

1.3. Biological contaminants

1.3.1. Types of contaminants

Contamination is one of the greatest limitations in the productivity of mass cultures. Some microalgal contaminants such as “protozoa”, zooplankton, fungi, bacteria, viruses, other algae, and even insects can cause serious economic losses (**Table 2**), due to their negative effect

on the overall productivity, such as reduction of microalgal concentration, stress, cellular alteration, degradation of the product quality and even destruction of the algal culture within a few hours after detection [21]. On the other hand, not all foreign microorganisms in a culture are harmful. Some microalgal species are able to grow and produce biomass that can be used for commercial ends with a tolerable level of contamination. Moreover, some species need additional macro- or micronutrients produced by other microorganisms and cannot be cultivated axenically [15].

In algal cultures, the most common interactions with contaminants are mutualism, competition, predation and parasitism. Mutualism is an interaction that benefits two populations. It can positively affect microalgal growth and even become essential (e.g., for Vitamin B₁₂ production by bacteria) which explains why sometimes it is impossible to maintain an axenic microalgal culture as it happens with the haptophyte *Tisochrysis lutea*. Competition is an interaction that benefits only one population, determined by environmental factors (e.g., nutritional factors and light intensity), which they compete for. Competitors in phototrophic cultures are other microalgae, while bacteria and fungi are the most common competitors in mixotrophic or heterotrophic cultures. Predators such as rotifers, microflagellates, amoeba and predatory bacteria are organisms that grow by feeding on microalgae, which often results into the death of the culture. On the other hand, parasites are organisms that grow using microalgae as their host and source of nutrients, thus, frequently maintaining them alive although in a weakened state. Parasites can be bacteria, virus and fungi, which can be endo- or ectoparasites, living inside or outside the cell, respectively [15].

Interactions such as competition are capable to reduce the nutrient yield up to 10 times. Predation and parasitism usually damage microalgal cultures the most, as in just a few days the biomass can decrease by 90% and sometimes, culture collapse occurs. Besides affecting the quantity of microalgal biomass production, contaminants can also affect the abiotic factors and produce toxins leading to cultivation limitations and quality problems for food safety and feed production [13,24]. An example of mutualism is the biomolecules produced for allelopathy, which are mostly secondary metabolites. These are known as allelochemicals and are produced by certain plants, algae, bacteria, coral, and fungi, which can have beneficial or detrimental effects on the target organism. Biomolecules with allelopathic function have other ecological roles, such as chemical defence and nutrient chelation. These molecules could be used as natural herbicides or agents for pest control in crops for sustainable agriculture and to improve microalgal cultivation [13].

Table 2: Summary of microalgal contaminants detection and mitigation strategies.

Taxon	Microalgal species	Contaminant		Culture system	Detection	Mitigation	References
		Species	Type				
Cyanobacteria	<i>Arthrospira</i> sp.	<i>Brachionus</i> sp.	Grazer	Open pond	Microscopy	Urea and ammonium bicarbonate	[38]
	<i>Synechococcus elongatus</i>	<i>Hartmannella</i>	Grazer	Open pond	Molecular methods	Isolate mutants	[39]
	<i>Synechocystis</i> sp.	<i>Colpoda steinii</i>	Grazer	Closed PBR	Microscopy	Anoxic conditions	[40]
	<i>Synechocystis</i> sp.	<i>Poterioochromonas</i> sp.	Grazer	Open pond	Microscopy	High pH	[41]
	<i>Synechocystis</i> sp.	<i>Pannonibacter phragmitetus</i>	Parasite	Closed PBR	Agar plates	High pH	[42]
Ochrophyta	<i>Asterionella formosa</i>	Chytridiomycota	Parasite	Lake	Epifluorescence microscopy	Unknown	[43]

Chlorophyta	<i>Chlorella kessleri</i>	<i>Brachionus calyciflorus</i>	Grazer	Laboratory	Microscopy	Copper ion	[44]
	<i>Chlorella sorokiniana</i>	<i>Vampirovibrio chlorellavorus</i>	Grazer	Closed PBR	Molecular methods	Benzalkonium chloride	[45]
	<i>Chlorella sp.</i>	<i>Phycodnaviridae</i>	Parasite	Laboratory	Molecular methods	Unknown	[46]
	<i>Graesiella sp.</i>	<i>Rhizophyidium scenedesmi</i>	Parasite	Open pond	Molecular methods	Unknown	[47]
	<i>Haematococcus pluvialis</i>	<i>Coelastrella sp.</i>	Competitor	Closed PBR	Molecular methods	Unknown	[48]
	<i>Scenedesmus dimorphus</i>	<i>Vernalophrys algivore</i>	Grazer	Closed PBR	Microscopy	Unknown	[49]
	<i>Scenedesmus dimorphus</i>	<i>Amoebophilidium protococcarum</i>	Parasite	Open pond	Microscopy	Target specific stages of life cycle	[50]
	<i>Scenedesmus obliquus</i>	Bacteria	Parasite	Closed PBR	Agar plates	Granular activated carbon	[51]

1.3.1.1. Competitors

Competitors such as other microalgae are inevitable and have been reported broadly. They appear when the initial culture is not monoaxenic, and when other microalgae are capable of growing more rapidly than the strain being produced, competing for nutrients or light. For certain ends, such as anaerobic digestion, it is possible to have both species growing. However, for food and feed products, mixed cultures cannot be used [15]. Contamination by other microalgae can be most problematic, since its occurrence can be asymptomatic and very difficult to detect by microscopy. As an example, the contamination of *Haematococcus pluvialis* (Chlorophyta) by the microalga *Coelastrella sp.* (Chlorophyta) (**Table 2**) is capable of reducing the biomass yield and quality [48]. Fungi can also be competitors of microalgae, due to their ability to use growth conditions appropriate for microalgae to proliferate. However, it has been previously reported that some fungal species do not grow well in nutrient-rich media because they are often outcompeted by other microorganisms. Therefore, usually non-pathogenic aquatic fungi do not pose a significant problem [52].

Competition between different microalgae is achieved by direct cell contact, resource consumption and allelopathy. Direct cell contact occurs when the concentration of microalgal cells reaches higher values, and less space is available and cells collide, resulting in competition, where dominant species outgrow the production strain, such as *Cochlodinium polykrikoides* that inhibits *Akashiwo sanguinea* growth. Resource competition occurs when the capability of the environment to supply resources is smaller than the potential biological requirement. For example, *Microcystis novacekii* can compete with *Scenedesmus quadricauda* for ammonium supply. Allelopathy is a biological phenomenon by which an organism produces biochemicals that kills or inhibits the growth of another. For instance, *Pridinium aciculiferum* can kill *Rhodomonas lacustris* by secreting a specific toxin [25].

1.3.1.2. Grazers

The major group of contaminants and most difficult to prevent are the grazers, usually eukaryotes present in microalgal cultures, with a larger in size with ameboid and/or ciliated/flagellated forms such as microflagellates, amoeba, ciliates, copepods, rotifers and other small organisms that prey on microalgae

Figure 2). Besides microalgae, they also consume bacteria and fungi, which have a significant impact on the community of microorganisms, thus significantly reducing the biomass yield [52].

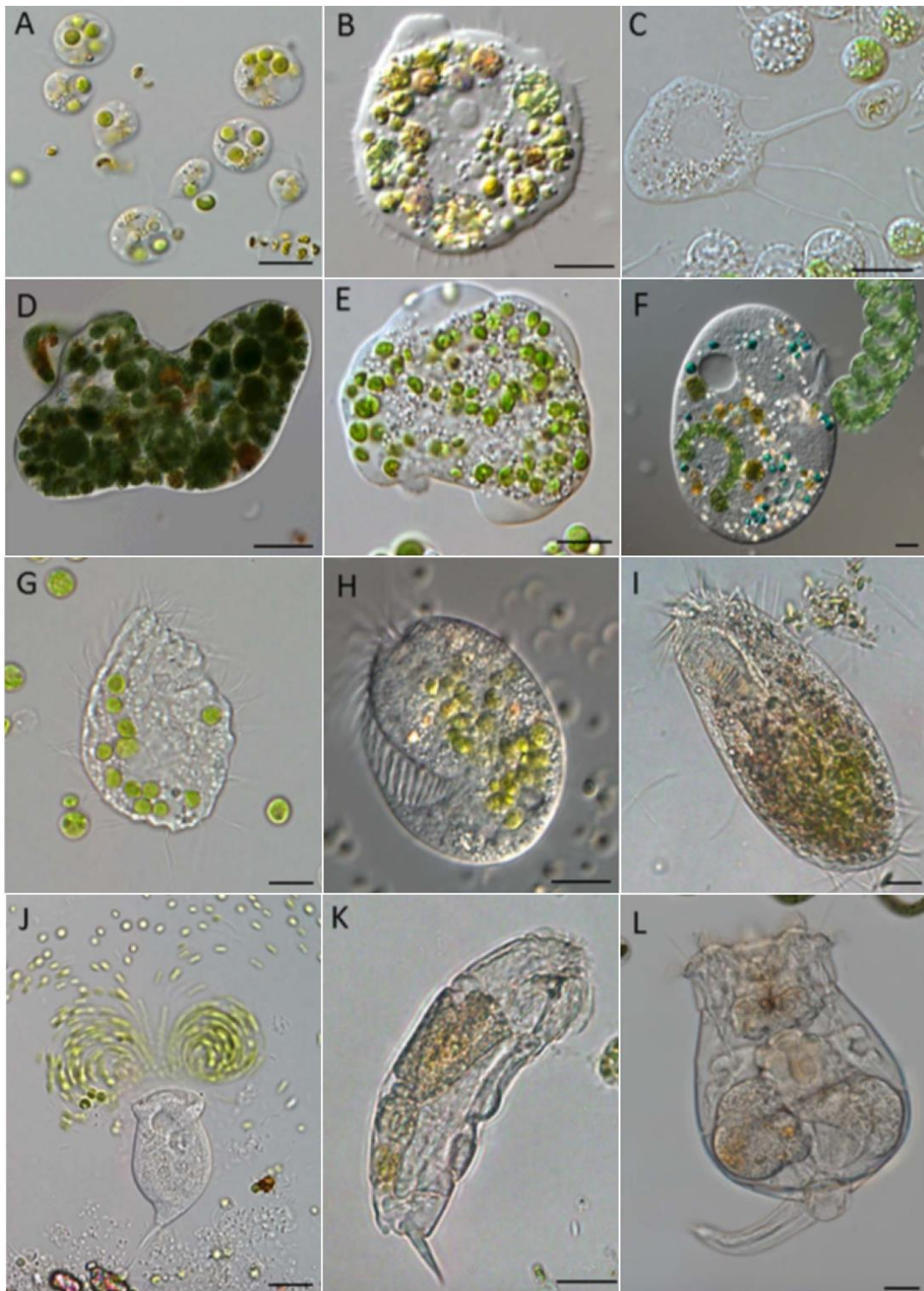


Figure 2: Microzooplanktonic grazers: A. *Poteriochromonas malhamensis* and *Chlorella*; B. *Nuclearia* and *Spirulina*; C. *Nuclearia* and *Scenedesmus*; D. Heterolobosean amoebae and *Spirulina*; E. *Saccamoeba* and *Nannochloropsis*; F. *Frontonia* and *Spirulina*; G. *Colpoda* and *Chlorella*; H. *Euplotes* and *Nannochloropsis*; I. *Sterkiella histriomuscorum* and *Scenedesmus*; J. *Vorticella* and *Scenedesmus*; K. *Lecane inermis* and *Chlorella*; L. *Brachinous plicatilis* and *Spirulina*. Scale bar = 10 μ m. [6].

Top-down control, such as grazing, is a key aspect of the food web, having a significant influence on ecosystems and functioning of the microbial loop. In marine ecosystems, the major grazers are larger zooplankton, with the potential to reduce algal concentrations and production to low levels in few days. Some microorganisms and zooplankton can also form resistant resting stages (e.g., cysts and spores), posing a major threat to open systems by spreading with wind currents and to closed systems by staying viable for many years in sediments and biofilms [6].

Grazers are known to be the main biological contaminants due to their ability to quickly affect the culture and destroy it in just a few hours. Grazers range from macroscopic insects to microflagellates, barely larger than their prey. In open systems such as raceways, insect larvae have already been reported as a grazing biological contaminant of *Spirulina* cultures [6], as well as the amoeba *Hartmannella*, previously reported to prey on the cyanobacterial *Synechococcus elongatus* cultures [39]. Furthermore, the chrysophyte *Poterioochromonas malhamensis* is a known grazer of *Chlorella* spp. (Chlorophyta) mass productions in flat panels and open pond systems but has also been shown to prey on other microalgal strains [39]. In closed PBR systems, *Colpoda steinii* has been reported to prey on *Synechocystis* sp. cultures and is associated with a very rapid decline of the algal numbers within 2-3 days [40] (**Table 2**).

1.3.1.3. Parasites

Parasites can be classified as endo- or ectoparasites. Endoparasites develop inside their host (nucleus remains inside). Once parasites enter the cell wall, kill the host and digest them entirely, or preserve the host alive until the end of the maturation process. To penetrate the host, they can produce a pseudopodium-like structure or an apical complex-derived structure, digesting the cell coverings and the inside by means of external and internal enzymes or simply by phagotrophy (thus becoming predators). Ectoparasites develop outside their host, as they can partially penetrate the host, although their nucleus remains always outside. These parasites can penetrate their host through germ tubes between thecal plates (e.g., fungi) or be active phagotrophs and feed by endocytosis, pinocytosis or phagocytosis [53].

Microalgal cultures are affected by several freshwater and seawater types of fungi and/or pseudofungi, usually belonging to the phylum Chytridiomycota and Oomycota, respectively. These freshwater contaminants tend to cause higher reduction of microalgal population than the seawater contaminants. Contaminants such as *Paraphysoderma sedebokerensis* have been found in cultures of *Scenedesmus* and *Chlamydomonas* [15]. Chytrids from the phylum *Blastocladiomycota* are also known parasites of *Haematococcus pluvialis* (Chlorophyta) [54] (**Table 2**).

On the other hand, bacteria are the most important contaminants which can be co-cultivated and help the growth of microalgae, or be a potential threat due to toxin productions, competition and direct lysis. With this type of contamination, microalgal cultures are more susceptible to the growth of other pathogens. Bacteria such as *Vibrio* can reduce the nutritional quality of the biomass and *Pseudomonas* can compete for nutrients and inhibit the microalgal growth [15]. Some bacteria such as *Cytophaga*, *Myxobacter* and *Bacillus* were found in cultures of *Scenedesmus*, *Chlorella*, *Chlorococcum*, and *Ankistrodesmus*, inhibiting microalgal growth [15] (**Table 2**).

Viruses are also well known for their interactions with microalgae and cyanobacteria. Indeed, they can also significantly reduce microalgal biomass in just a few days. They usually change the cell structure and diversity, due to their short and fast replication cycle and high specificity of infection [25]. The contamination of this group has still little information. Viruses attach the cell wall, digest a small part of the cell covering and inject DNA into the microalgal cell. To replicate themselves, they use host replication and transcription machinery, which can overwhelm the host cell response against the viral infection. Usually, low growth rates are observed, and a viral outbreak happens [52]. Viruses are able to infect both prokaryotic cyanobacteria and eukaryotic algae. The LPP virus has previously been reported to infect several hosts such as the cyanobacteria *Lyngbya* sp., *Phormidium* sp. and *Plectonema* sp. [25]. Cultures of *Heterosigma akashiwo* (Raphidophyte) presented parasites that inhibit its growth, such as the virus HaV [55] (**Table 2**).

1.3.2. Detection and quantification of contaminants

The determination and quantification of different contaminants in microalgal cultures is a challenging task. When a microalgal culture is highly contaminated, the effects are obvious by eye. The culture usually changes in its overall hue, leading to, for example, a reduction in their green colour, which is typical of Chlorophyta cultures, and an increase of a brownish coloration. Concomitantly, the cell concentration decreases while grazers or other contaminants increase, and the microalgae lyse and die. However, at this point it is usually too late to apply mitigation strategies to control the contaminant and save the culture [6].

Monitoring health and productivity of algal ponds, including early detection and control of contaminants, is important to avoid significant culture damage and economic losses for the microalgal producer. Over the last few years, techniques have been developed aiming to control the contamination in mass cultures of algae and to identify not only natural defence

mechanisms, but also genes and genetic pathways that could be used as protective strategies for cultivation [39]. For early detection, a minimum of daily sampling at a number of points in each production unit (flat panel, pond, bioreactor) is needed. Furthermore, sampling of sediments and/or any biofilms, if present, should be included, as these may be potential sources of an inoculum that could result in infection [6].

Quantification of biological contaminants and their impact on microalgal cultures requires the measurement of cell concentration, biomass concentration and elemental composition. Data from different analytical methods need to be integrated and for each investigated parameter a compromise among accuracy, sensitivity, cost, labour and time has to be found, depending on the aims of the analysis. The dry weight of the biomass is a fundamental parameter that needs to be known and calculated for every analysed species to quantify the impact of biological contaminants. In pure cultures cultivated under controlled conditions, the concentration of contaminants can be obtained with a correlation between cell concentration and dry weight. However, it is not a constant value for all species [24].

Microscopy is the simplest and most common approach to detect and enumerate contaminants (**Figure 3**). It allows to directly distinguish and estimate the growth of different contaminants. Several methods of imaging can be used from optical to confocal, interference and electron microscopy. One of the disadvantages of microscopy is that it requires an experienced operator for reliable results, and it is time consuming for higher number of samples [15]. Optical microscopy is used to measure cell concentration of microorganisms directly in their living environment. It is reliable to quantify and count separately different microorganisms in mixed cultures.

Direct cell counting is used to determine the total contamination in microalgal cultures with chambers, such as Hausser 3200, Sedgwick-Rafter, Nageotte haemocytometer and Neubauer haemocytometer [24]. In order to count bacteria and/or viruses, cells are stained with fluorescence dyes for DNA, such as propidium iodide, SYTO 9, acridine orange, fluorescein diacetate, DAPI and SYBRGreen and visualised using an epifluorescence microscopy. The correct dye must be chosen to avoid signal interference with the autofluorescent pigments of microalgae. For morphological analysis, scanning electron microscopy (SEM) and transmission electron microscopy (TEM) are the most used techniques down to a few nanometres. With SEM the structure of microorganisms, the establishment of an axenic culture and the interactions between microorganisms can be seen. With TEM, the contaminant concentration analysis of complex samples (e.g., activated sludge and environmental samples) can be measured. However, these techniques are expensive and time consuming [24].

Plate counting is often used in microbiology to count microorganisms (**Figure 3**). The sample is spread onto a plate to form colonies. It is a cost-effective and easy-to-perform method, which does not require expensive materials and there are several protocols available. However, some microorganisms do not grow on plates and, therefore, this technique might not be reliable. When the samples are complex with diverse microorganisms, it is difficult to grow all of them under the same cultivation conditions. Furthermore, it can take days or weeks to obtain results, which means it will probably be too late to find a mitigation strategy [24].

Flow cytometry is a high throughput technique that analyses a large number of cells in mixed populations of cultures in a short time (1,000–35,000 events/s), being able to count and measure different properties of the microorganisms directly in the sample (**Figure 3**). Cells are separated by a fluidic system, an incident laser hit the cell which produces signals with different fluorescence emissions that will further be detected by optical filters and light detectors. Microorganisms are distinguished by size, internal complexity as well as fluorescence (e.g., chlorophyll autofluorescence). This methodology is beneficial in the control of biological contaminants in mass cultures in order to identify the microorganism responsible for the contamination. However, its capacity is limited in identifying strains with similar phenotypes and to single cell microorganisms [15]. Despite its high potential, the application of this technique is still at its infancy and standardized protocols for analysis are missing.

When coupled with fluorescence-activated cell sorting (FACS), flow cytometry can process and measure up to 20 different light scatter and fluorescence properties of thousand cells per second. Separation of cells or populations is achieved which enables the selection of strains with improved traits [56]. Imaging flow cytometry is the same high throughput technique as conventional flow cytometry. However, when passing through the laser point, photographic images can be captured, and a lower number of events is registered (300 and 1,000 events/s). These images can be analysed using software and higher amount of cellular information is obtained. Rather than producing a single pixel for every parameter measured, it produces 2D images of several pixels capable of capturing cell aggregates and pluricellular structures [24]. It can detect a wide range of grazers (e.g., amoeba, flagellates, ciliates and zooplankton) at concentrations as low as <1 individual ml^{-1} such as *Brachionus calyciflorus* in *Chlorella* cultures with cell concentrations as high as 10^7 cells ml^{-1} [6]. Mass cytometry also operates as flow cytometry. Nonetheless, in this technique, the mass of each cell is analysed. In this case, the laser detector is replaced by an inductively coupled plasma (ICP) detector. When the cell suspension reaches the detector, cells are nebulized with Ar gas and are confined into small droplets. These droplets pass through an aerosol splitter and are injected with an inductively

coupled plasma to produce ions. The cells are sent to a mass detector to be analysed with different parameters (up to 40) [24].

Non-genetic biomarkers could also be used to measure microorganism concentrations and detect contaminants, since some chemical molecules can be specifically produced only by some groups of organisms (**Figure 3**). For example, molecules such as pigments (e.g., chlorophyll, carotenoids and phycocyanin), lipids, carbohydrates, sterols and proteins can be used. For microalgae, the most analysed pigment is chlorophyll *a* since the contaminants are usually heterotrophic and do not possess chlorophyll. Even if it is cheap and fast for large number of samples, specific molecules are required, and the contamination needs to be a fraction of the whole biomass [24].

Molecular techniques have been developed and allow the identification and detection of different contaminants in microalgal cultures (**Figure 3**). These techniques can determine single specific molecules, allowing the identification of different species or strains in a sample. Therefore, molecular approaches are the most specific and sensitive techniques to early detection of contaminants since they are based on polymerase chain reaction (PCR) and amplify molecules even when DNA is extracted from a low concentration of cells. Usually, the regions of DNA that are used for the identification of microorganisms are the genes encoding the small subunit (SSU) and large subunit (LSU) ribosomal RNA, and the respective internal transcribed spacers (ITS1 and ITS2). With these regions, it is possible to design PCR primers with high specificity. The polymorphism between the 18S (SSU) genes of microalgae is enough for the differentiation of genera, allowing to identify contamination by other microalgae [15].

Through monitoring microalgal cultures using quantitative PCR (qPCR), contaminants may be detected at levels as low as one in 10^8 microalgal cells as well as the exact concentration of each specific DNA sequence [57]. Second Generation Sequencing (NGS) is used to analyse the microbiome of different cultures and is able to identify the microorganism responsible for the culture collapse. For example, in mass cultures of *Nannochloropsis salina*, several grazers were identified with this technique, such as *Brachionus* and *Chaetonotus*, as well as the ciliate *Acineta*, the parasite *Vampyrella* and the amoeba *Nolandella* [6]. However, the high sensitivity of DNA analysis means that every step must be carefully carried out and optimized.

Many commercial kits are already used to extract DNA from microalgal samples. After the extraction, the molecular analyses can be qualitative (presence/absence and relative abundance of species) or quantitative (exact concentration of each specific DNA sequence can be measured in the sample). After amplification, the DNA sequences can be detected using gel electrophoresis, sequenced and compared with other sequences using genetic databases (e.g.,

GenBank and BLAST) [24]. There are several other new alternatives to identify biological contaminants in algal cultures, such as metagenomics, metatranscriptomics, and metaproteomics.

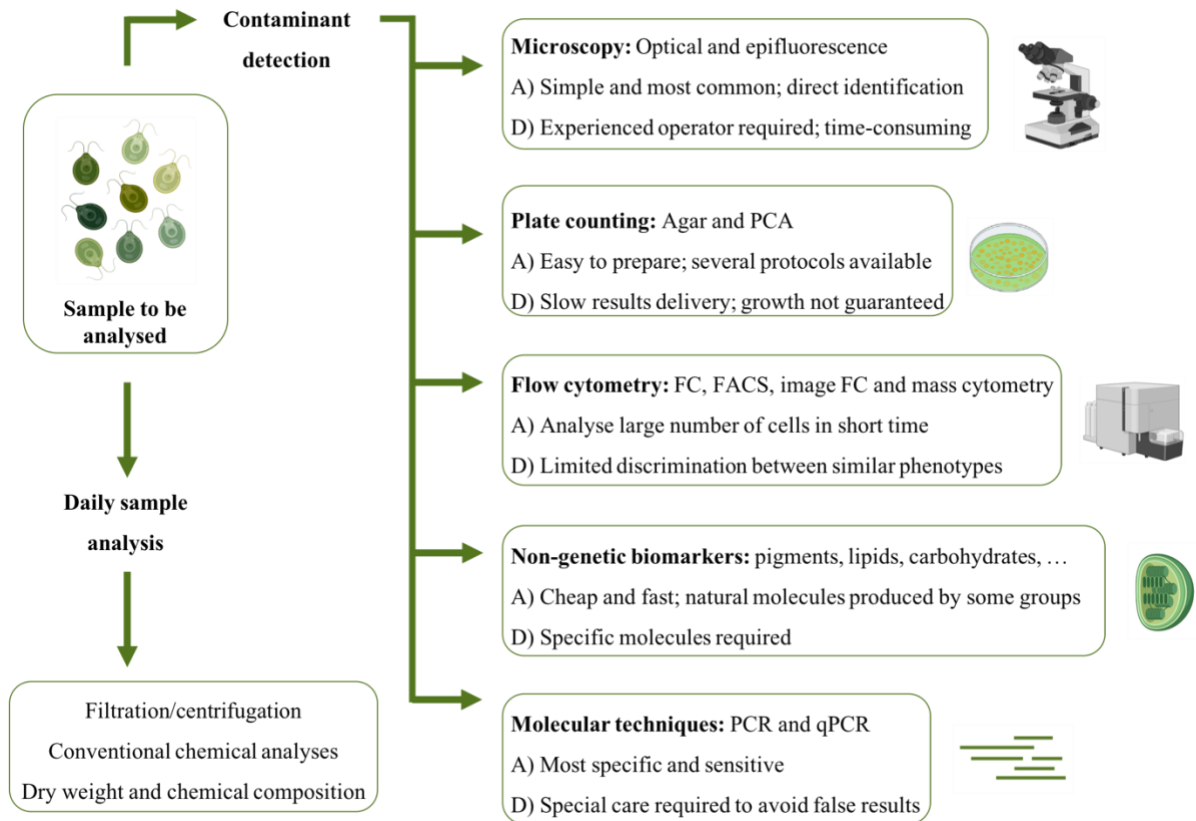


Figure 3: Schematic flow diagram on how to analyse microalgal cultures and detect biological contaminants, as well as the advantages (A) and disadvantages (D) of each detection method [24] (www.biorender.com).

1.3.3. Mitigation strategies

Contamination in microalgal cultures is a factor that cannot be avoided. Despite the existence of control mechanisms, these are not always effective and sometimes they can become costly, especially due to the large number of possible contaminants and the lack of information about their biology. For this reason, it is necessary to investigate specific methodologies for each culture and search new substances of natural origin to avoid problems of toxicity in cultures [15]. Strategies can be preventive (avoid the entry of contaminants) or corrective (control or eliminate the contamination). Disinfection of equipment and the aseptic handling of inocula are the most common strategies; nevertheless, it is generally doable only at the laboratory and it is not possible at pilot scale. Some of the strategies currently used to combat

biological contamination are environmental, physical, chemical and biological strategies (**Table 2**). However, there is no single methodology able to address all contaminations [15].

The most used strategies to control contaminants in commercial microalgal cultures is the application of environmental pressure, such as extreme temperature, light intensities, pH or salinity. Some microalgae are able to endure those extreme conditions of cultivation, which may act as a competitive advantage in relation to contaminants when grown in liquid medium [13]. Although this strategy is used to prevent the growth of foreign microalgae, bacteria and grazers, it can lead to losses of biomass and productivity. To cultivate microalgal species unable to grow in extreme culture conditions, other methods have been proposed and implemented to reduce the impact of contamination, such as the culture parameters [23]. For example, reducing the culture pH to 3 for 1-2 h was shown to eliminate flagellates; increasing the salinity to 20% was shown to inhibit the development of amoeba/ciliates in *Dunaliella* cultures [25].

The physical strategies, such as filtration and physical disruption (sonication) are also used world-wide. Since microalgal cells are relatively small (5-100 microns), filtration can be considered as an effective method to remove biological organisms with large volumes of cell size (>200 microns in length), such as rotifers and copepods. However, eggs and developing young individuals cannot be completely removed. In order to eliminate the smaller biological contaminants thoroughly, the culture should be continuously filtered over 3-4 days [15]. A slow sand filter can be used to treat the incoming water, which can effectively filter out all particles larger than 10 microns. As most protozoan contaminants are larger than 16 microns, a very low concentration of grazers is expected in the effluent. Wastewater treatment methods also have many protocols for coagulation of cyst and oocyst as well as filtration techniques that could be employed to remove grazers [52]. Physical disruption (sonication) is another method that belongs to the physical strategies. While several microalgae are resistant to mild sonication, larger organisms require less energy input for disruption. Zooplankton required less exposure time and ultrasonic energy (3-9 s, 6-19 J/mL) when compared to bacteria and phytoplankton (1 to 22 min, 31 to 1240 J/mL). Therefore, this method is effective for larger contaminants but less so for the smaller contaminants [58]. Other physical processes such as sterilization, ultraviolet light application, and pasteurization can be used, especially in the water medium before inoculation. For this reason, they can be combined with other methodologies in order to obtain the desired results [15].

Chemical strategies are the most feasible to counteract biological contamination and/or induce the biological contaminant to separate from the algal cells. After separation, the biomass can be concentrated in a special compartment of the photobioreactor from which it can be

discarded [13]. Despite its low specificity (both contaminants and microalgae are targeted), the addition of chemical compounds is very effective. To determine the appropriate agents and concentrations to perform the control, determination of the minimum inhibitory concentration for contaminants is required as well as the tolerance of the desired microalga, and tests to avoid damage and loss of the cultures are mandatory. Commonly used chemical agents are antibiotics, fungicides, pesticides, salts, aldehydes, and peroxides. For example, the combination of Celangulin and Toosendanin (1:9) exterminated the rotifers *Brachionus plicatilis* from *Chlorella* and *Nannochloropsis* cultures [15]. A different report showed that quinine (10 mg/L) is effective to eliminate ciliates and had low damage on *Dunaliella salina* cells [25].

Biological strategies are still a work in progress, but very promising as it does not produce any chemical residues and allows the growth of a favourable bacterial population, for example. For toxic dinoflagellates, some studies showed that both virus infection and algicidal effects from bacteria can be host specific and kill them specifically when they reach a certain population size. For harmful bacteria, some strains such as *Aeromonas* can adapt to low concentrations of organic substrate and outcompete the growth of *Vibrio alginolyticus* in microalgae cultures [26].

1.4.Aims and objectives

Because of biological contaminations, the productivity of microalgal mass cultures is reduced and the collapse of the cultures may occur leading to high production costs. Contaminants are species-specific and their taxonomical classification down to genus and species level is still unknown. Therefore, in this thesis molecular methods will be used to identify harmful contaminants in industrial microalgal cultures focusing on eukaryotic taxa.

Molecular approaches were chosen because they are highly specific and sensitive techniques allowing for a detection of contaminants at an early stage. This is important to be able to implement mitigation strategies at a timepoint before culture collapse. This thesis is integrated in the Algaesolutions project and is therefore carried out in close cooperation with the microalgal producing companies Necton and Allmicroalgae.

Taking these aims into consideration the specific objectives of this thesis are to:

- ⇒ Identify eukaryotic contaminants collapsing industrial microalgal cultures using NGS.
- ⇒ Generate contaminant-specific primers for early detection of specific contaminants.
- ⇒ Identify the scale-up step where the contaminant is first detected.
- ⇒ Develop possible mitigation strategies to avoid culture collapse

2. Materials and methods

2.1. DNA extraction

For DNA extraction, PowerSoil Pro DNA kit (QIAGEN) was used. A negative control was made using distilled water. The kit protocol was followed with some adaptations. All centrifugations were conducted at 20,817 *g* if not otherwise indicated. To collect the biomass, samples were centrifuged for 5 min at 5,752 *g* and the supernatant was discarded. After centrifugation, approximately 50 to 100 mg of wet biomass were left, depending on each sample, of which a maximum of 1 mL was transferred into the “PowerBead Pro Tube” and 800 μ L of CD1 buffer were added. Afterwards, the Mixer Mill MM400 (Retsch) was used for 5 min at 30 Hz to disrupt the cells. To ensure supernatant and beads separation, a centrifugation step of 2 min was performed. For DNA elution, 50 μ L of Solution C6 was added to the centre of the filter membrane, centrifuged and the procedure repeated by adding additional 50 μ L of the same solution. DNA stock was stored immediately at -20°C until further utilization.

Genomic DNA stock quality was checked on agarose gel and quantified with NanoDrop One (Thermo Scientific) in order to be used for Next Generation Sequencing (NGS) analysis.

2.2. NGS analysis

Illumina Miseq sequencing was performed by MrDNA using the 18S region with the universal primers, euk1391F (5'-GTA CAC ACC GCC CGT C-3') and EukBr (5'-TGA TCC TTC TGC AGG TTC ACC TAC-3') [59] leading to about 100-bp sequences of all eukaryotic organisms present in the culture. Data obtained known as Zero-radius Operational Taxonomic Unit (zOTU) was screened having in account the number of reads and that each zOTU identifies a unique sequence able to classify groups even if they are closely related. After selecting zOTUs for each microalgal culture, bioinformatic analysis was performed in separate for each culture in order to identify possible microorganisms related to the sequences. The first step was to compare each zOTUs sequence to the sequences present in the National Centre for Biotechnology Information (NCBI) [60] using the nucleotide Basic Local Alignment Search Tool – BLAST [61].

Afterwards, phylogenetic analysis was performed in “À la carte” mode at Phylogeny.fr [62] using similar sequences to the contaminant identify by BLAST. Multiple alignments were performed using MUSCLE (v 3.5) [63], while Maximum likelihood (PhyML, v 3.0) [64] and Distances (BioNJ, v 3.6) [65] were used to build phylogenetic trees. Tree visualization was

conducted with the software FigTree (v 1.4.3). The results of phylogenetic trees were compared to published images and literature as well as with microscopic observations of possible contaminants. Therefore, it was possible to verify that the phylogeny obtained corresponded to the phenotype and/or image observed of what was thought to be the contaminants that caused culture collapse.

2.3. Primer design

Once the sequences of possible harmful contaminants were associated to a family, genus or species, coverage of the target the gene coding for the 18S ribosomal RNA (rRNA) of these microorganisms available in publications was confirmed in order to find specific primers already published. Moreover, several primers pairs were designed in-house using bioinformatic tools, namely primer-BLAST [66], CLC Main Workbench (v 21.0.4) (QIAGEN) and Geneious Prime (v 2021.2.2) (Biomatters Ltd.).

Primers of 18 to 22 bp were designed with a specific 3' end for the sequence of the contaminant small subunit gene (SSU), melting temperature (T_m) between 50 and 60°C, GC content higher than 40% and with an amplicon length between 100 and 1,500 bp. Several consensus 18S sequences of the genus or phylum of the possible contaminants as well as of the affected microalgae, such as *T. lutea*, *P. tricornutum*, *Tetraselmis chui* and *Chlorella vulgaris*, were aligned together in order to design primer pairs with specificity to the 18S ribosomal DNA (rDNA) sequence of the target contaminant, while excluding *in silico* primers aligning with the respective orthologous microalgal genes.

2.4. PCR optimization and sequencing

PCR optimization and tuning of the conditions are very important for a correct amplification of the target sequence. All amplifications were performed using a GoTaq G2 Flexi DNA polymerase (Promega Kit) in a MiniAmp Plus Thermal cycler (Applied Biosystems). All PCR products were visualized on agarose gel using GelRed (Biotium) staining [67].

A master mix with a final volume of 20 μ L was prepared containing 1X Colourless GoTaq Flexi Buffer, 2.5 mM of magnesium chloride, 0.05 mM of dNTPs (2 mM each), 1U of GoTaq G2 and 1 μ L of DNA being assayed. Different primer combinations and concentrations of 0.2 and 0.5 μ M of each primer were tested. The thermocycler programmes consisted of an initial heating up to 95°C for 5 min and a final extension of 72°C for 10 min. The annealing temperature (50 - 65°C), extension time (1 - 1.5 min) and number of cycles (25 - 45) were varied

to find the optimal conditions for the expected amplicon. For the standard PCR conditions, the annealing temperature was 2°C lower than the melting temperature of the primer pair. The extension time was 1 min or 1.5 min if the product length was under or over 1,000 bp, respectively. The number of cycles was 30, following the protocol of the GoTaq polymerase.

Furthermore, the stock DNA of the most contaminated sample was used to make several DNA dilutions, in a range between 0.0002 - 77% of reads (relative abundance) of the possible zOTU contaminant. This was made in order to test the sensitivity of the primers and to detect contaminants at lower concentrations until the limit of detection was reached.

The samples with only one specific PCR product were sequenced using an Applied Biosystems 3130XL DNA sequencer (Life Technologies, CCMAR). The sequences obtained from Sanger DNA sequencing were compared to the previously identified sequences to confirm the specificity of the primer to amplify only sequences of the contaminant and not of the contaminated microalgal species or even of other unrelated co-contaminants.

2.5. Sampling procedure during the scale-up process

The scale-up process was followed from the laboratory to industrial scale, sampling 50 ml of biomass and process water of each step to find out the source of contamination (**Figure 4**). Samples were stored at -20°C until DNA extraction. The sampling process started with the culture collection to ensure axenic conditions at laboratory scale were attained.

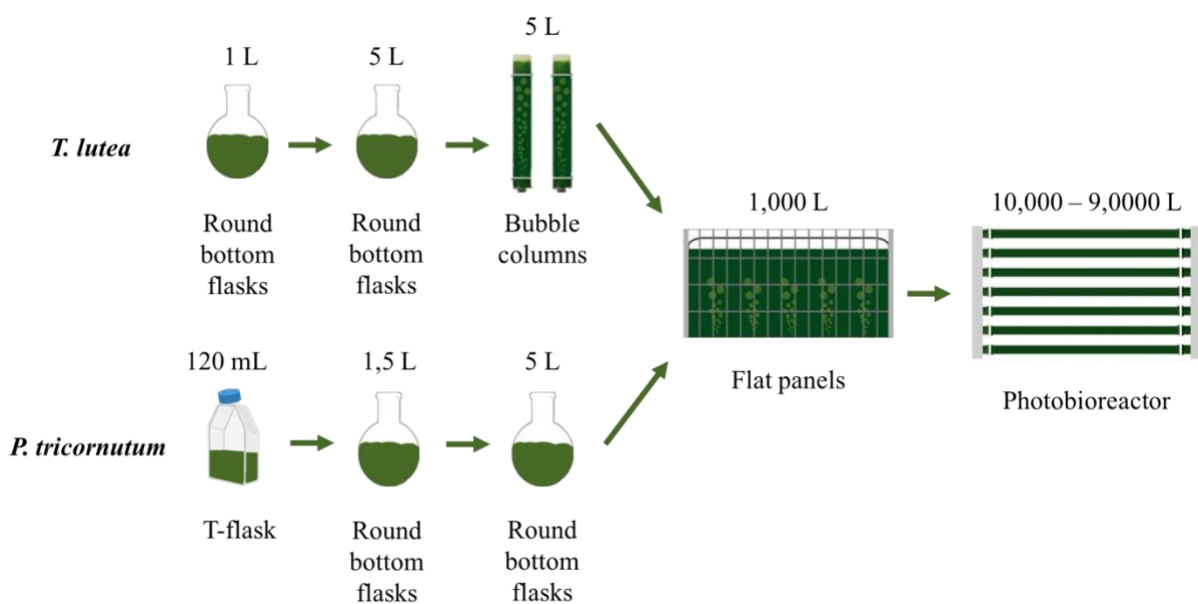


Figure 4: Diagram of the scale-up procedure used for both *T. lutea* and *P. tricornutum* at Necton and Allmicroalgae, respectively.

At the facilities of Necton, *Tisochrysis lutea* was scaled up to 1-L round bottom flasks, which were further transferred to 5-L round bottom flasks. These round bottom flasks were used as inocula for indoor 5-L bubble columns. The outdoor scale-up included 1,000-L flat panels and finally 20,000-L tubular photobioreactors. At Allmicroalgae, *Phaeodactylum tricornerutum* was scaled up in T-flasks of 120 mL. Then, the cultures inside the T-flasks were transferred to 1.5-L round bottom flasks, which were further scaled up to 5-L balloons. These round bottom flasks were used to inoculate 1,000-L flat panels located in greenhouses. For the final step of the scale-up process, outdoor photobioreactors of different sizes were inoculated (small – 10,000 L, medium – 35,000 L and large – 90,000 L).

2.6. Cultivation and microscopic observations of the contaminants

Contaminated *T. lutea* and *P. tricornerutum* cultures were provided by Necton and Allmicroalgae, respectively. The cultures were grown in 100-mL Erlenmeyer flasks (50 mL working volume) under continuous light at a photon flux density (PFD) of $38 \pm 9 \mu\text{mol s}^{-1} \text{m}^{-2}$ with a photoperiod of 24h and agitation of 140 rpm at an average temperature of $30 \pm 5^\circ\text{C}$.

The medium used for the contaminant of *T. lutea* was the actively growing microalga in sterile seawater with a salinity of 33 ppt enriched with 4 mL/L of Nutribloom™ as nutrients (Phytobloom, by Necton), with a final nitrate concentration of 8 mM. As for the contaminant of *P. tricornerutum*, the media was composed of the microalga grown in sterile artificial seawater with a salinity of 33 ppt supplemented with modified ALGAL medium (MAM) [68], optimized for diatoms (**Table 3**). Both microalgal cultures were cultivated in 1-L glass reactors with artificial light at a PFD of $140 \mu\text{mol s}^{-1} \text{m}^{-2}$ with a photoperiod of 24h under continuous filter sterilized (0.2 μm) air bubbling of 0.4 L/min. Cultures containing the contaminant were reinoculated every 7 to 10 days by the following procedure: 1 mL of the previous contaminated culture was added to a new Erlenmeyer flask containing 50 mL of the actively growing microalgal culture.

For *T. lutea*, further analysis was made about the life cycle of its contaminant. An experiment of 21 days was conducted using three healthy microalgal cultures inoculated with contaminated cultures with an age of 7, 14 and 21 days, which represent the different life stages of the contaminant. The experiment was carried out in biological triplicates and under the same cultures conditions as described **above**.

Table 3: Composition of 1x concentrated MAM.

	Reagents	Concentrations	Unit
Macronutrients	NaNO ₃	12.0	mM
	KH ₂ PO ₄	0.6	mM
Micronutrients	EDTA-Na	19.2	μM
	ZnCl ₂	3.0	μM
	ZnSO ₄ •H ₂ O	3.0	μM
	MnCl ₂ •4H ₂ O	3.0	μM
	Na ₂ MoO ₄ •2H ₂ O	0.3	μM
	CoCl ₂ •6H ₂ O	0.3	μM
	CuSO ₄ •5H ₂ O	0.3	μM
	MgSO ₄ •7H ₂ O	6.0	μM
Iron	FeCl ₃ •6H ₂ O	60.0	μM
	EDTA-Na	60.0	μM
Silica	Na ₂ SiO ₃ •9H ₂ O	0.3	mM

2.7. Analysis of growth parameters

The contaminated microalgal cultures were observed every day under the microscope (Zeiss Axioscope 5 Z2) using the 40x lens and pictures were taken and analysed by ZEN blue software (v. 3.3) to better understand their life cycle. In order to follow the growth of the cultures, optical density measurements were performed using HITACHI Spectrophotometer UH5300 set to a wavelength of 750 nm.

Cell count (CC) was correlated with optical density (OD) to measure the cell concentration of *T. lutea* cultures ($y = 8E+06x$, $R^2 = 0.9714$, **Figure A1**) and *P. tricorutum* cultures ($y = 3.52E+05x$, $R^2 = 0.9959$, **Figure A2**). Cellular concentrations were measured using 10 μ L of microalgal culture in a Neubauer chamber (**Equation 1**) and 1 μ L/mL of acid Lugol's solution (1%) to fixate the cells. Each count was kept between 30 to 300 cells in order to obtain significant cell numbers without increasing the error. If higher, cells were diluted by adding seawater or artificial seawater.

T. lutea growth was also followed by correlating OD and dry weight (DW) ($y = 0.7743x$, $R^2 = 0.971$, **Figure A3**). In order to estimate the biomass concentration, dry weight was measured using 5 mL samples filtered by vacuum pump through pore glass fibre filter (0.7 μ m), followed by washing with 5 mL of ammonium sulphate (31.5 g/L) to remove the remaining residues such as salts. The filters were dried in an oven for 24 hours at 100 °C and weighed using the GH-202 analytical balance (A&D Weighing).

Dissolved nitrates in the supernatant were determined spectrophotometrically using the method described previously in Schulze et al., 2017. Briefly, a correlation curve was established using sodium nitrate (NaNO₃ - 8 mM) at the concentrations of 0.25, 0.5, 1, 2 and 4 mM, in order to calculate the concentration of dissolved nitrates present in the supernatant of the samples. For each sample, 50 μ L of supernatant were added to a mixture of 930 μ L of NaCl (35 g/L) and 20 μ L of HCl (1 M). To separate algal biomass from the growth medium, 1 mL of sample was centrifuged for 6 min at 3,000 g and 20 °C (Eppendorf Centrifuge 5430R). As negative control seawater was used. Optical density was measured using a quartz cuvette at the wavelengths of 220 nm and 275 nm in order to determine the nitrates and interference of some debris present in the supernatant, respectively. After the measurements, the dissolved nitrates were calculated using **Equation 2** obtained with the correlation curve ($y = 0.1733x$, $R^2 = 0.9989$, **Figure A4**).

Salinity was measured using the HI96822 Seawater Refractometer (HANNA). If needed, salinity was lowered or increased by the addition of distilled water (DW) or brine water (BW - 442 ppt), respectively. The pH was measured using non-bleeding pH-indicator strips (MColorpHAST™). The pH was adjusted to a lower or higher value with the respective addition of hydrochloric acid (HCl - 1 M) or sodium hydroxide (NaOH - 2 M) solution.

Equation 1: Cellular concentration (cells/mL) = Number of cells x 10⁴ x Dilution

Equation 2: Dissolved nitrates (mM) =
$$\frac{(\text{OD}_{220} \times \text{Dilution}) - 2 \times (\text{OD}_{275} \times \text{Dilution})}{0.1733}$$

2.8. Mitigation trials

2.8.1. 6-well plate screening

For the first screening, several environmental and chemical agents were tested using microalgae infected with their respective contaminant while non-contaminated microalgal cultures served as a control for growth performance of the algae.

The environmental pressure applied to the contaminants were different salinities and pH, and the chemical tests were different concentrations of germanium dioxide (GeO₂), potassium phosphate (K₂HPO₄), sodium dodecyl sulphate (SDS) and hydrogen peroxide (H₂O₂) based on previous publications (**Table 4**). All treatments were performed in triplicate using in total 60 mL of *T. lutea* inoculated with 500 µL of contaminated culture for 6 days. The growth conditions used are described **above**. The growth of microalgae and contaminants was monitored by microscopic observations and optical density measurements (OD₇₅₀), harvesting 500 µL of culture for all measurements.

Table 4: Concentrations of the performed mitigation treatments.

Type	Treatments	Concentrations					Unit	Ref.
		Lower		Medium	Higher			
Environmental pressure	Salinity	45	50	55	60	80	ppt	[70]
	pH	6		-	10		-	[41]
Chemical tests	Germanium dioxide (GeO ₂)	0.25	0.5	1	2	4	mg/L	[71]
	Potassium phosphate (K ₂ HPO ₄)	2		10	20		mM	[70]
	Sodium dodecyl sulphate (SDS)	20		-	40		mg/L	[72]
	Hydrogen peroxide (H ₂ O ₂)	0.028		-	0.056		mL/L	[73]

2.8.2. Lab-scale assays in 100-mL Erlenmeyer flasks

As negative control, microalgae were grown without contaminants while a contaminated culture under normal growth conditions served as positive control for culture collapse. The environmental mitigation assays using salinity and pH were adjusted before the distribution of the culture to Erlenmeyer flasks, and the chemical mitigation agent, germanium dioxide, was added after the addition of the culture to the flasks. All experiments for *T. lutea* and *P. tricornutum* were carried out in triplicates, for 14 and 4 days, respectively. The biochemical and morphological analysis performed for this assay were pH, optical density measurement (OD₇₅₀), determination of nitrates concentration in the medium, microscopic observation and cell counting (Neubauer chamber).

2.9. Statistical analysis

All statistical analyses were performed using XLSTAT PREMIUM (v 2022.5.1.1386). The data was evaluated by one-way ANOVA with Tukey's multiple comparison tests, with a confidence level of 95%. Graphs were plotted using Microsoft Excel (v 16.43 1108).

3. Results and Discussion

3.1. Biological contaminants of *Tisochrysis lutea*

3.1.1. NGS analysis

Samples of contaminated cultures from different timepoints and of different reactors during the growth of *T. lutea* were taken during the industrial production in order to extract high-quality DNA that was sent to be sequenced using Next Generation Sequencing (NGS) technology (Illumina MiSeq short read technology), in addition to a sample of distilled water as negative control (**Table 5**).

Table 5: Samples sequenced by NGS.

Company (species)	Sample Name	Observations
Necton (<i>T. lutea</i>)	Inoculum	Inoculum, non-contaminated
	ETO3 3/3/21	Highly contaminated culture from a photobioreactor
	ETO4 22/7/20	Collapsed culture from a photobioreactor
	ETO4 22/7/20	Collapsed culture from a photobioreactor
	PBR4 22/7/20	Highly contaminated culture from a photobioreactor
Negative control	NC	Negative control

The results obtained from NGS showed in total 224 zOTUs. Before the classification of each zOTU, it was important to take into account the contaminants concentration existing in the extracted samples sent for NGS analysis. Different samples had the same zOTU, however, at different concentrations ranging from 0 to 31,801 reads. Because it is unlikely that zOTUs with less than 100 reads are the main cause of the culture collapse, only zOTUs with more than 100 reads were considered to identify genetically which contaminant is harming the microalgal culture. Therefore, only 112 zOTUs were further characterised. The sequences were analysed using BLAST, taking into account the expected (E)-value ($\sim 1 \times 10^{-50}$) and percentage of identity (>95%) (**Figure 5**).

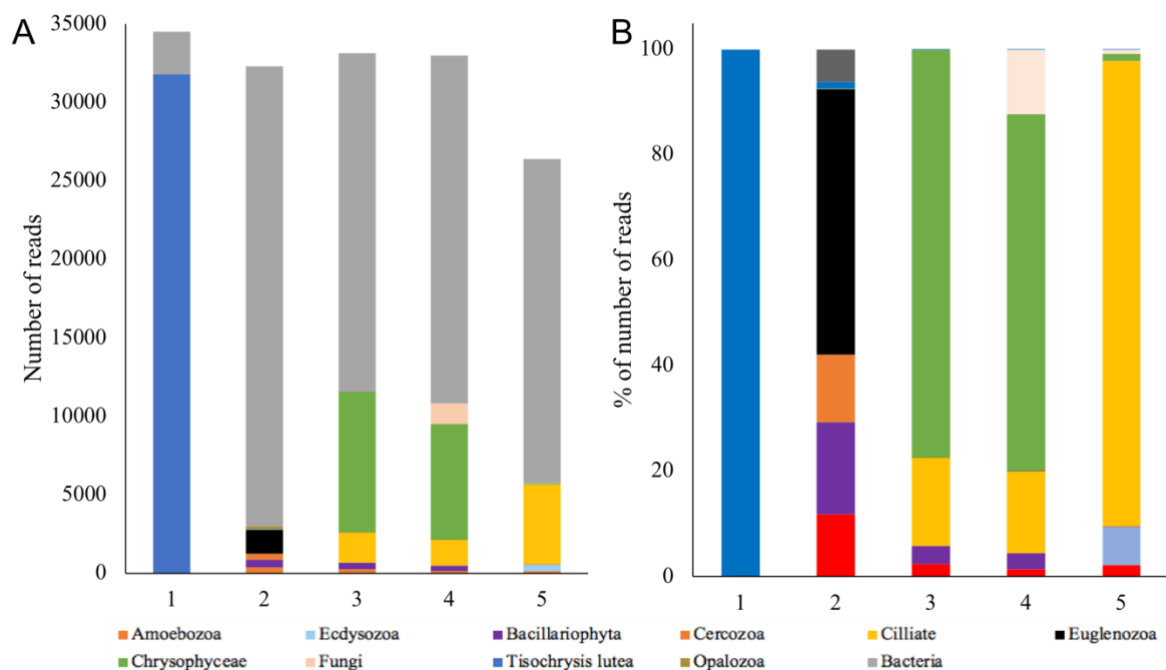


Figure 5: Abundance of relevant taxa obtained by NGS in inoculum and contaminated samples of *T. lutea*, namely: 1) Inoculum, 2) ETO3 3/3/21, 3) ETO4 22/7/20, 4) ETO4 22/07/20 and 5) PBR4 22/07/20; with bacteria shown as total number of reads (A) and without bacteria shown as percentage of abundance (B).

The samples of *T. lutea* revealed ten different taxa of possible contaminants related to the Amoebozoa (true amoeba), Bacillariophyceae (diatoms), Bacteria, Cercozoa (a biodiverse group of microflagellates and amoeba-like microorganisms), Ciliophora (ciliates), Ecdysozoa (animals), Euglenozoa (includes microorganisms related to *Euglena* and *Leishmania*), Chrysophyceae (“golden” microflagellates with sometimes amoeba-like life stages), Fungi and Opalozoa (a heterotrophic clade belonging to the megagroup Stramenopiles, which includes brown algae and diatoms) [74]. When looking at the different taxa, bacteria were identified in every sample, at a lower concentration in the inoculum (2,713 reads) and higher in the photobioreactors (20,000 to 30,000 reads) (**Figure 5A**). Even though the primer pairs were designed to amplify eukaryotic 18S rDNA, fragments from bacterial 16S rDNA can also be amplified, as well as archaeal or eukaryotic genes other than those coding for rRNA. This is a consequence of the need for primers with lower specificity for amplifying a higher diversity of eukaryotic organisms [75,76]. Nevertheless, the bacteriome was not the focus of this study and therefore it was not further analysed. Eukaryotic contamination was not present in the inoculum, which only appeared at higher concentrations in the photobioreactors (from 2,966 to 11,572 reads) (**Figure 5B**).

Contaminants belonging to Amoebozoa, ciliates and Chrysophyceae were present in the samples from the same year (2020), showing a similar pattern of organisms when compared to the sample from the year after (2021), which only had Amoebozoa in common. The most abundant contaminant in 2021 belonged to Euglenozoa (50%). However, in 2020, the most abundant contaminants were Chrysophyceae (77%) and ciliates (88%). The samples from the same day (ETO4 22/7/20) presented similar results, with Chrysophyceae as the main contaminant (around 72%) and ciliates, Bacillariophyta and Amoebozoa with about 16%, 3% and 2% of number of reads, respectively (**Figure 5B**). Therefore, the NGS results seemed to have been reliable due to their congruency. The most abundant zOTUs, Chrysophyceae (zOTU4), ciliates (zOTU9) and Euglenozoa (zOTU28) were chosen for further analysis. Literature research and phylogenetic characterisation were used to find out the most likely candidate causing the culture collapse.

The BLAST results of zOTU4 showed an (E)-value of 2×10^{-56} and 99% of identity to the "golden algae" *Paraphysomonas* (Chrysophyceae). To confirm this result, a phylogenetic analysis was performed on the Chrysophycean contaminant (zOTU4) by comparison with known sequences of the genus *Paraphysomonas* using sequences of the genus *Ochromonas* as outgroup. The zOTU4 contaminant shared a node with a branch support value of 0.82 with *Paraphysomonas longispina* and *Paraphysomonas foraminifera* and, therefore, with this phylogenetic analysis, it was not possible to resolve these two taxa (**Figure 6**). For that reason, zOTU4 might belong to any of these two species or a closely related one. Nevertheless, there are misidentifications of some microalgae classified as *P. foraminifera* [77]. Therefore, the Chrysophycean contaminant has only been identified as belonging to the genus *Paraphysomonas*. The species from this genus are known for being colourless chrysoomonads forming cysts, with numerous silica scales on its cell body only seen by electron microscopy. Moreover, this microflagellate is a known grazer of bacteria, such as *Vibrio natrigens*, and of Haptophyta microalgae such as *T. lutea* and *Pavlova lutheri* [78]. When both preys are present in the same environment, the contaminant will preferably ingest the phytoplankton rather than the bacteria. However, when the bacteria are the only organism, the contaminant will actively prey on it.

For zOTU9, the BLAST results showed an (E)-value of 8×10^{-49} and 100 % of identity for the ciliate *Euplotes*. Therefore, phylogenetic analysis was performed on the zOTU9 contaminant to compare with known sequences of the genus *Euplotes*. Sequences of the family *Aspidiscidae* were used as outgroup. The zOTU9 contaminant did not share a node with any of the sequences used and was clearly separated from *Euplotes magnicirattus* with a branch with

maximum support (**Figure 7**). Ancestral nodes were in general not significant, except for the root node, which showed maximum support, suggesting that this contaminant belongs to the genus *Euplotes* but to a species yet to be described or with a sequence not deposited on the nucleotide databases. Nevertheless, *Euplotes* ciliates have been shown to graze on microalgae such as *Chlorella vulgaris*, *Dunaliella salina*, and *Nannochloropsis salina* and to collapse them in a few days [6]. However, no further analysis was made for zOTU9, since there are several ways to eliminate ciliates, such as quinine sulphate (50 mg/L) and SDS (45 mg/L) [79]. Furthermore, contaminants such as *Euplotes vannus* can easily be inhibited by extracellular secretions produced in a medium from highly concentrated *Nannochloropsis oceanica* cultures, being an example of how to manage biological infections in large-scale cultivation of microalgae using allelopathy [80].

Finally, zOTU28 showed an (E)-value of 2×10^{-57} and 100% of identity with *Euglenozoa* taxa. Therefore, phylogenetic analysis was performed on zOTU28 to compare with known sequences of the phylum *Euglenozoa*. Sequences of the phylum *Heterolobosea* were used as outgroup. The zOTU28 contaminant shared a node with a branch support value of 0.7 with *Diplonemida sp.* and uncultured marine *Diplonemida* (**Figure 8**). For that reason, zOTU28 might belong to the family *Diplonemidae*. The Euglenozoan contaminant has been shown to ingest microalgal species, such as the marine diatom *Coscinodiscus concinnus* [81]. These contaminants are colourless biflagellated organisms with phagotrophic feeding on several types of microalgae and are rarely found to graze on bacteria [82]. However, no further analysis was made for this contaminant, since the biological agent responsible for collapsing the *T. lutea* cultures was not similar to a *Diplonema* flagellate as observed by microscopy.

Scale: 0.01

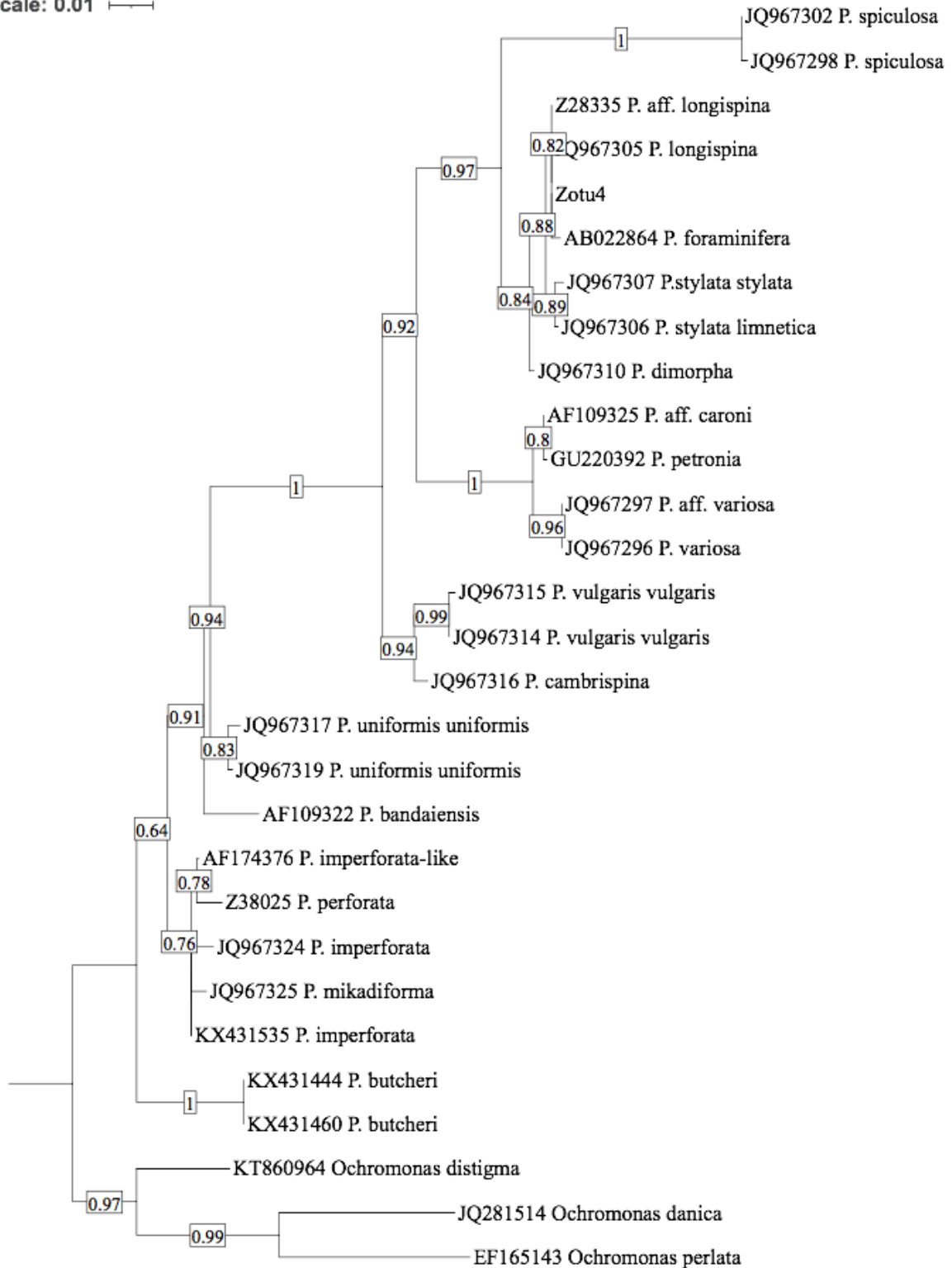


Figure 6: Distance-based (BioNJ) phylogenetic tree of the Chrysophyceae zOTU4 present in highly contaminated cultures of *T. lutea*. Several 18S rDNA sequences belonging to the genus *Paraphysomonas* have been added to determine the root node by means of an outgroup.

Scale: 0.01

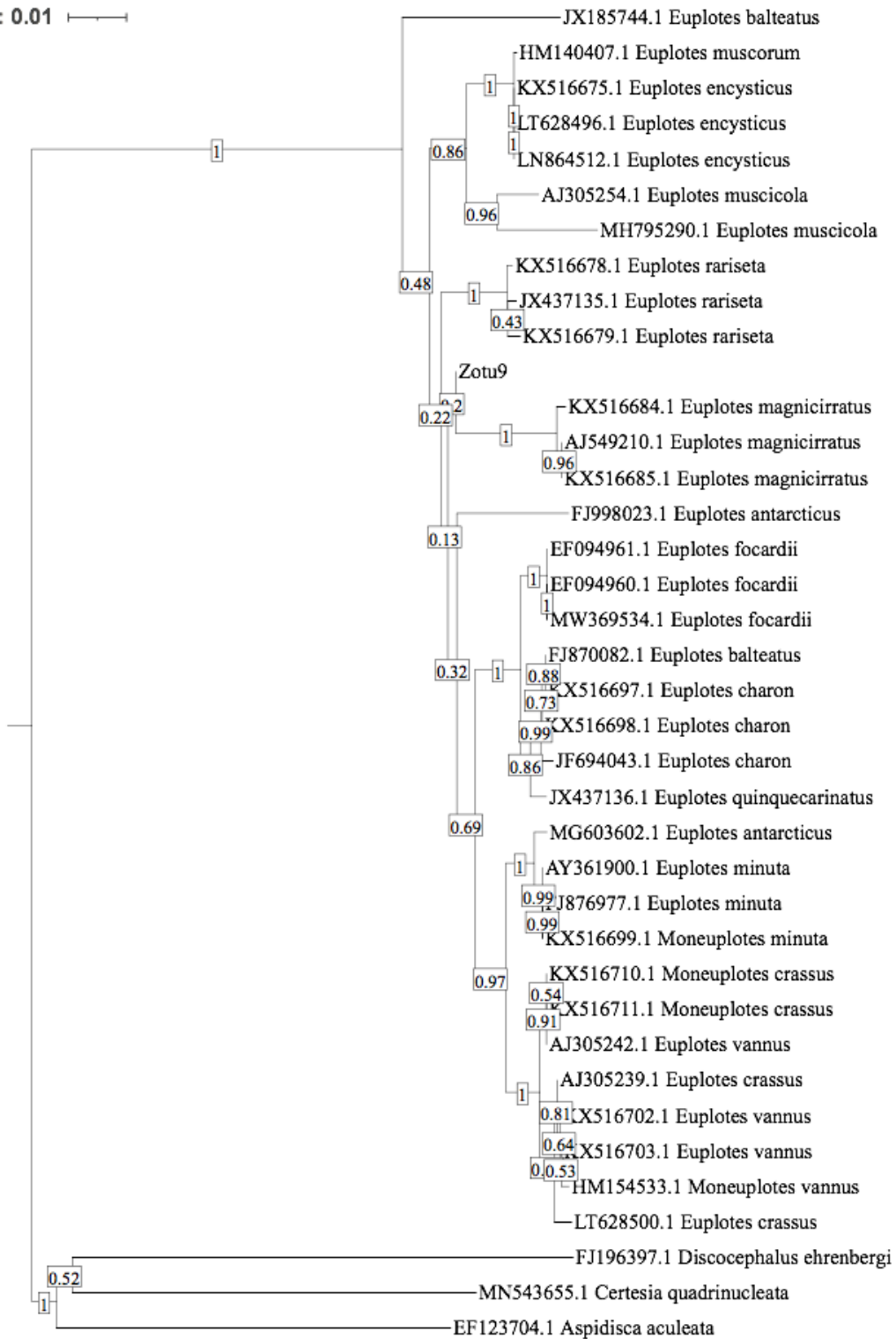


Figure 7: Distance-based (BioNJ) phylogenetic tree of the ciliate zOTU9 present in highly contaminated cultures of *T. lutea*. Several 18S rDNA sequences belonging to the genus *Euplotes* have been added to determine the root node by means of an outgroup.

Scale: 0.2

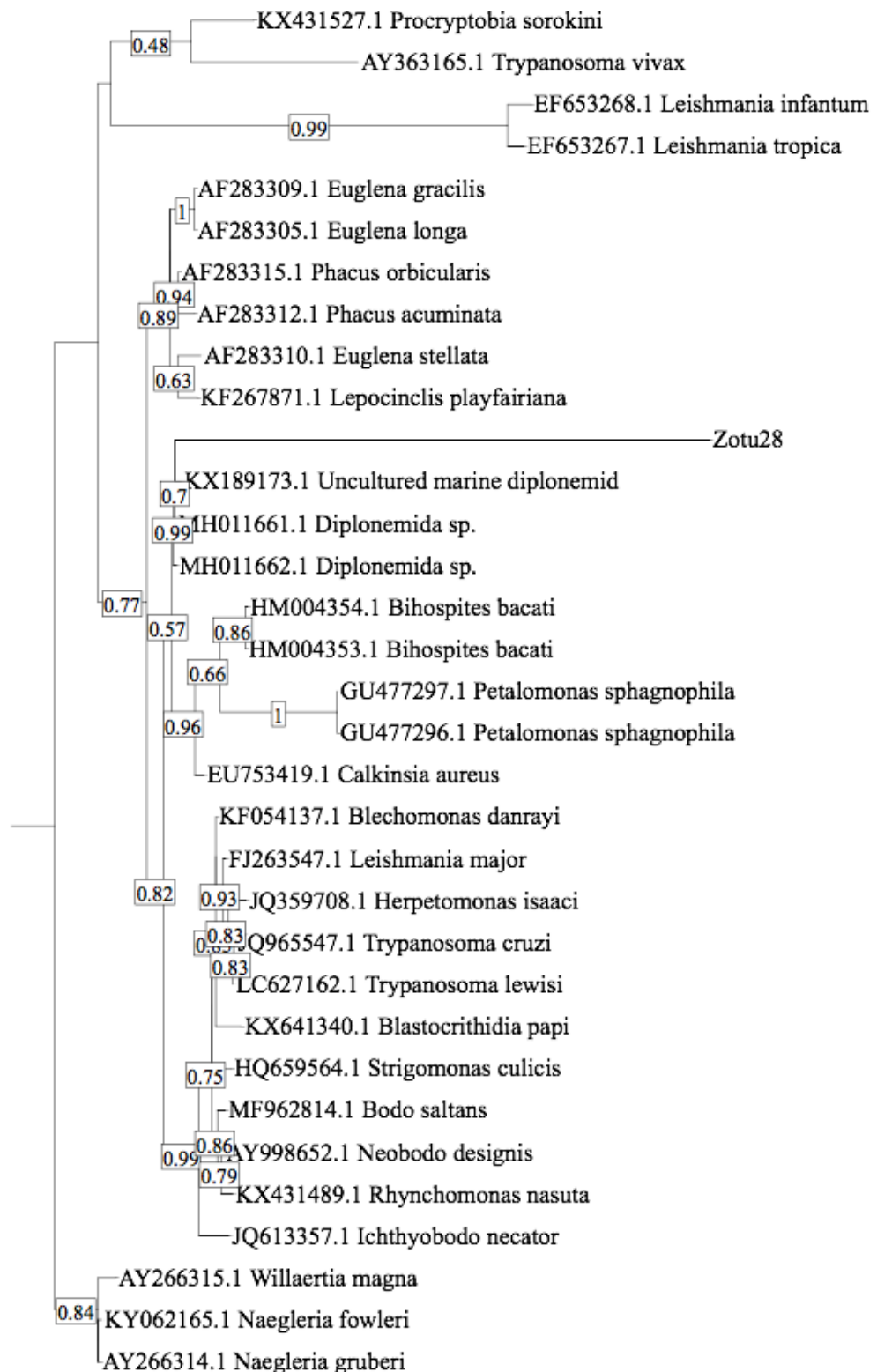


Figure 8: Maximum likelihood (PhyML) phylogenetic tree of the Euglenozoan zOTU28 present in highly contaminated cultures of *T. lutea*. Several 18S rDNA sequences belonging to the phylum *Euglenozoa* have been added to determine the root node by means of an outgroup.

3.1.2. Primer design and optimization

After the phylogenetic analysis and literature research described previously, the Chrysophycean contaminant (zOTU4) revealed to be the main cause of *T. lutea* cultures collapse. Therefore, a further literature research was made in order to find optimized primer pairs which targets Chrysophyceae. However, only one primer pair was found. Therefore, primers were designed in-house, after aligning several *Paraphysomonas* sequences as well as microalgal species using the Qiagen CLC Genomics Workbench (**Table 6**). The primers were then tested with standard PCR conditions and extracted DNA samples of four different microalgal cultures as well as the four contaminated cultures of *T. lutea*.

Table 6: List of contaminant-specific 18S primers developed for *T. lutea* contaminant.

Name	Sequence 5'-3'	Characteristics			Ref.
		Tm (°C)	GC content (%)	Amplicon length (bp)	
Chryso_240	GGAAACCAATCCA GGGC	55.2	59	500	[83]
Chryso_651	CTATTTTACTCAC AGTAAATGACGAA	56.9	31		
Paraphysomonas_1F	CTATACTGTGAAA CTGCGAATGGC	61	46	1,000	In-house
Paraphysomonas_1R	CCCGAAAGTATAA ATATCACAGTCC	59.7	40		
Paraphysomonas_1376F	TTAGAGGGACTTT CGGTGACT	57.9	48	200	In-house
Paraphysomonas_1549R	TCTATCCCTAACA CGATACACA	56.5	41		

The first primer pair (Chryso_240/Chryso_651) had an expected band size of 500 bp. However, an amplicon of more than 500 bp appeared in samples from a highly contaminated photobioreactor (ETO4 22/7/20) (**Figure 9A**). A likely reason for this is due to GelRed, which is a large molecule that binds to DNA and is known to retard the migration of amplicons, making them appear larger in terms of molecular size [67]. In order to increase the intensity of the bands and test the primer pair, further optimizations were made. The first change was the annealing temperature, which was decreased from 60 to 55°C, in order to improve the specificity of the amplification. The same amplicon of about 500 bp appeared in the highly contaminated samples, however, additional bands of higher molecular length (>1,000 bp) also appeared (**Figure 9B**). When the number of cycles was increased to 35, even more amplification products were generated. However, several bands with different sizes became visible, indicating the amplification of unspecific regions of the genome(s) present in the sample (**Figure 9C**). To further increase the specificity, the annealing temperature was increased from 55 to 62 °C. The final result was a multiband pattern (**Figure 9D**), which showed that the selected primer pair was not specific enough in order to detect the target contaminant. For that reason, no further optimizations were made. Nevertheless, the target sequence of 500 bp was amplified in one of the highly contaminated samples (ETO4 22/7/20) without other amplicons, suggesting that the primer could bind specifically to the target sequence. The PCR product of the contaminated sample was sent to be sequenced for further analysis.

The second primer pair (Paraphysomonas_1F/Paraphysomonas_1R) assayed resulted into a 1000-bp amplicon, as expected. The first PCR test amplified the 18S rDNA of the *P. tricornutum* sample with a multiband pattern. Similar results were obtained with two samples (ETO3 3/3/21 and ETO4 22/7/20) highly contaminated with *Paraphysomonas*, as scored by microscopy, resulting in a single band (**Figure 10A**). However, the DNA fragment amplified in *P. tricornutum* sample had a length of about 1,000 bp, suggesting that the primer pair was not specific to the contaminant target sequences as it was able to amplify microalgal 18S rDNA as well. Furthermore, it only amplified one of the highly contaminated samples (ETO4 22/7/20), further highlighting its poor reliability. Therefore, no further analysis was made.

The third primer pair (Paraphysomonas_1376F/Paraphysomonas_1549R) assayed had an amplicon with an expected molecular length of 200 bp. The first PCR test resulted, however, in the amplification of a multiband pattern with the *P. tricornutum* sample with higher molecular sizes (>500 pb). Conversely, the two highly contaminated samples (ETO4 22/7/20) showed a thick single band with the expected size (**Figure 10B**). In fact, this 200-bp amplicon was obtained with all contaminated samples. Therefore, this primer pair seemed to be a suitable

candidate to target *Paraphysomonas*. Further optimizations were made, starting with an increase in the number of cycles to 35, in order to allow the generation of more amplification products and test the specificity of the primer. A multiband pattern appeared in all samples except for the highly contaminated sample (ETO4 22/7/20) (**Figure 10C**). Therefore, the annealing temperature was increased from 55 to 58°C, resulting in single amplicons with the expected size in all contaminated samples (**Figure 10D**), suggesting that the primer pair was specific for the target contaminant. For that reason, the third primer pair was selected for further analysis using the optimized PCR conditions (**Table 7**).

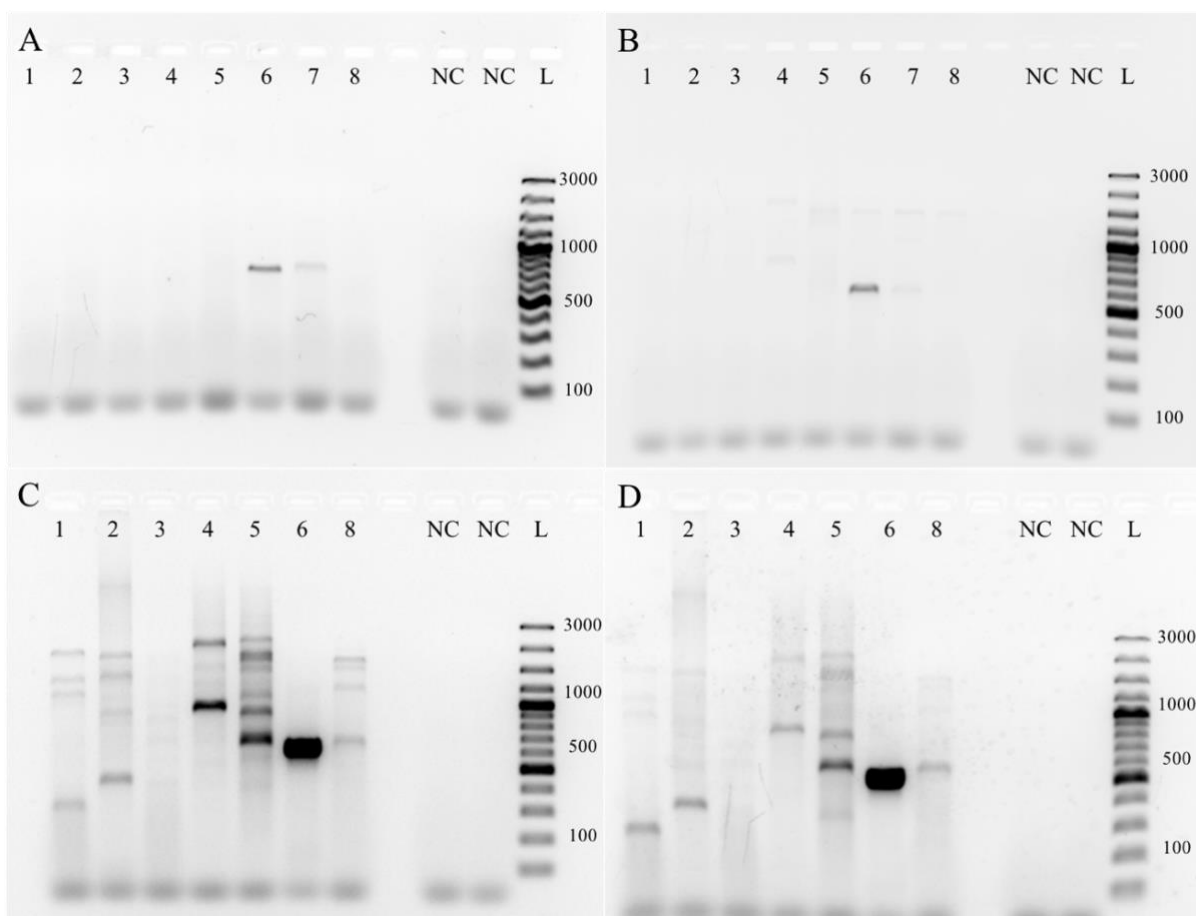


Figure 9: Optimization steps from amplification products of *Paraphysomonas* 18S rDNA using the primer pair Chryso_240/Chryso_651 from DNA of different microalgal samples, namely 1) *Tetraselmis chui*, 2) *Chlorella vulgaris*, 3) *T. lutea* and 4) *P. tricorutum* as well as of *T. lutea* samples contaminated with *Paraphysomonas* sp.: 5) ETO3 3/3/21, 6) ETO4 22/7/20, 7) ETO4 22/07/20 and 8) PBR4 22/07/20. Samples of the negative control (NC) and of the 100-bp DNA ladder (L) were also loaded on the gel.

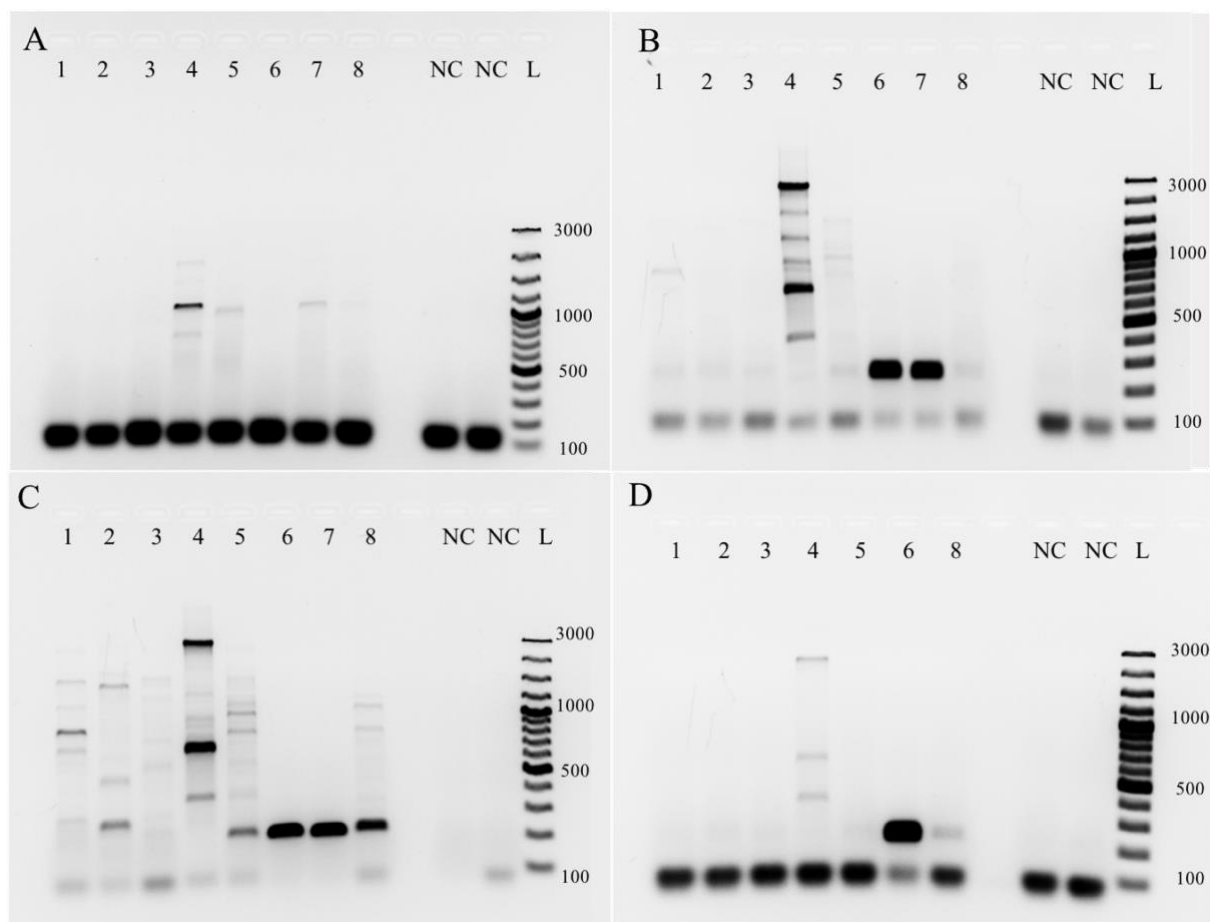


Figure 10: Optimization steps from amplification products of *Paraphysomonas* 18S rDNA using the primer pair Paraphysomonas_1F/Paraphysomonas_1R (A) and the primer pair Paraphysomonas_1376F/Paraphysomonas_1549R (B, C and D); from DNA of different microalgal samples, namely 1) *Tetraselmis chui*, 2) *Chlorella vulgaris*, 3) *T. lutea* and 4) *P. tricornutum*, as well as of *T. lutea* samples contaminated with *Paraphysomonas* sp.: 5) ETO3 3/3/21, 6) ETO4 22/7/20, 7) ETO4 22/07/20 and 8) PBR4 22/07/20. Samples of the negative control (NC) and of the 100-bp DNA ladder (L) were also loaded on the gel.

Table 7: Optimized PCR conditions of the third primer pair.

Steps	T (°C)	Time (min)	Cycles
Denaturation	94	5	-
Denaturation	94	0.5	35
Annealing	58	0.5	
Extension	72	1	
Extension	72	10	-

Once the PCR conditions were optimized, a sensitivity test was made. Several DNA dilutions of the least and the most contaminated samples ETO3 3/3/21 and ETO4 22/7/20, respectively, in order to find out the limit of detection of the selected primer pair. It was possible to detect *Paraphysomonas* at a relative abundance as low as 0.0049% (

Figure 11). Furthermore, the detection limit was even lower than what was found from NGS (0.07%), which makes the Paraphysomonas_1376F/Paraphysomonas_1549R a very specific and sensitive primer pair for the detection of *Paraphysomonas*.

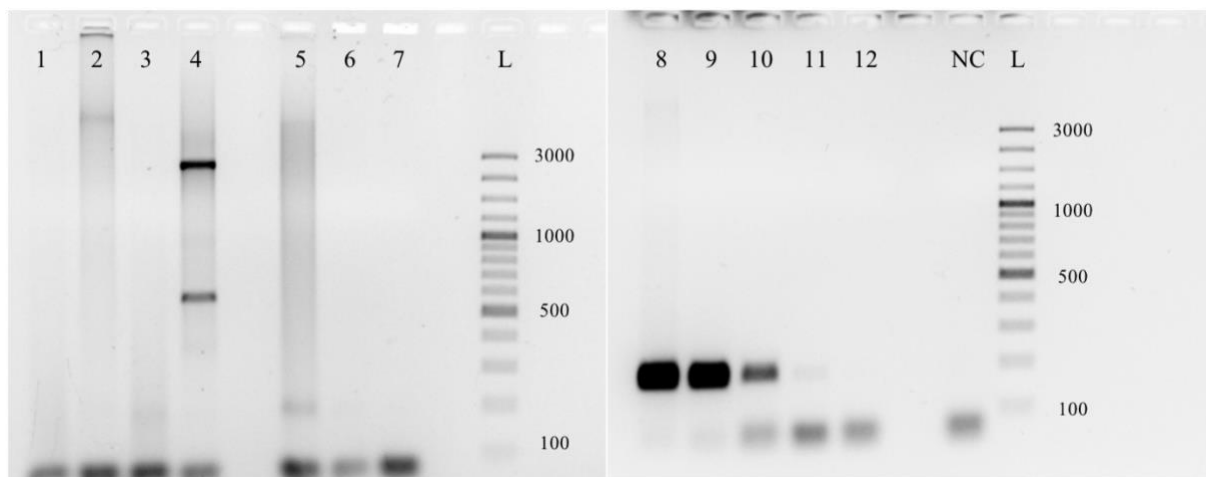


Figure 11: Amplification products of *Paraphysomonas* 18S rDNA using the primer pair Paraphysomonas_1376F/Paraphysomonas_1549R from DNA of different microalgal samples, namely 1) *Tetraselmis chui*, 2) *Chlorella vulgaris*, 3) *T. lutea* and 4) *P. tricorntutum*, as well as of *T. lutea* samples contaminated with *Paraphysomonas sp.* (% of relative abundance): 5) ETO3 3/3/21 (0.07), 6) ETO3 3/3/21 (0.0028), 7) ETO3 3/3/21 (0.000112), 8) ETO4 22/07/20 (77), 9) ETO4 22/07/20 (3.08), 10) ETO4 22/07/20 (0.1232), 11) ETO4 22/07/20 (0.004928), 12) ETO4 22/07/20 (0.00019712), negative control (NC) and 100 bp ladder (L).

3.1.3. Life cycle of contaminant

In order to study the life cycle of the chrysophyte able to cause the collapse of *T. lutea* cultures, light microscope observations were performed every day by pipetting only 4 μ L of culture to the microscope slide in order to fixate the larger cells with the cover slip, without the addition of chemicals. For cell counting, only 1 μ L/L of Lugol's solution (1%) was used in order to fixate and differentiate all of the contaminant cells from the microalgae. Following several weeks of microscopic observation, different life stages of the *Paraphysomonas* chrysophyte, present in *T. lutea* cultures, were identified.

After being inoculated in new media, the first stage seen under light microscope were small flagellated cells of about 2 μ m of length, incapable of feeding on *T. lutea*, most probably

due to the larger size of the prey (**Figure 12A**). Subsequently, the chrysophyte started to develop into flagellated amoeba-like cells of about 15-20 μm , which are capable of feeding on several microalgae (**Figure 12B-E**). Once the culture collapsed, and there were no microalgae left, the flagellated amoeba-like cells became smaller, about 10-15 μm , and started feeding on each other (**Figure 12F**). Some days after the collapse, the contaminants started to disappear and only cell detritus were visible under the microscope. However, when a collapsed culture was used as inoculum for a fresh culture of *T. lutea*, the contaminant was able to grow again. This result suggests that a resistant form is retained in these cultures, most likely in the form of cysts, but they might be, nevertheless, too small or too infrequent to be readily visible by microscopy.

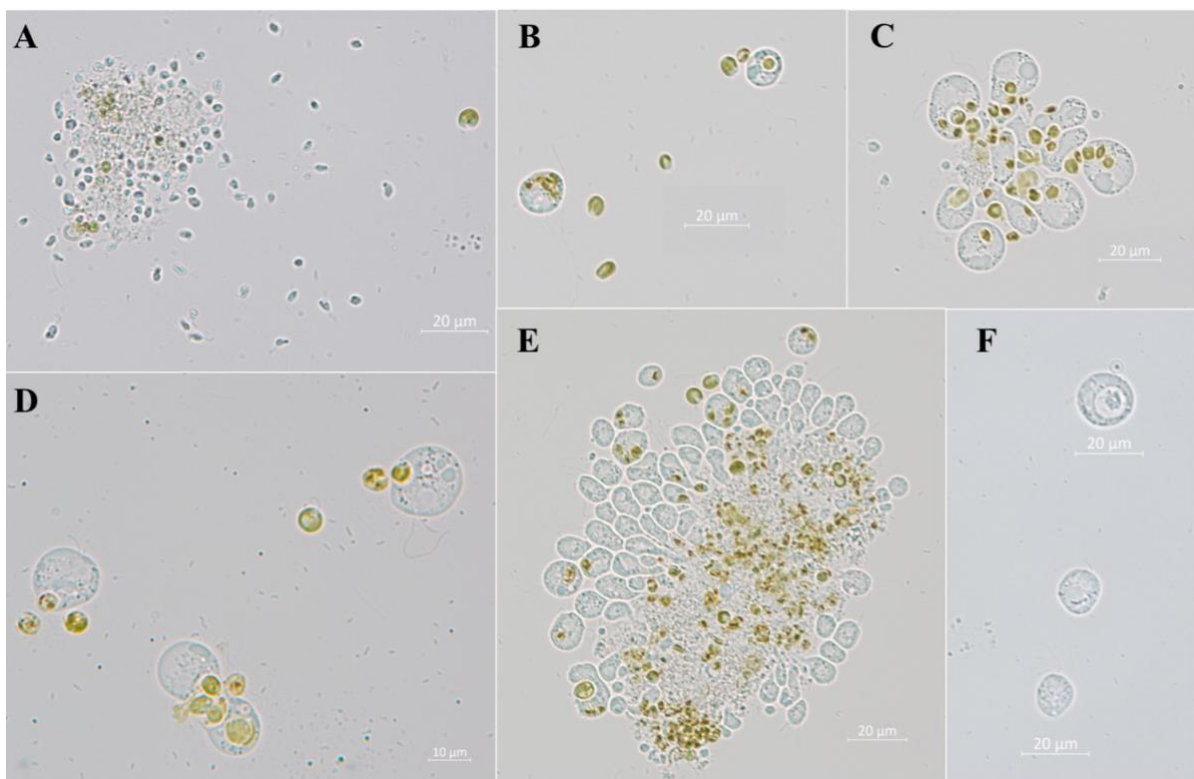


Figure 12: Life stages of the flagellated *Paraphysomonas sp.*, feeding on *T. lutea*: small flagellated cells (A); large flagellated amoeba-like cells feeding on microalgae (B, C, D and E); and medium flagellated amoeba-like cells feeding on themselves (F).

Indeed, *Paraphysomonas* has been shown to graze on several phytoplankton species as well as bacteria, and when there was no food left, grazed on themselves [84]. It was also shown the ability to produce resting stage cells named stomatocysts, formed endogenously and species-specific. This ability allows cells to survive in adverse environmental conditions and to disperse around the world. Apart from the cyst formation, their heterotrophic capacity, small

size and rapid growth are characteristics that enable these microscopic predators to outcompete other species [70]. This may explain why the detection of this contaminant is always attained at a too late stage, precluding any measures for saving the microalgal culture in time. Therefore, molecular methods might be once more a viable strategy to provide an early detection methodology of the grazer, being also a more practical method to readily identify the culture-collapsing microorganism.

Within the family Paraphysomonadaceae, there are only four silica-scaled genera, one of which is the genus *Paraphysomonas*. Species from this genus have been described as colorless heterotrophic free-swimming chrysophytes, with spherical, oval or elongated shape [77]. The two important characteristics of this genus are the silica scales and the flagella. These organisms are covered by silica scales, about 0.5-1.02 μm in diameter, only visible under electron microscope, which have a species-specific morphology. Furthermore, cells possess one longer flagellum with tubular hairs and one shorter, smoother flagellum, with about 4.9-12 and 1.8-2.7 μm of length, respectively [85].

To analyze the capacity of the contaminant to collapse the microalgal culture, three different collapsed cultures were tested. For this experiment, *T. lutea* was inoculated with cultures of *Paraphysomonas* with different lifetimes, as described **above**. The one-, two- and three-week-old *Paraphysomonas* cultures used for this experiment had several medium-sized flagellated amoeba-like cells feeding on themselves, few medium-sized flagellated amoeba-like cells and with only cell detritus visible, respectively.

The first culture of *T. lutea* to collapse was the one-week-old culture (**culture C**), which exhibited a significantly cell count decrease, from 5×10^6 cells to 2×10^6 cells/mL between day 2 and day 4, respectively, showing the collapse of the culture upon two days after the inoculation. The second culture to collapse was the two-week-old (**culture B**), which significantly decreased from 7×10^6 cells to 2×10^6 cells between day 4 and day 7, respectively, collapsing after seven days. The third microalgal culture did not collapse after 21 days of growth, representing the same exponential growth curve as the negative control (**culture A**). However, it was expected that the three-week-old would collapse after 10 days, following the behaviour of the previous cultures (**Figure 13**).

Such result suggests that there was too little number of cysts present in the last contaminated culture used to inoculate *T. lutea* with this chrysophycean predator. Indeed, even though 1 mL of the three-week-old culture was taken as inoculum, it most probably did not contain enough cysts to outgrow and collapse *T. lutea* culture within 21 days of the experiment. To conclude, this experiment demonstrated that if present in lower amounts, or in its resting

stage (cysts), *Paraphysomonas* is not capable to collapse an actively growing microalgal culture in 21 days. Nevertheless, when a culture of fresh *T. lutea* was inoculated into a new photobioreactor, it collapsed after 3 to 4 days. Therefore, a considerable number of cysts able to resist the cleaning chemicals used to sterilize the photobioreactor must remain in a sediment or between pipe joints, where it is not possible to clean, rapidly developing into its flagellate stage and overpowering the microalgal culture.

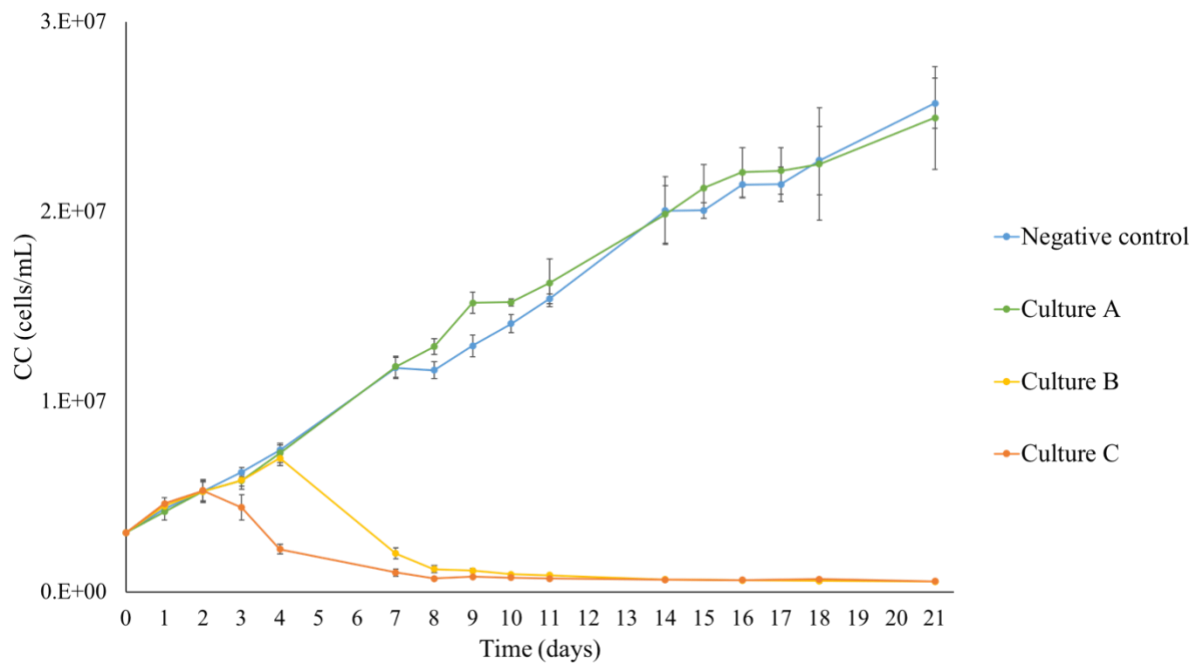


Figure 13: Growth curve of *T. lutea* cultures without contaminant (Negative control) and inoculated with contaminated cultures: three-week-old (Culture A); two-week-old (Culture B); and one-week-old (Culture C). $n=3$, mean \pm SD.

3.1.4. Growth and mitigation trials

Following the study of the life cycle of *Paraphysomonas*, several mitigation strategies were tested in order to control or eliminate the contaminant without harming *T. lutea*. Both contaminant and microalgal growth were followed in order to understand how the mitigation affected them. It was possible to see the start and the complete collapse of the culture by scoring it visually through the colour of the microalgal culture, as its original brown colour (**Figure 14A**) turned into a yellowish hue (**Figure 14B**), becoming fully transparent at a later stage (**Figure 14C**). As described **above**, CC was correlated with OD in order to measure the cell concentration of *T. lutea* cultures (**Figure A1**). Therefore, OD₇₅₀ was measured and the formula obtained with the correlation was used to express the results in cells/mL.

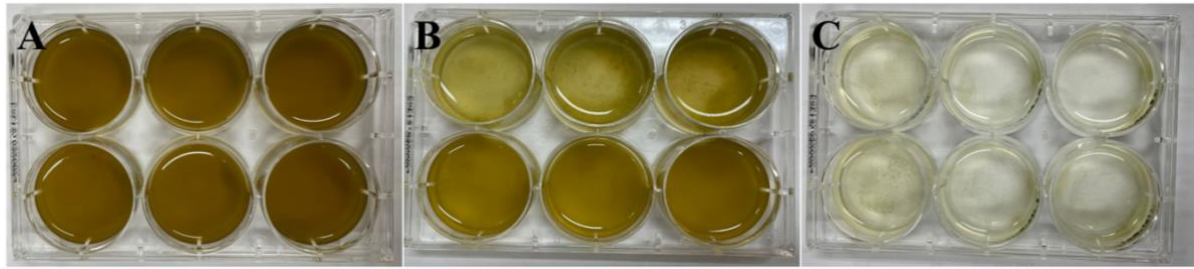


Figure 14: 6-well plates trials with *T. lutea* cultures contaminated with *Paraphysomonas*. A) healthy culture, B) culture at its early stages of collapse and C) fully collapsed culture.

As the first mitigation strategy, different measures of environmental pressure were tested, since the conditions are easy to control and are more cost-effective. Therefore, preliminary trials were performed with increased salinities, namely 60 and 80 ppt as compared to the control condition of 33 ppt. Cultures were incubated for 7 days, in order to identify which conditions might inhibit the growth of the contaminant. For this purpose, *T. lutea* culture inoculated with *Paraphysomonas* and at a salinity of 60 ppt displayed similar growth to that of the uncontaminated *T. lutea* culture (**negative control**), suggesting that this mitigation measure could be successfully used to control the contaminant. Moreover, the culture with a salinity at 80 ppt did not collapse; however, *T. lutea* cells looked stressed and became smaller. Thus, even though high salinity seemed to be a promising mitigation strategy, it did compromise the growth of the microalgal culture, suggesting that other options should be explored. Based on previous reports of the genus *Paraphysomonas*, strains were mainly found in freshwater environments, and few species were found in brackish or marine environments with salinities lower than 35 ppt, which might explain the sensitivity of this strain to high salinity [70]. On the other hand, *T. lutea* is known to be a halotolerant species, growing in environments with a salinity range of 35-75 ppt, which correlates well with results found in this study [86].

The next trials were performed, repeating the trials at lower salinities, but using chemical mitigation strategies as well to find out the optimal concentration inhibiting the contaminant development and proliferation. Trials were performed in 6-well plates to be able to test 2 different concentrations in biological triplicates in one plate and, therefore, assaying several mitigation agents at the same time under the same biological conditions. The growth curve of all cultures of *T. lutea* were analysed for 6 days (**Figure 15**). The culture without the presence of *Paraphysomonas* (**negative control**) started with a *T. lutea* cell concentration of 5×10^6 cells/mL, exhibiting a lag phase from day 0 to day 2 with no significant increase in the number of cells. Between day 2 and 3, the culture entered the exponential phase with a significant increase of the microalgal number of cells from 7×10^6 to 1.6×10^7 cells/mL. After

day 3, *T. lutea* reached the stationary phase with no significant increase in cell number, leading to a cell concentration of 1.9×10^7 cells/mL on day 6. Overall, *T. lutea* cultures without contamination had a healthy growth with a dark brown colour (**Figure 14A**). The culture with the presence of *Paraphysomonas* (**positive control**) did not show a significant increase in *T. lutea* cell concentration during the 6-day experiment. Indeed, flagellated amoeba-like cells feeding on *T. lutea* started to appear on day 2 accompanied by the change of the culture appearance from a brown to a yellowish colour (**Figure 14B**). On day 6, no microalgae were seen by microscopy and the cultures became transparent (**Figure 14C**). However, upon the cell concentration of *T. lutea* obtained from the correlation curve, there were 3.8×10^6 cells/mL on day 6. Interestingly, these results show how unreliable OD₇₅₀ measurements are when a mixed culture is analysed. In fact, OD measures the light scattering caused by every particle present in the sample, which includes cell detritus of lysed cells or contaminant cells. Therefore, any attempt at correlating OD with the cell count might result in estimated cell concentrations that never reach 0 cells/mL.

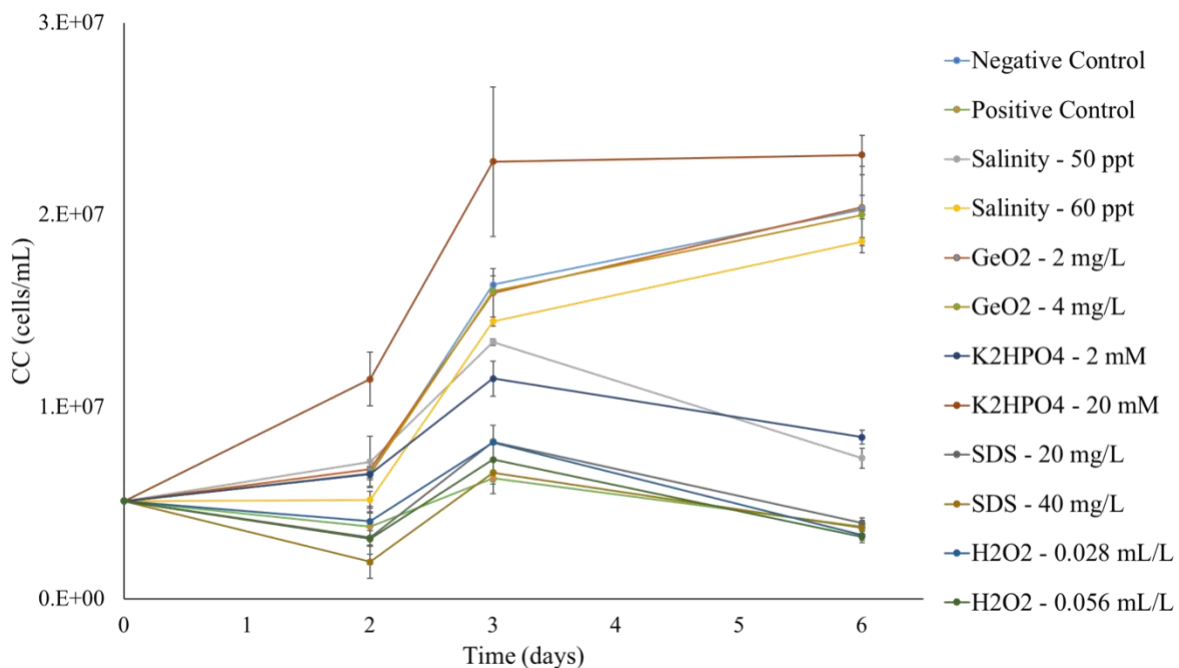


Figure 15: Growth curve of *T. lutea* cultures without (negative control) and with contaminant (positive control). Several mitigation agents such as salinity at 50 and 60 ppt, GeO₂ at 2 and 4 mg/L, K₂HPO₄ at 2 and 20 mM, SDS at 20 and 40 mg/L, H₂O₂ at 0.028 and 0.056 mL/L were tested on the cultures of *T. lutea* with *Paraphysomonas* in order to avoid culture collapse. $n=3$, mean \pm SD.

T. lutea cultures contaminated with *Paraphysomonas* and salinity of 60 ppt had a very similar growth when compared to the negative control, without any significant differences. Few small flagellated cells were visible by microscopy; however, the culture was of dark brown colour (**Figure 14A**). With a salinity of 50 ppt, the culture also had a similar growth to the negative control until day 3. However, a yellowish colour (**Figure 14C**) started to appear and a decrease in *T. lutea* cell counts (7.3×10^6 cells/mL) on the last day became apparent, which was significantly different from that of the negative control. In addition, flagellated amoeba-like cells feeding on *T. lutea* were present in the culture.

The cultures treated with both concentrations of GeO_2 (2 and 4 mg/L) had a very similar growth as the negative control with no significant differences. No contaminants were visible using microscopical observation and the culture displayed a dark brown colour (**Figure 14A**). Germanium dioxide, which belongs to the IV group of the periodic table of elements, possesses no known biological function to any living plant or animal [71]. Nevertheless, it was reported in aquatic environments in a range of 0.07-2.2 mg/L. GeO_2 is a possible substitute for silicon and has been shown to inhibit the growth of diatoms such as *Skeletonema costatum*, at concentrations of 1-10 mg/L, due to their silica frustules [71]. Since the cells of *Paraphysomonas* sp. also contain silica, GeO_2 might be incorporated into its outer cell coverings, leading to cell division arrest or inhibition of its DNA polymerase, therefore compromising the proliferation of this predator [87].

The treatment using 2 mM of K_2HPO_4 had a similar growth to the negative control until day 2, and on day 3, the number of *T. lutea* cells decreased to 1.5×10^7 cells/mL, with a significant difference from the 1.6×10^7 cells/mL of the negative control. Until day 6, the culture collapsed with the appearance of flagellated, transparent amoeba-like cells, resulting in a significantly lower number of microalgae cells when compared to those of the negative control, 8.4×10^6 and 1.9×10^7 cells/mL, respectively. At 20 mM of K_2HPO_4 , the culture had a significant increase of number of cells in all data points when compared to the negative control and did not collapse. However, when seen under the microscope, the microalgae were stressed, smaller and the culture was full of cell detritus. Therefore, the increased number of cells obtained from the correlation curve was an artefact of the OD_{750} measurements that were correlated with the cell number since the presence of cell detritus in the samples can interfere with the measured absorbance. K_2HPO_4 supply is consumed by *Paraphysomonas* and their growth can increase in its natural habitat. However, in culture media, if supplied as the only phosphate, this potassium salt can become toxic for the contaminant. Indeed, previous studies showed the inhibitory effect of dipotassium phosphate on chrysophytes [70]. In this study, the growth of the contaminant

was inhibited by higher concentration of K_2HPO_4 . However, *T. lutea* cells were also affected by this compound.

The treatments with sodium dodecyl sulphate (SDS) and hydrogen peroxide (H_2O_2) at both tested concentrations had no effect on the contaminant, showing growth similar that of the positive control during all of the experiment without any significant differences. Several flagellated amoeba-like cells were visible after 3 days and the cultures became transparent on the last day (**Figure 14C**). Although SDS (8-10 mg/L) is an anionic surfactant that was shown to completely eliminate contaminants such as *Poterioochromonas sp.* and *Hemiurosomoida sp.* from *Chlorella* cultures [72], this chemical was ineffective to inhibit or eliminate *Paraphysomonas*. This observation is most probably related with the outer cell coverings of the contaminant, which is protected by silica scales. Since SDS targets the cell membrane of the cells, it was not effective in controlling *Paraphysomonas*. On the other hand, H_2O_2 is an oxidizing agent through the formation of radicals that can affect carbohydrates, lipids, proteins and nuclei acids. It is known to be effective against several microorganisms, including dormant forms, and it was shown to be effective as a fungicide against the zoosporic chytrid fungi infection in *Haematococcus pluvioalis* cultures at concentrations as low as 0.0028 mL/L [73]. Nevertheless, it was not successful in controlling the development of *Paraphysomonas*, most probably due to the protection afforded by its silica scales.

To conclude this search for a working mitigation strategy, the only agent that was successful in controlling and eliminating *Paraphysomonas* from *T. lutea* cultures were salinity of 60 ppt, and GeO_2 at 2 and 4 mg/L. These treatments were successful in mitigating the development and proliferation of the contaminant while sustaining the normal growth of *T. lutea*. Other studies correlate with these results, since it was previously reported that *P. vestita* is capable of growing at high salinities; however, for this particular species, the predatorial cells became immobile under these stressful conditions. In addition, these results are consistent with the fact that GeO_2 inhibits the growth of diatoms by competing with frustule-building enzymes for silicon [87]. The cultures with the treatments K_2HPO_4 at 2 mM, salinity of 50 ppt, SDS and H_2O_2 at both concentrations were not successful in controlling or mitigating the growth of *Paraphysomonas*.

A second 6-day experiment was made with the same treatments, however, at different concentrations of the mitigating agents, though using the same culture conditions as the previous. Salinity of 60 ppt, GeO_2 at 2 mg/L and K_2HPO_4 at 20 mM were tested once more as well as lower concentrations of each. H_2O_2 was tested at the same concentrations, though being added to the culture every day (**Figure 16**). The culture without the presence of

Paraphysomonas (**negative control**) started with a *T. lutea* cell concentration of 5×10^6 cells/mL and had a lag phase from day 0 to day 3 with no significant increase in the number of cells. Between day 3 and 6, the culture grew exponentially with a significant increase in the number of microalgal cells, from 3×10^6 to 1×10^7 cells/mL on the last day, with a dark brown colour (**Figure 14A**). The culture with the presence of *Paraphysomonas* (**positive control**) had a similar growth from day 0 to day 1 to the negative control. However, a significant decrease occurred from day 1 to day 3 with microalgal cell concentrations dropping from 5.8×10^6 to 1.6×10^6 cells/mL, when flagellated amoeba-like contaminants feeding on *T. lutea* started to appear. On day 6, no microalgae were seen under the microscope and the culture was transparent (**Figure 14C**) with a significant theoretical decrease of *T. lutea* cells to 8.8×10^5 when compared to day 0; however, no microalgae cells were seen under the microscope.

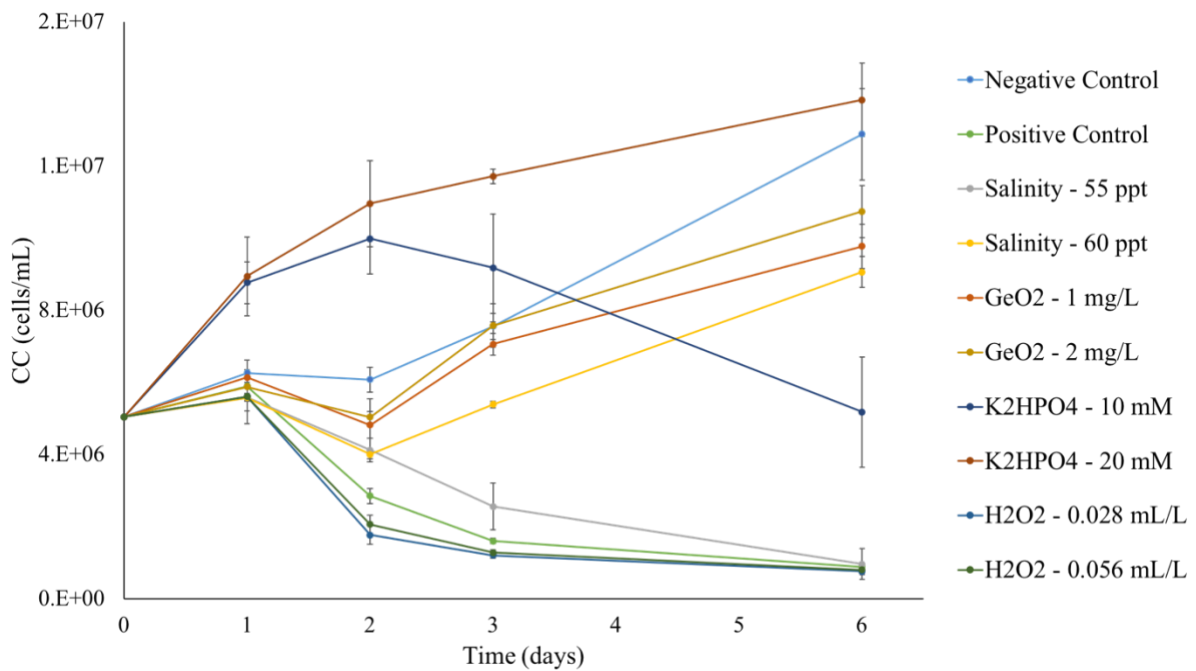


Figure 16: Growth curve of *T. lutea* cultures without (negative control) and with contaminant (positive control). Several mitigation agents such as salinity at 55 and 60 ppt, GeO_2 at 1 and 2 mg/L, K_2HPO_4 at 10 and 20 mM, SDS at 20 and 40 mg/L, H_2O_2 at 0.028 and 0.056 mL/L were tested on the cultures of *T. lutea* with *Paraphysomonas* in order to avoid culture collapse. $n=3$, mean \pm SD.

During the experiment, *T. lutea* cultures contaminated with *Paraphysomonas* treated with increased salinity (60 ppt) and both concentrations of GeO_2 (1 and 2 mg/L) had a similar growth when compared to that of the negative control without any significant differences. No

contaminants were visible by microscopy and the cultures were dark brown (**Figure 14A**) with around 1×10^7 cells/mL of *T. lutea* on the last day.

The treatment using 20 mM of K_2HPO_4 had a similar result from the last experiment, with higher values in all off the data points. Even if there were no significant differences from the negative control on the last day, the culture was full of cell detritus and the microalgae were stressed. The culture treated with K_2HPO_4 at 10 mM had an overall growth significantly different from the other cultures. Until day 2, this culture had a similar growth with no significant differences from the culture treated with K_2HPO_4 at 20 mM, reaching 1×10^7 cells/mL of *T. lutea* with many cell debris seen under the microscope. However, after day 2 until day 6, the culture decreased significantly with the presence of flagellated amoeba-like cells feeding on *T. lutea* until a microalgal cell concentration of 5×10^6 cells/mL with a transparent culture on the last day (**Figure 14C**).

The cultures treated with salinity of 55 ppt and H_2O_2 at both concentrations had a similar growth when compared to the positive control, with no significant differences. Several flagellated amoeba-like cells with a significantly decrease of *T. lutea* cells from 5.6×10^6 to 2×10^6 cells/mL on day 2, with the collapse of the cultures until the last day (**Figure 14C**).

Therefore, the only mitigations successful to control and eliminate the *Paraphysomonas* in *T. lutea* cultures were once more salinity of 60 ppt and GeO_2 from 1 to 4 mg/L. These treatments were successful to control the development and proliferation of the contaminant and maintain normal growth of *T. lutea*. The treatments with K_2HPO_4 did not mitigate the contaminant, resulting in a culture with microalgae with a stressed phenotype and many cell debris. The cultures with the treatment salinity below 60 ppt, SDS and H_2O_2 were not successful in controlling or mitigating *Paraphysomonas* either.

With these results, a third experiment was performed with the same cultures conditions for 3 days (**Figure 17**). The limitation of using high salinity became once again apparent, as a salinity of 60 ppt did not prevent the contaminant from growing and collapsing the culture. Therefore, GeO_2 was also tested at concentrations of 0.25 and 0.5 g/L to determine the lowest effective concentration of this mitigation agent. Furthermore, a combination between the two treatments was tested in order to change as little as possible the culture conditions. Therefore, salinity of 45 ppt was tested with the addition of the aforementioned concentrations of GeO_2 . The culture without the presence of *Paraphysomonas* (**negative control**) started with a *T. lutea* cell concentration of 2×10^6 cells/mL and had an exponential growth from day 0 to day 3, reaching 8×10^6 cells/mL and a dark brown colour on the last day (**Figure 14A**). The culture with the presence of *Paraphysomonas* (**positive control**) had a similar growth from day 0 to

day 1 from the negative control. However, a significant decrease occurred between day 1 and day 3 with the microalgal cell concentration dropping from 3.3×10^6 to 8×10^5 cells/mL when flagellated amoeba-like contaminants feeding on *T. lutea* started to appear and the culture turned yellowish (**Figure 14B**).

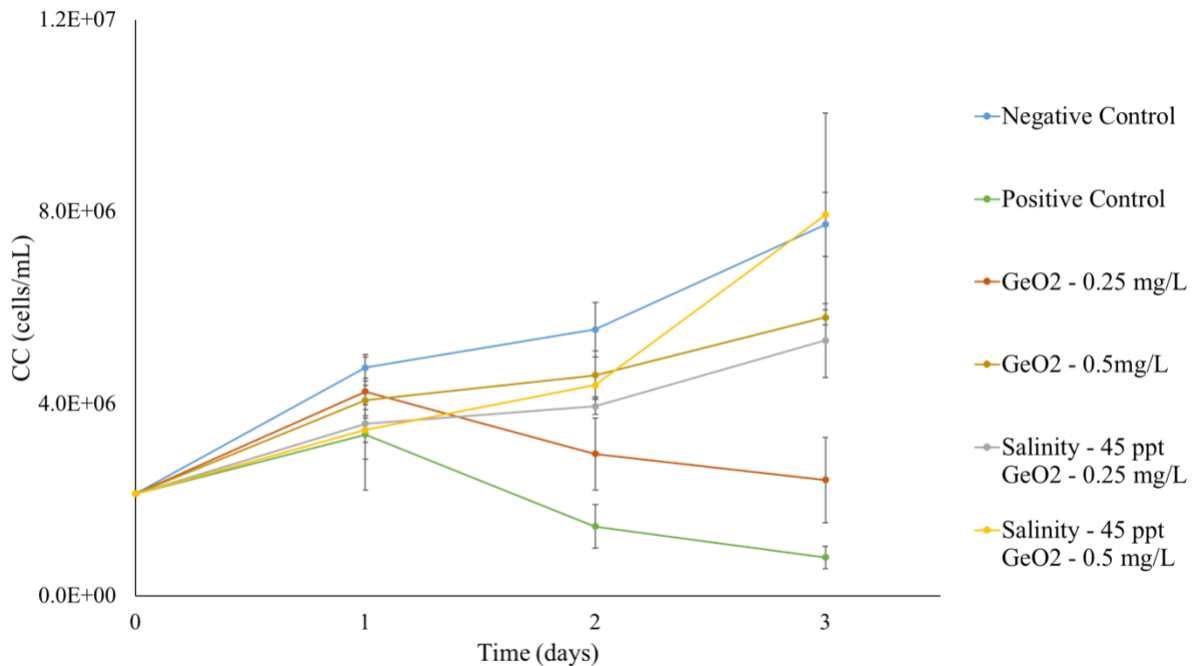


Figure 17: Growth curve of *T. lutea* cultures without (negative control) and with contaminant (positive control). Several mitigation agents such as GeO₂ at 0.25 and 0.5 mg/L, salinity at 45 with GeO₂ at 0.25 and 0.5 mg/L were tested on the cultures of *T. lutea* with *Paraphysomonas* in order to avoid culture collapse. $n=3$, mean \pm SD.

T. lutea cultures contaminated with *Paraphysomonas* treated with GeO₂ at 0.25 mg/L had an overall similar growth to that of the positive control, however, with significant differences. On the last day, the culture presented a higher *T. lutea* cell concentration of 2.4×10^6 cells/mL when compared to that of the positive control (8×10^5 cells/mL); however, some flagellated amoeba-like cells feeding on microalgae could be observed and the culture turned yellowish (**Figure 14B**). The cultures treated with GeO₂ at 0.5 mg/L alone or with a higher salinity of 45 ppt combined with 0.25 mg/L of GeO₂ presented the same growth without significant differences between them. However, on day 3, these cultures had a significantly lower number of *T. lutea* cells (around 6×10^6 cells/mL) when compared to that of the negative control (8×10^6 cells/mL) and small flagellated cells of the predator were visible in the culture. Microalgal cultures treated with salinity of 45 ppt and 0.5 mg/L of GeO₂ had a significantly lower number of *T. lutea* cells when compared to the negative control on day 1 and 2. However,

on day 3, the number of *T. lutea* cells increased to 7.9×10^6 cells/mL with no significant differences to that of the negative control, with a dark brown colour (**Figure 14A**).

These results showed that GeO_2 at lower concentrations than 1 mg/L or with a higher salinity of 45 ppt together with the addition of 0.25 mg/L of GeO_2 were not sufficient to control the development and proliferation of the contaminant. However, the combination of salinity of 45 ppt and 0.5 mg/L of GeO_2 appeared to be sufficient to control the growth of the contaminant and prevent culture collapse.

Thus, it is possible to conclude that three mitigations were successful in controlling the proliferation of the *Paraphysomonas* in 6-well plates, namely very high salinity such as 60 ppt, GeO_2 at 0.5 mg/L with increased salinity (45 ppt), and GeO_2 alone at 1 mg/L. Therefore, additional assays were performed in 100-mL Erlenmeyer flasks in order to assess the impact of these mitigation measures on both microalgae and contaminants upon scale-up. Cell counts of both *T. lutea* cells and *Paraphysomonas* cells, as well as nitrates concentrations were determined. The biomass concentration of *T. lutea* cultures was determined using the OD_{750} measurements performed during the trial and the formula obtained from the correlation curve described **above**, of OD and DW (**Figure A3**).

In the first Erlenmeyer experiment, *T. lutea* cultures were treated with a salinity of 60 ppt for 14 days. The culture of *T. lutea* without contaminant (**negative control**) did not grow significantly during the experiment, remaining in the stationary phase, due to the high cell concentration of the culture being assayed, namely 2×10^7 cells/mL (**Figure 18**). This resulted in a poor consumption of nitrates (**Figure 20**), with a starting value close to that of the growth medium, 11.7 mM. This led to a biomass concentration of 1.7 g/L on day 0 (**Figure 19**) with no significant changes until day 14. However, the culture did consume nitrates, decreasing the levels of this nutrient to 9.6 mM on day 14. The culture of *T. lutea* with contaminant (**positive control**) had no significant growth from day 0 to day 2. Between day 2 and day 4, a significant drop in microalgal cell counts and biomass occurred, from 1.3×10^7 cells/mL and 1.8 g/L to 3.0×10^6 cells/mL and 1.2 g/L, respectively. Concomitantly, the cell counts of the contaminant rose to 2.3×10^6 cells/mL. After the collapse of *T. lutea* on day 7 (**Figure 14C**), the contaminant cell concentration dropped significantly down to 8.8×10^5 cells/mL and on the last day only 1.0×10^5 cells/mL were left. These collapsed cultures showed no significant nitrate consumption during the experiment (≈ 0.5 mM).

The culture of *T. lutea* without contaminant treated with a salinity of 60 ppt (**algae**) showed results similar to those of the negative control throughout the experiment. No significant changes and differences were observed on day 14 regarding the number of cells,

biomass and nitrates, with the culture revealing a dark brown colour (**Figure 14A**). The culture of *T. lutea* with contaminant treated with a salinity of 60 ppt (**algae + contaminant**) had a similar growth to that of the negative control with no significant differences until day 9, reaching *T. lutea* cell and biomass concentrations of 1.1×10^7 cells/mL and 1.9 g/L, respectively. Until day 11, the culture exhibited a significant decrease in microalgal cells and biomass, down to 3.5×10^6 cells/mL and 0.8 g/L, respectively. This was correlated with a surge of contaminants, reaching a concentration of 2.6×10^6 cells/mL of contaminants, which decreased significantly to 7.2×10^5 cells/mL on day 14 (**Figure 14C**). The consumption of nitrates had no significant differences from the negative control.

These results demonstrated that salinity of 60 ppt has no significant effect on the normal growth of *T. lutea* cultures for 14 days. Furthermore, higher salinity was successful to control the development and proliferation of *Paraphysomonas* for 7 more days, when compared to a *T. lutea* culture contaminated without any treatment.

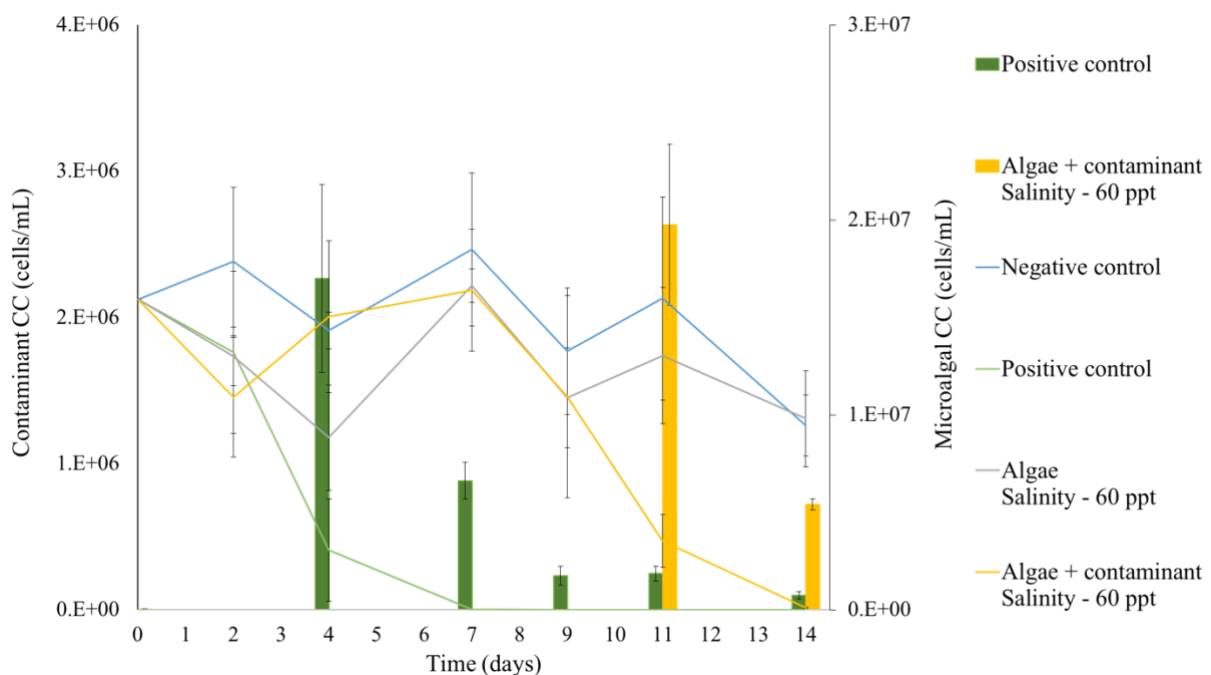


Figure 18: Growth of *T. lutea* (lines) cultures and *Paraphysomonas* contaminant (bars) using cell counts over 14 days of cultivation. Non-contaminated cultures (negative control) and contaminated cultures (positive control) at a standard salinity of 33ppt were compared with treatments at a salinity of 60 ppt. $n=3$, mean \pm SD.

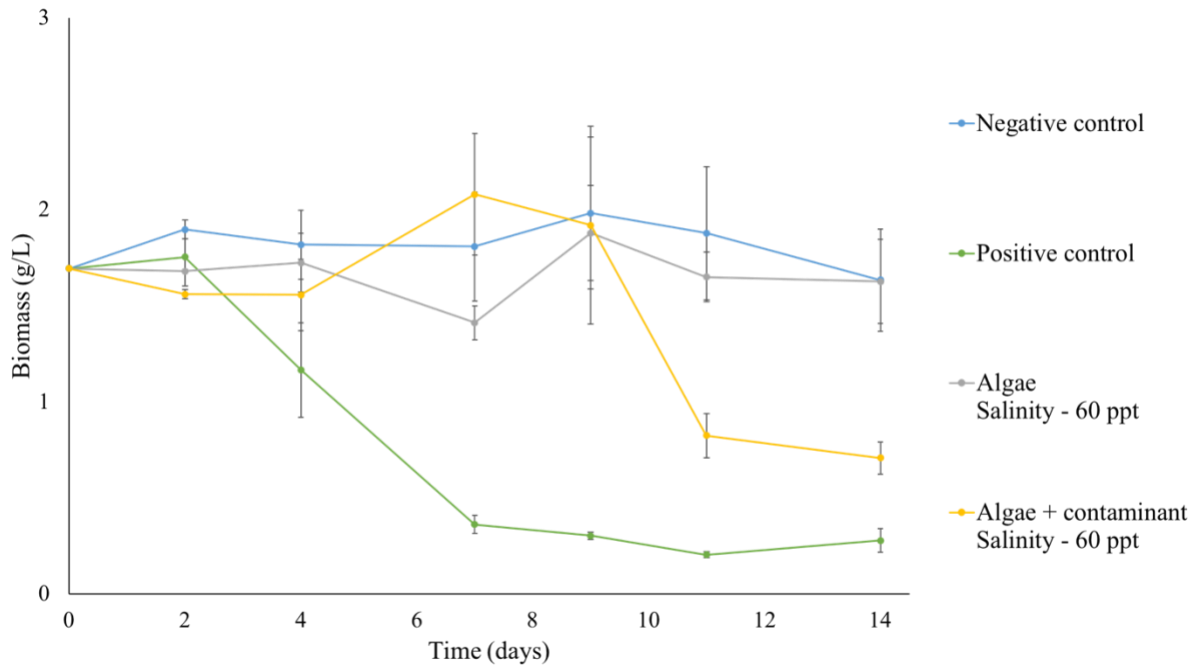


Figure 19: Growth curve of *T. lutea* cultures without (negative control) and with contaminant (positive control). Salinity of 60 ppt was applied to the non-contaminated culture of *T. lutea* (Algae), and cultures with *T. lutea* with *Paraphysomonas* (Algae + contaminant). $n=3$, mean \pm SD.

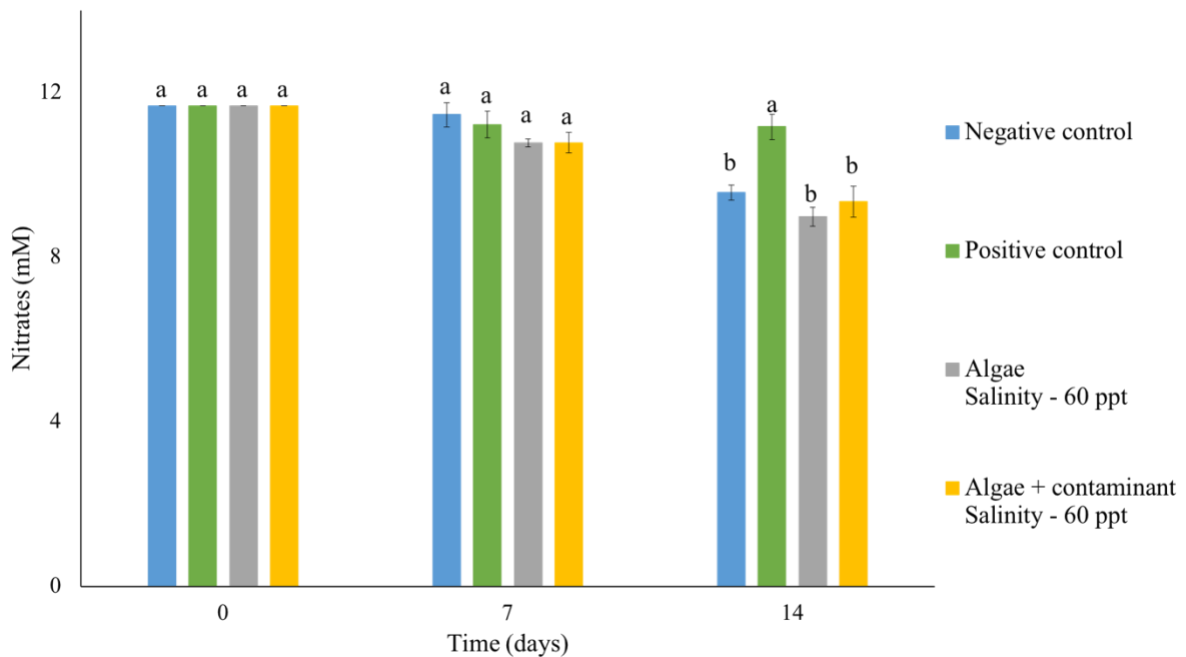


Figure 20: Nitrates measurements of *T. lutea* cultures without (negative control) and with contaminant (positive control). Salinity of 60 ppt was applied to the non-contaminated culture of *T. lutea* (Algae), and cultures of *T. lutea* contaminated with *Paraphysomonas* (Algae + contaminant). $n=3$, mean \pm SD. Different letters over the bars indicate significant differences between samples ($p < 0.05$, ANOVA Tukey).

For the second Erlenmeyer experiment, *T. lutea* cultures were treated with a salinity of 45 ppt and GeO₂ at a concentration of 0.5 mg/L for 7 days under the same culture conditions as used in the previous experiment. The culture of *T. lutea* without contaminant (**negative control**) remained in the stationary phase throughout the experiment due to the initial high concentration of microalgal cells (**Figure 21**) and nitrates (**Figure 23**), 2×10^7 cells/mL and 11.7 mM, respectively, leading to a biomass concentration of 1.7 g/L of on day 0 (**Figure 22**). No significant differences occurred until day 7 for microalgal cell, biomass and nitrates concentrations, with a dark brown colour on the last day (**Figure 14A**). The culture of *T. lutea* with contaminant (**positive control**) had no significant growth from day 0 to day 2. Between day 2 and day 4, a significant decrease in microalgal cell counts and biomass took place, dropping from 1.3×10^7 cells/mL and 1.8 g/L to 3.0×10^6 cells/ml and 1.2 g/L, respectively. This coincided with a rapid increase of *Paraphysomonas* on day 4, displaying cell concentrations as high as 2.3×10^6 cells/mL. On day 7, the cell concentration of the contaminants dropped significantly to 8.8×10^5 , most probably because they ran out of prey as no microalgal cells could be observed (**Figure 14C**). The culture had no significant nitrate consumption during the experiment (0.5 mM).

The culture of *T. lutea* without contaminant treated with a salinity of 45 ppt and GeO₂ at 0.5 mg/L (**algae**) showed results similar to that of the negative control, occurring no significant changes. On day 7, this culture also had a similar concentration of microalgal cells, biomass and nitrates, with a dark brown colour (**Figure 14A**). The culture of *T. lutea* with contaminant treated with salinity of 45 ppt and GeO₂ at 0.5 mg/L (**algae + contaminant**) had a similar growth to that of the negative control with no significant differences until day 4, reaching a microalgal cell concentration of 1.1×10^7 cells/mL and a biomass content of 1.9 g/L. However, contaminants appeared, reaching a cell concentration of 5.7×10^5 cells/mL. Therefore, by day 7, a significant decreased in the microalgal biomass, down to 0.5 g/L, occurred, with the total collapse of the *T. lutea* culture (0 cells/mL), while the cell concentration of the predator rose as high as 1.5×10^6 cells/mL (**Figure 14C**). The consumption of nitrates had no significant differences when compared to that of the negative control.

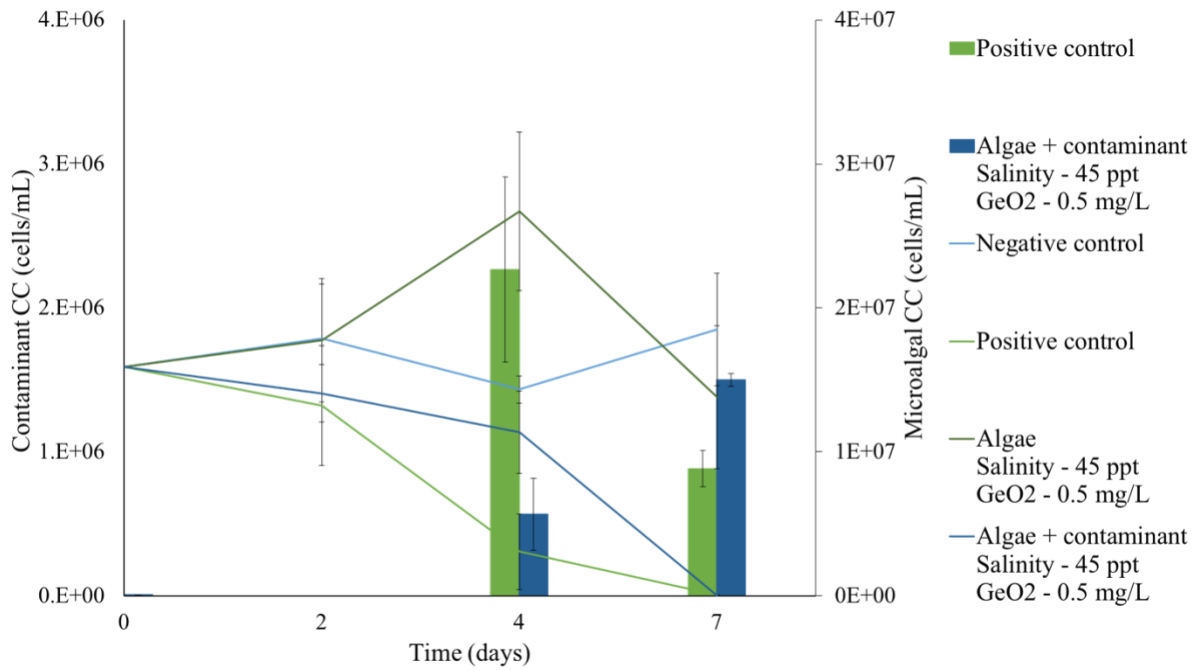


Figure 21: Growth of *T. lutea* (lines) cultures and *Paraphysomonas* contaminant (bars) using cell counts over 7 days of cultivation. Non-contaminated (negative control) and contaminated (positive control) cultures at standard salinity of 33 ppt were compared with treatments at a salinity of 45 ppt and GeO₂ at 0.5 mg/L. $n=3$, mean \pm SD.

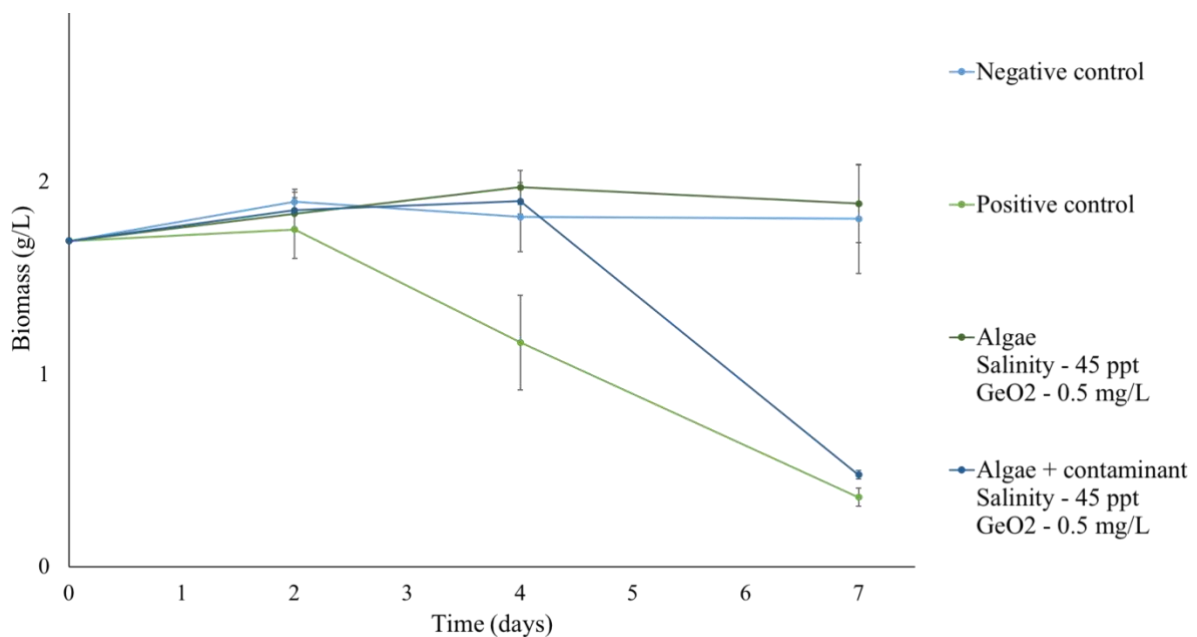


Figure 22: Growth curve of *T. lutea* cultures without (negative control) and with contaminant (positive control). Salinity of 45 ppt and GeO₂ at 0.5 mg/L were applied to the culture of *T. lutea* only (algae), and cultures with *T. lutea* contaminated with *Paraphysomonas* (algae + contaminant). $n=3$, mean \pm SD.

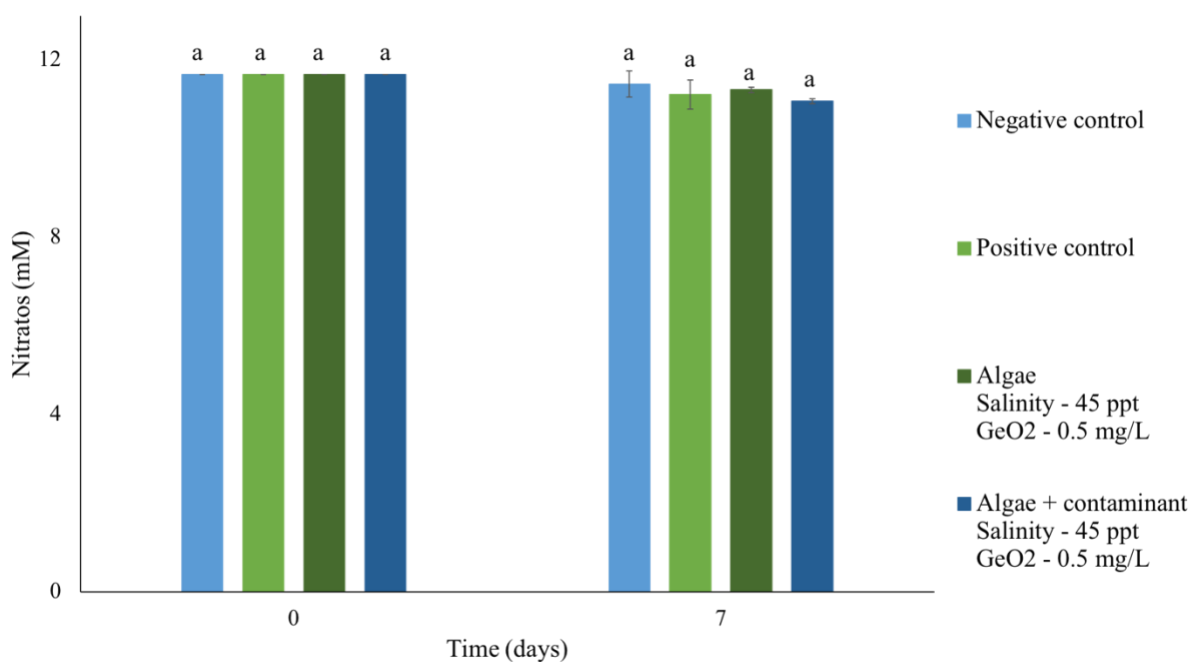


Figure 23: Nitrates measurements of *T. lutea* cultures without (negative control) and with contaminant (positive control). Salinity of 45 ppt and GeO₂ at 0.5 mg/L were applied to the uncontaminated culture of *T. lutea* (algae), and cultures of *T. lutea* with *Paraphysomonas* (algae + contaminant). $n=3$, mean \pm SD. Different letters over the bars indicate significant differences between samples ($p<0.05$, ANOVA Tukey).

These results showed that a salinity of 45 ppt and GeO₂ at 0.5 mg/L has no significant effect on the normal growth of *T. lutea* cultures. However, this mitigation was not successful in controlling the proliferation of *Paraphysomonas*, which collapsed the microalgal culture two days after the contaminated *T. lutea* culture without any treatment (**positive control**). Nevertheless, the 6-well plate experiment with the treatment salinity of 45 ppt and GeO₂ at 0.5 mg/L described before was successful in preventing any significant surge of *Paraphysomonas*. This could be explained by the short duration of the trial, which were only 3 days, when compared to that of the 100-mL Erlenmeyer trials, which took seven days.

To ensure we did not miss the appearance of the contaminant due to the short duration of the last trial, one last experiment was performed with *T. lutea* cultures treated with GeO₂ at 1 mg/L for 14 days. The culture of *T. lutea* without contaminant (**negative control**) presented an exponential growth during the entire experiment, starting with a lower concentration of microalgae cells (**Figure 24**) and biomass (**Figure 25**), namely 4.0×10^6 cells/mL and 0.3 g/L respectively, and lower level of nitrates (7.2 mM), when compared to the previous experiments, on day 0 (**Figure 26**). Microalgal cell counts and biomass increased significantly every 3 days, reaching a maximum of 2.1×10^7 cells/mL and 1.9 g/L on day 14, respectively, with a dark

brown colour (**Figure 14A**). Nitrates were consumed significantly from day 0 to day 7 (>1 mM/day). However, from this latter day onwards only 0.9 mM were consumed. The culture of *T. lutea* with contaminant (**positive control**) had no significant growth changes as compared to the negative control until day 4, reaching microalgae cell and biomass concentrations of 7×10^6 cells/mL and 0.6 g/L, respectively. Nevertheless, contaminants cells were already present on day 3 (5.3×10^4 cell/mL) and increased significantly to 6.1×10^6 cells/mL on day 4. *T. lutea* culture collapsed completely on day 7 with no microalgal cells left (**Figure 14C**) while contaminants cells further increased to a concentration of 8.8×10^5 cells/mL. Until day 11, the number of contaminants decreased significantly to 1.4×10^5 cells/mL and were no longer present in the culture until day 14. The nitrate consumption was not significant throughout the experiment (<1 mM).

The culture of *T. lutea* without contaminant treated with a salinity of 45 ppt and GeO_2 at a concentration of 0.5 mg/L (**algae**) had no significant differences to the negative control throughout the experiment. On day 14, this culture also had a similar number of cells, biomass and nitrates consumption when compared to those of the negative control, as well as a dark brown colour (**Figure 14A**). The culture of *T. lutea* with contaminant treated with a salinity of 45 ppt and GeO_2 at a concentration of 0.5 mg/L (**algae + contaminant**) had no significant differences to the negative control until day 10, reaching microalgal cell and biomass concentrations of 1.4×10^7 cells/mL and 1.4 g/L, respectively. Nevertheless, contaminants cells were present in the culture on day 8, reaching a concentration of 3.3×10^4 cells/mL. Between day 10 and day 11, a significant decrease occurred in the number of cells and biomass of *T. lutea*, to 4.7×10^6 cells/mL and 0.9 g/L respectively, with a significant increase of the number of contaminants to 9.1×10^5 cells/mL in the culture. The culture collapsed on day 14 with no microalgae left and a cell concentration of 2.9×10^5 cells/mL of contaminants (**Figure 14C**). The nitrates were significantly consumed during the experiment (2 mM).

These results showed that for 14 days, GeO_2 at 1 mg/L has no significant effect on the growth of *T. lutea* cultures. Furthermore, this mitigation was successful to control the development of *Paraphysomonas* for 7 more days, when compared to a contaminated *T. lutea* culture without any treatment.

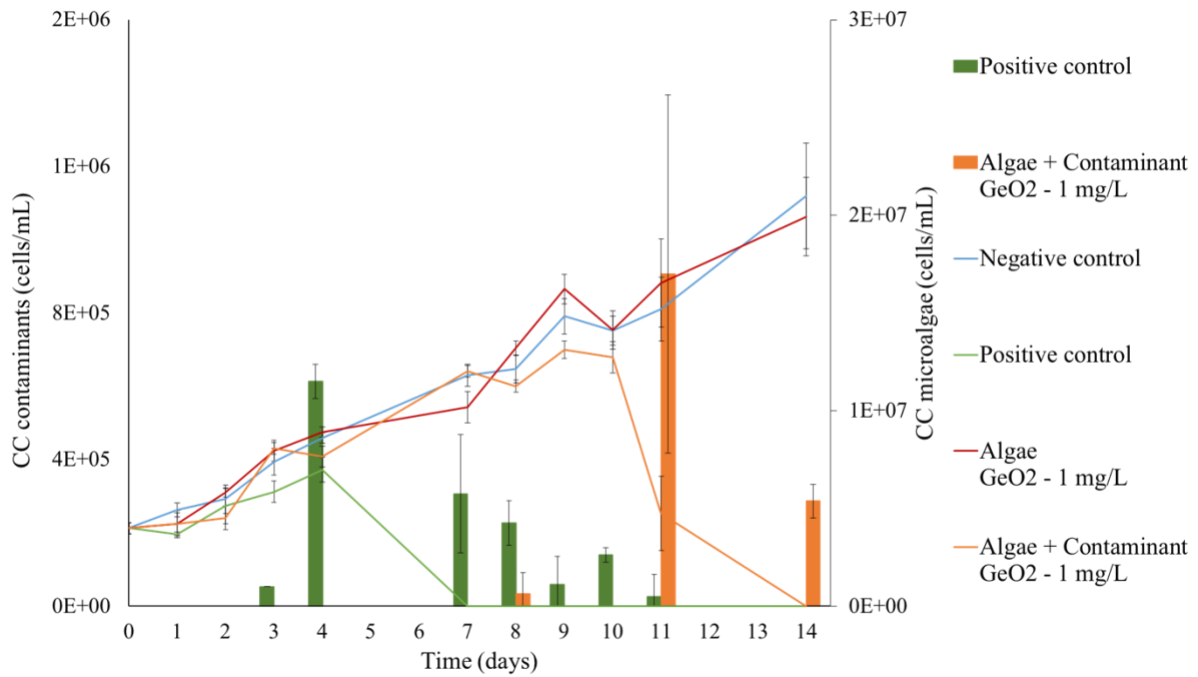


Figure 24: Growth of *T. lutea* (lines) cultures and *Paraphysomonas* contaminant (bars) using cell counts over 14 days of cultivation. GeO₂ at 1 mg/L was applied to the uncontaminated culture of *T. lutea* (Algae), and cultures with *T. lutea* with *Paraphysomonas* (Algae + contaminant). $n=3$, mean \pm SD.

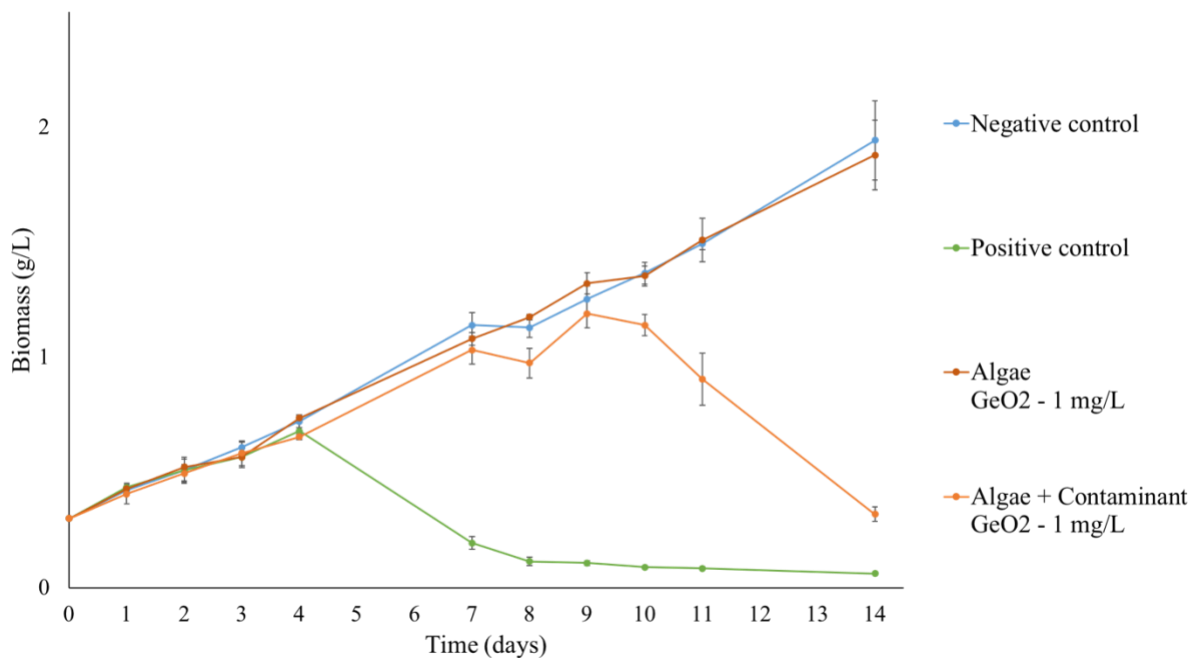


Figure 25: Growth curve of *T. lutea* cultures without (negative control) and with contaminant (positive control). GeO₂ at 1 mg/L was applied to the uncontaminated culture of *T. lutea* (Algae), and cultures with *T. lutea* with *Paraphysomonas* (Algae + contaminant). $n=3$, mean \pm SD.

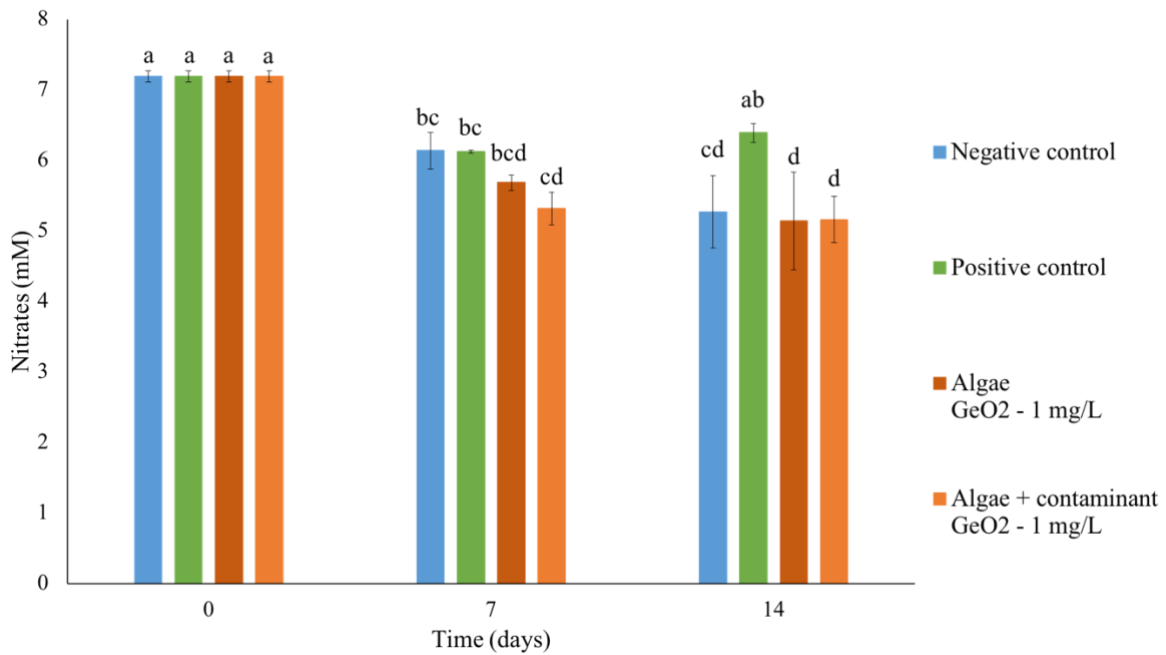


Figure 26: Nitrates measurements of *T. lutea* cultures without (Negative control) and with contaminant (Positive control). GeO₂ at 1 mg/L was applied on culture of *T. lutea* only (Algae), and cultures with *T. lutea* contaminated with *Paraphysomonas* (Algae + contaminant). $n=3$, mean \pm SD. Different letters over the bars indicate significant differences between samples ($p < 0.05$, ANOVA Tukey).

To sum up, the successful treatments were either a salinity of 60 ppt or 1 mg/L of GeO₂. Both mitigations strategies showed similar results and had the ability to control the proliferation of *Paraphysomonas* for one additional week, when compared to the positive control, without harming *T. lutea*. Nevertheless, the chemical mitigation is apparently the best candidate for a mitigation strategy. Once the environmental pressure is applied to the microalgal cultures, it will not be possible to increase salinity once the contaminants reappear, because it will harm the microalgal culture. Therefore, the proposed environmental strategy can only control the growth of the contaminant only once and for one week. However, it might be possible to add more GeO₂ once *Paraphysomonas* appears in the culture. For that reason, the chemical mitigation seems to be most suitable option to control the development and proliferation of this chytrid predator in *T. lutea* cultures.

3.2. Biological contaminants of *Phaeodactylum tricornutum*

3.2.1. NGS analysis

Extracted high quality DNA of different samples from contaminated cultures of *P. tricornutum* taken during the industrial production was sent to be sequenced using NGS technology (Illumina MiSeq short read technology). One sample of distilled water was sent as negative control (**Table 8**).

Table 8: Samples sequenced by NGS.

Company (species)	Sample Name	Observations
Allmicroalgae (<i>P. tricornutum</i>)	Inoculum	Inoculum, non-contaminated
	S3 12/3/21	Small photobioreactor 3, highly contaminated
	S4 12/3/21	Small photobioreactor 3, highly contaminated
	S4 14/3/21	Small photobioreactor 4, highly contaminated
	M5 17/3/21	Medium photobioreactor 5, highly contaminated
Negative control	NC	Negative control

In total, 223 zOTUs were obtained from the NGS results. A minimum level of each zOTU was taken into account (>100 reads) therefore, only 97 zOTU were analysed, in concentrations from 0 to 34,992 reads. After comparing the sequences to the known sequences of NCBI using BLAST, *P. tricornutum* samples revealed possible contaminants of seven different taxa related to the Bacteria, Cercozoa (a biodiverse group of microflagellates and amoeba-like microorganisms), Chlorophyta (green algae), Chrysophyceae (“golden” microflagellates with sometimes amoeba-like life stages), Ciliophora (ciliates), Excavata (includes the group discobids, photosynthetic parasites and free-living heterotrophic microorganisms) and Euglenozoa (includes microorganisms related to *Euglena* and *Leishmania*) [74] (**Figure 27**).

The inoculum of *P. tricornutum* was free of contamination, while all reactor samples represented different taxa of contaminants. Some bacterial 16S rDNA fragments were amplified, showing bacteria in all reactor samples. Reactor S3 12/3/21 showed the highest bacterial load (23,119 reads), and the lowest eukaryotic contamination (1,080 reads), when

compared to the other reactors (**Figure 27A**). Reactor S4 had one predominant eukaryotic contaminant belonging to the megagroup Excavata (20%), which increased four-fold after two days (84%). Reactor M5 17/3/21 had the most diverse contamination, belonging to Cercozoa (33%), ciliates (5%) and Excavata (24%) (**Figure 27B**). Therefore, for the most abundant zOTUs, Excavata (zOTU2) and Cercozoa (zOTU8), literature research was made as well as phylogenetic characterisation to identify the most likely candidate for collapsing the culture of this diatom.

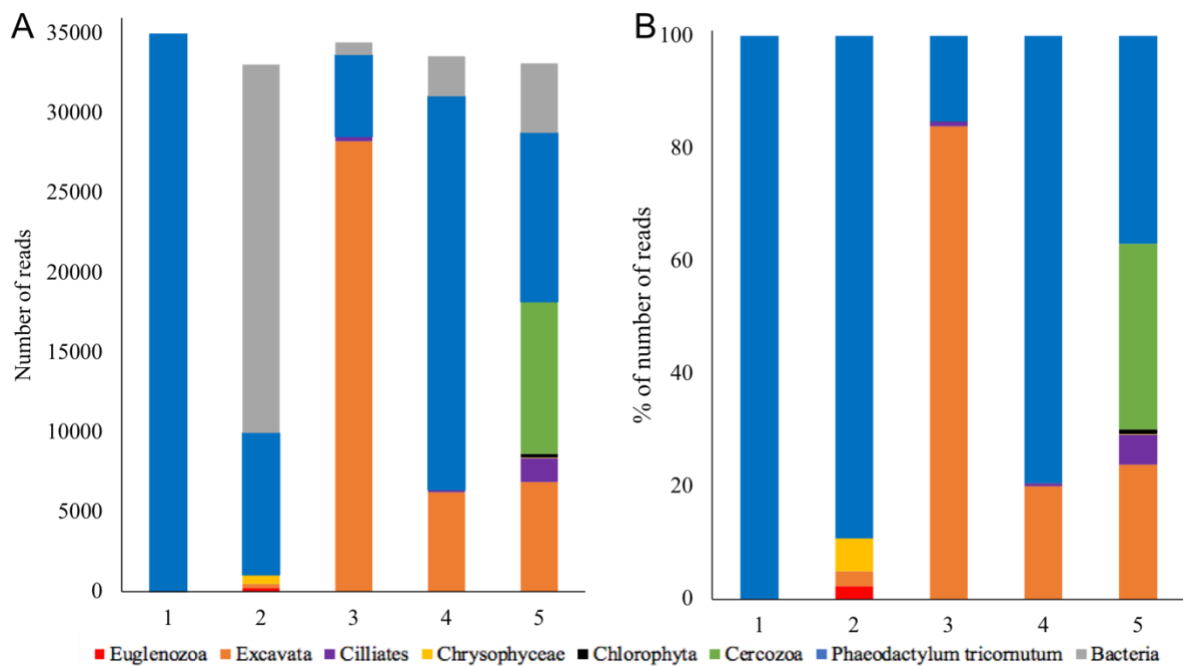


Figure 27: Abundance of relevant taxa obtained by NGS in inoculum and contaminated samples of *P. tricornutum*, namely: 1) Inoculum, 2) S3 12/3/21, 3) S4 14/3/21, 4) S4 12/3/21 and 5) M5 17/3/21; with (A) and without (B) bacteria being shown as percentage of abundance.

The BLAST results of zOTU2 showed an (E)-value of 3×10^{-45} and 96% of identity to the amoeba *Heterolobosea* sp. (Excavata). Phylogenetic analysis was performed on the Excavata contaminant (zOTU2) to compare with known sequences of the phylum *Heterolobosea* using sequences of the clade *Discoba* as outgroup. The zOTU2 contaminant did not share any node with the sequences used, however, it was closely related to sequences from *Euplaesiobystra hypersalinica* and *Heteramoeba clara*, suggesting that this contaminant belongs to the same phylum (**Figure 28**). Moreover, it was not possible to identify this predator down to the species level, as it seems to be a novel species that has not been described as yet. Therefore, the Excavata contaminant has only been identified as belonging to the phylum

Heterolobosea, a sister clade of the Euglenozoa, which contains microorganisms such as *Euglena* and *Leishmania*. Literature research revealed that this contaminant is the most likely candidate responsible for culture collapse, since it has been found to graze on microalgae, such as the cyanobacterium *Spirulina* sp. [6]. Furthermore, heterolobosean cells can be amoeboid or amoebiflagellated. Some are able to switch between a flagellated and amoeboid phase during their life cycle and form resistant cysts when stressed [88].

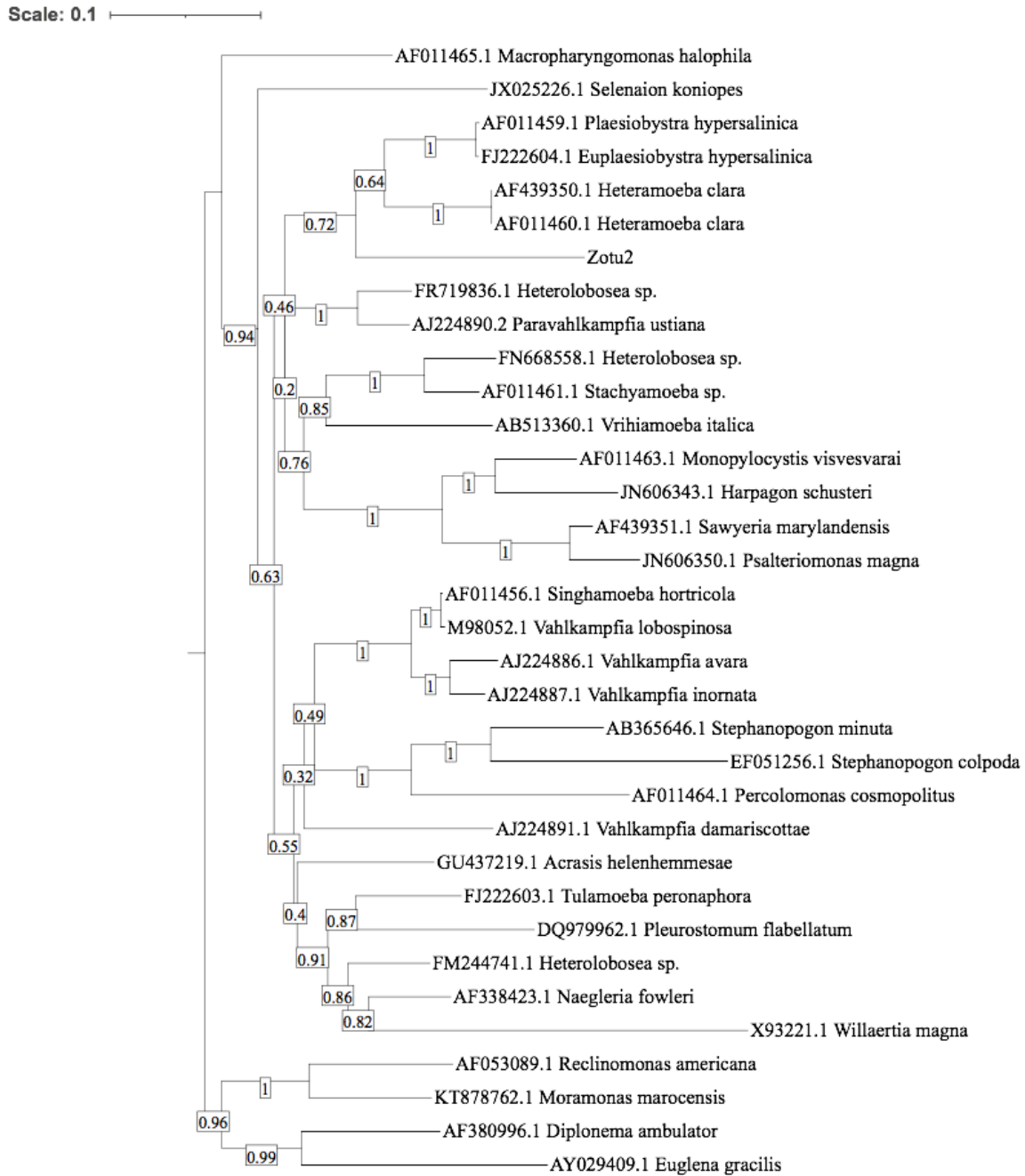


Figure 28: Distance-based (BioNJ) phylogenetic tree of the Excavata contaminant (zOTU2) of cultures of *P. tricorutum*. Several 18S rDNA sequences belonging to the clade Discoba have been added to find the tree root by means of an outgroup.

For zOTU8, the BLAST results showed an (E)-value of 2×10^{-35} and 99% of identity to the zooflagellate *Helkesimastix* sp. (Cercozoa). To confirm this result, a phylogenetic analysis was performed on the zOTU8 contaminant with known sequences of the superfamily Sainouroidea using sequences of different families belonging to the phylum Cercozoa as outgroup. The zOTU8 contaminant shared a node with the sequence *Helkesimastix marina* with a branch support of 0.99, suggesting that the cercozoan contaminant belongs to the genus *Helkesimastix* (**Figure 29**). This microorganism is known to be a non-amoeboid, semi-rigid, unciliated, gliding marine zooflagellate that has been shown to be a cannibal or bacterivore; however, it has never been described as a grazer of microalgae [89]. Therefore, no further research was made, since the contaminant that was collapsing *P. tricorutum* cultures showed to be amoeba-like.

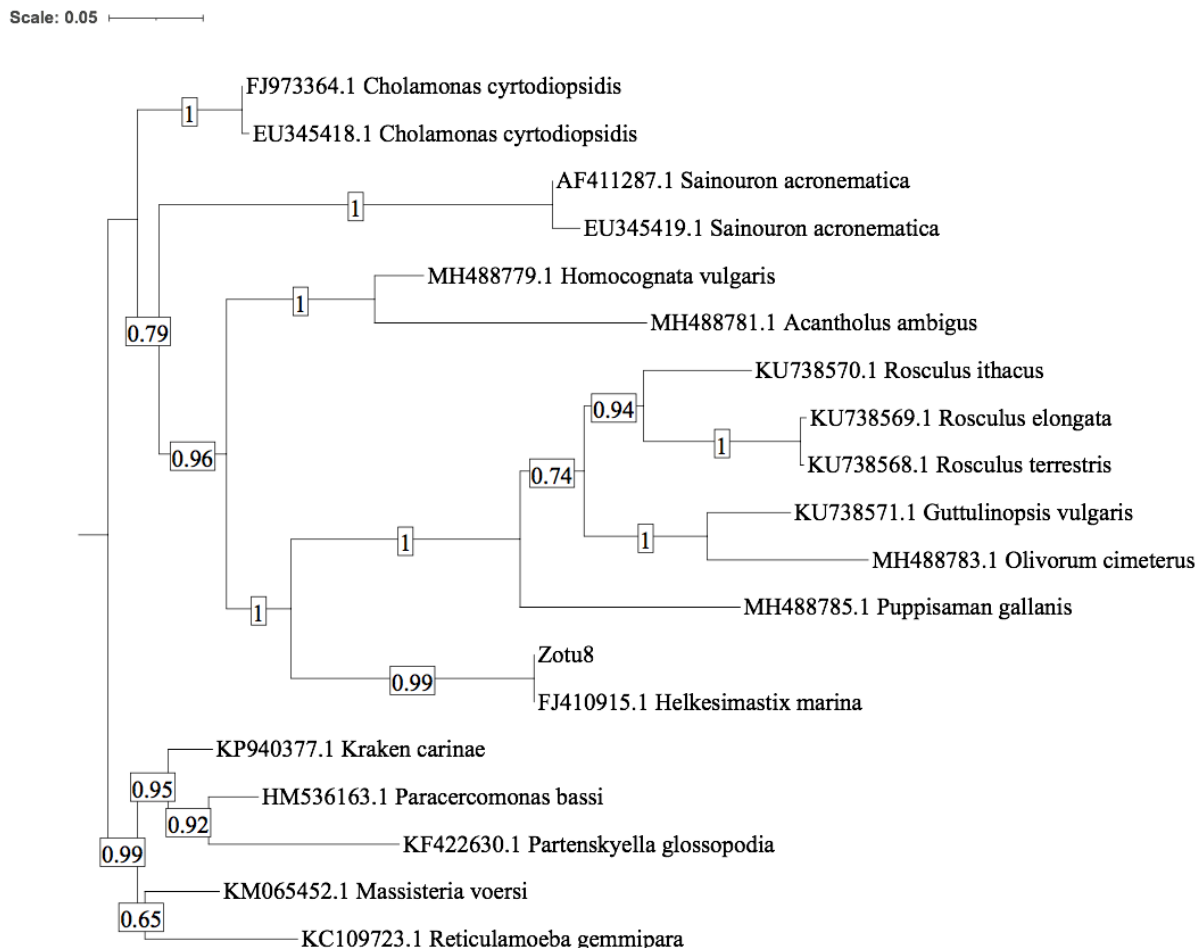


Figure 29: Maximum likelihood phylogenetic tree of the Cercozoa contaminant (zOTU8) of cultures of *P. tricorutum*. Several 18S rDNA sequences belonging to the superfamily Sainouroidea have been added to find the tree root by means of an outgroup.

3.2.2. Primer design and optimization

The heterolobosean contaminant (zOTU2) was identified to be the main cause of *P. tricorutum* culture collapse, as shown by microscopical observation and by the previous NGS and phylogenetic analyses as well as literature research. Only one optimized primer pair targeting heterolobosean DNA sequences was found upon literature research.

Therefore, it was concluded that additional primers needed to be designed in-house to increase the chances of success of finding specific primers for this contaminant. Several heterolobosean 18S rDNA sequences were aligned with those of microalgal species using the Qiagen CLC Genomics Workbench. To test all of the primers, standard PCR conditions were used as well as extracted DNA samples of four different microalgal cultures of *P. tricorutum*, as described before.

Table 9: List of contaminant-specific 18S primers developed.

Name	Sequence 5'-3'	Characteristics			Ref.
		Tm (°C)	GC content (%)	Amplicon length (bp)	
ACA5'	CTGGTTGATCCTG CCAGTATT	57.9	47.6	1300	[90]
Heterolobosea _ 3R	TACGCTGTATCGT CCCGTTG	59.4	55		In-house
Heterolo_spec _ 392F	CGCGTAAATTACC CAATCATAACA	57.6	38	200	In-house
Heterolo_spec _ 596R	CGTTTTAACTGCA GCAATATAGG	57.1	39		
Heterolo_spec _ 1186F	AATAGCCTTTTCT TGATTCTCTAATA	55.3	27	470	In-house
Heterolo_spec _ 1620R	GGACGTAGTCAAT GCGAGA	56.7	53		

The first primer pair (ACA5'/Heterolobosea_3R) was found in literature [90]. Since the preliminary tests of the primer pair, amplification showed a non-specific multiband pattern, the sequence of the reverse primer was optimized in-house. The generated primer pair was expected to amplify a DNA fragment of 1,300 bp. Under standard PCR conditions, the 18S rDNA of the sample S3 12/21 showed an amplification product with a band close to the expected region, whose migration is apparently retarded by the binding of GelRed as discussed before. The same was observed for the other three samples taken from the photobioreactors, showing thicker bands of the amplification product (**Figure 30A**). The primer pair seemed to be specific for the heterolobosean contaminant, since the most contaminated samples S4 and M5 (20-83% of number of reads) yielded bands of amplification products of higher intensity. Conversely, the less contaminated sample S3 (3%) showed thinner bands of the amplification products.

The second primer pair (Heterolo_spec_392F/ Heterolo_spec_596R) had an expected 200-bp amplicon length. With the standard PCR conditions, the 18S rDNA of the samples *T. chui* and S3 12/21 were amplified as well as the three other samples of the reactors (**Figure 30B**). The microalgal sample *T. chui* was previously sent by the company Allmicroalgae, however, there was no information about a eukaryotic contamination or an amoeba-like organism. Therefore, with this amplification product, it is possible that the same contaminant as the one found in *P. tricornutum* cultures is also present in *T. chui* cultures. Nevertheless, further research is needed to confirm this hypothesis.

The third primer pair (Heterolo_spec_1186F/ Heterolo_spec_1620R) amplified an expected product of 470 bp. Under standard PCR conditions, results similar to those obtained with the previous primer pair were obtained (**Figure 30C**). It also amplified the 18S rDNA of the sample of *P. tricornutum* with a multiband pattern, however, none of the bands represented the size of the amplification product of the target sequence.

To conclude, three robust primer pairs were design with promising results under standard PCR conditions (**Table 10**), with a limit of detection at a relative abundance of 2.6%. Even so the PCR conditions need to be optimized and the detection limit tested.

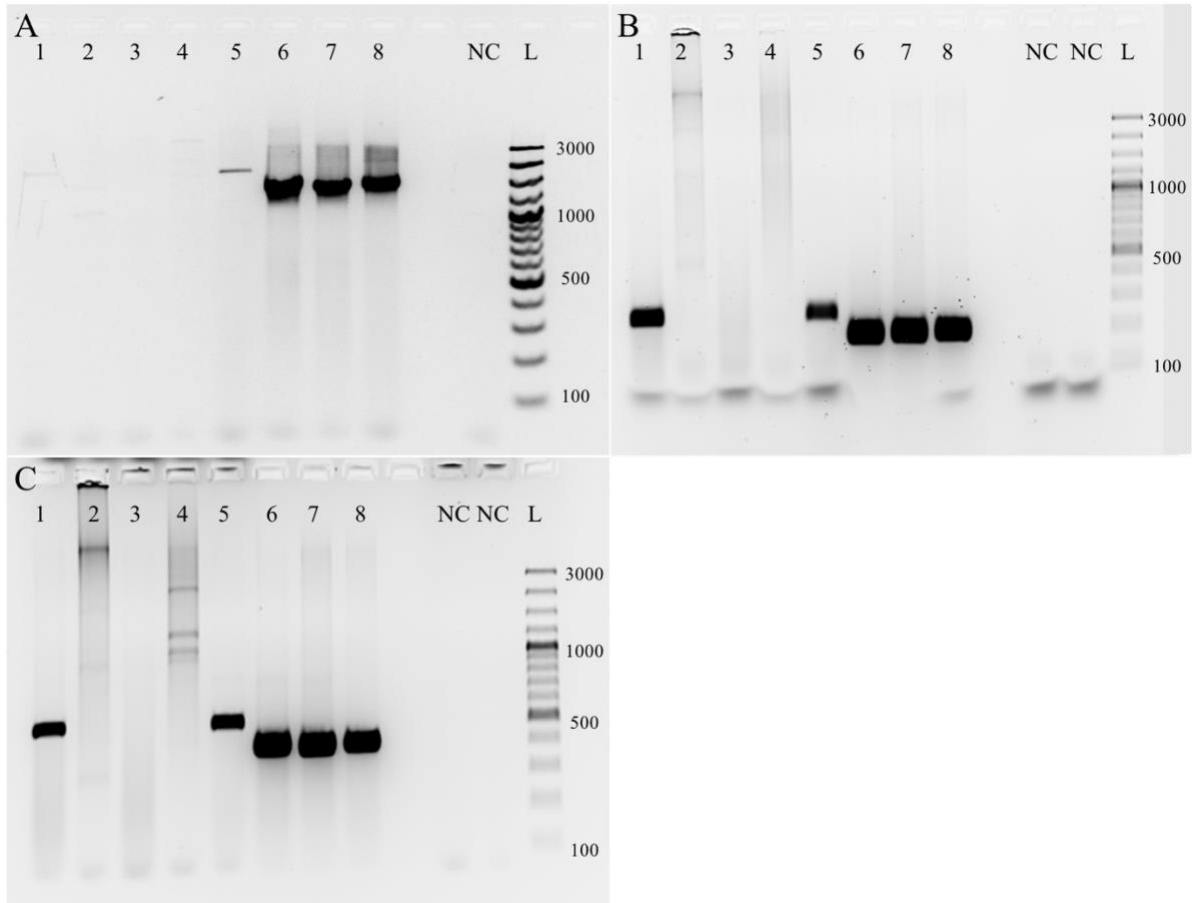


Figure 30: Amplification products of *Heterolobosea* 18S rDNA using the primer pair A) ACA5'/*Heterolobosea*_3R, B) *Heterolo_spec*_392F/*Heterolo_spec*_596R and C) *Heterolo_spec*_1186F/*Heterolo_spec*_1620R from DNA of different microalgal samples, namely 1) *Tetrasselmis chui*, 2) *Chlorella vulgaris*, 3) *T. lutea* and 4) *P. tricorutum*, as well as of *P. tricorutum* samples contaminated with *Heterolobosea*: 5) S3 12/3/21, 6) S4 14/3/21, 7) S4 12/3/21, 8) M5 17/3/21. A negative control (NC) and 100 bp ladder (L) were also loaded on the gel.

Table 10: PCR conditions of the pair primers.

Steps	T (°C)	Time (min)	Cycles
ACA5' / <i>Heterolobosea</i>_3R			
Denaturation	94	5	-
Denaturation	94	0.5	30
Annealing	55	0.5	
Extension	72	1.5	

Extension	72	10	-
Heterolo_spec_ 392F / Heterolo_spec_ 596R			
Denaturation	94	5	-
Denaturation	94	0.5	30
Annealing	55	0.5	
Extension	72	1	
Extension	72	10	-
Heterolo_spec_ 1186F / Heterolo_spec_ 1620R			
Denaturation	94	5	-
Denaturation	94	0.5	30
Annealing	53	0.5	
Extension	72	1	
Extension	72	10	-

3.2.3. Life cycle of the heterolobosean contaminant

The contaminated culture of *P. tricornutum* was observed by optical microscopy in order to understand the life cycle of its predator. The first stage seen after inoculating the heterolobosean contaminants in fresh media had a round-shaped morphology with an apparent size of about 5-10 μm (**Figure 31A**). At a later stage, larger amoeboid cells of about 20-30 μm feeding on microalgae started to appear. The cells became even larger (30-50 μm) and continued to feed on microalgae (**Figure 31B-E**). Once the culture collapsed and there were no *P. tricornutum* cells left, the predator kept increasing in size to more than 50 μm without feeding on microalgae (**Figure 31F**). When the microalgal culture was completely collapsed, showing only cell debris, some round-shaped cyst-like forms could still be seen, being most probably the resting stage of this diatom predator. Several types of organisms, such as ciliates and some amoebas made difficult the observation of the contaminant. Additionally, *P. tricornutum* is a winter strain, resulting in the fact that samples with the heterolobosean contaminant preying on

this diatom can only be obtained during the winter. Samples of cultures containing the predators of *P. tricorutum* were received before summer with a type of behaviour that changed during the summer. Indeed, the optimal temperature of heterolobosean amoebas, such as *Vahlkampfia signyensis*, is only 10 °C, being unable to grow at 30°C degrees [91]. Because of the temperature range of the laboratory, it was only possible to further study the life cycle of this predator after the summer, once the temperature decreased.

Heterolobosea is a phylum composed of free-living amoeboid and amoeboflagellated microorganisms that belong to the supergroup Excavata, found in diverse environments, as well as extreme hypersaline environments. An important aspect of these microorganisms is their life stages: some are known as microflagellates only, amoeba only, or amoeboflagellates that can switch from an amoeboid stage to a flagellated stage, and vice-versa [90]. They are mainly known to feed on bacteria by phagocytosis with a characteristic eruptive cytoplasmic flow that allow them to move and feed. However, they have been found to prey on microalgae as well. Furthermore, many species of the phylum Heterolobosea are able to differentiate into cysts in harsh conditions [90].

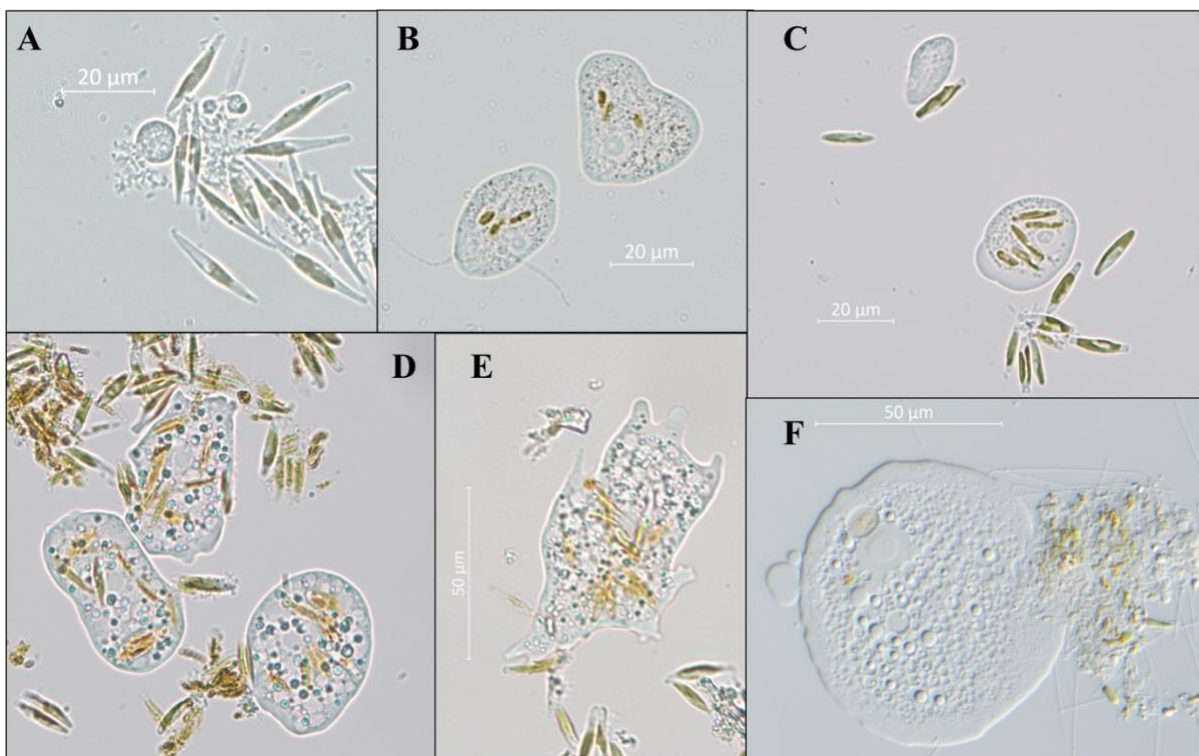


Figure 31: Life stages of the non-flagellated heterolobosean amoeba feeding on *P. tricorutum*: cysts (A); large amoeboid cells feeding on microalgae (B, C, D and E); and even larger amoeboid cells no longer feeding on microalgae, in this case due to cell lysis, with the remnants of the intracellular contents on the right side of the micrograph containing partially digested diatom cells (F).

The amoeba present in this group usually contain round nucleus clearly visible in the body, as well as large food vacuoles where the preys are kept. However, they are often morphologically indistinguishable, and their morphology cannot be used in taxonomical assignment, in contrast to flagellates which are far more variable in their external morphology [88]. Therefore, it was not possible to identify the genus of this contaminant by microscopy. However, the contaminant of *P. tricornutum* did not show any flagellate stage. “Pure” amoebas are known to form cysts in old and young cultures, associated with prokaryotic aggregates. Cells contain food vacuoles, large rounded inclusions, which are possibly oil droplets and pink particles in vacuoles, but only in older cells [92]. Hence, the contaminant collapsing *P. tricornutum* cultures is most likely a “pure” amoeba belonging to the phylum Heterolobosea.

3.2.4. Growth and mitigation trials

Once the life cycle of *P. tricornutum* contaminant was analysed, literature research was carried out in order to find published mitigation strategies. Preliminary environmental pressure trials were tested in order to control or eliminate the contaminant. Trials were made with higher and lower pH (10 and 6, respectively), in order to see if basic or acid solutions inhibits the growth of the contaminant. With a pH of 10, the *P. tricornutum* culture contaminated with Heterolobosea showed normal growth when compared to the non-contaminated culture. Therefore, one experiment was performed. The collapse of *P. tricornutum* culture was visible by visual observation, the brown cultures becoming transparent with the presence of the predator. Interestingly, agglomerates began to appear in the culture, most likely cell debris due to predation of the heterolobosean contaminant.

As described **above**, correlation between OD and CC of *P. tricornutum* was performed in order to measure the cell concentration of the microalgal culture. This trial was made in 100-Erlenmeyer flasks, using culture with and without contaminants to understand how the mitigation can affect the microalgal culture for 4 days (

Figure 32). *P. tricornutum* culture without contaminant (**negative control**) started with a microalgal cell concentration of 6.8×10^5 cells/mL and showed a significant growth from day 0 to day 2, reaching a cell concentration of 1.3×10^6 cells/mL. However, the microalgal cell counts suffered a significant decrease from day 2 to day 4, reaching 8.0×10^5 cells/mL. This might be due to stress, namely high cell concentration from the start of the experiment. *P. tricornutum* culture with contaminant (**positive control**) growth until day 2 was not significant, reaching only a microalgal cell concentration of 7.2×10^5 cells/mL, having a few agglomerates

visible in the culture. On the last day, the number of *P. tricornutum* cells decreased significantly to 5.3×10^5 cells/mL, with the appearance of contaminants in the culture, seen through microscopic observation.

P. tricornutum culture without contaminant treated with pH 10 (**algae**) had a similar growth to that of the negative control without significant differences. The culture was dark brown, and the microalgal cells looked healthy. *P. tricornutum* culture with contaminant treated with pH 10 (**algae + contaminant**) had no significant differences to the positive control until day 2, reaching a microalgal cell concentration of 7.5×10^5 cells/mL, and contaminants were visible by optical microscopy. Until day 4, the number of cells showed a significant microalgal decrease to 5.3×10^5 cells/mL, the colour of the culture turned transparent, resulting into the collapse of *P. tricornutum* culture.

The mitigation strategy tested was pH, since it was shown in previous studies that a pH 11 was successful in controlling the development of contaminants without harming microalgal cultures [41], and *P. tricornutum* is known to show a healthy growth in high ranges of pH [92]. Nevertheless, pH 10 was not successful in controlling the development of the heterolobosean predator. Further mitigation strategies need to be tested, such as the chemical trials performed for *T. lutea* contaminant.

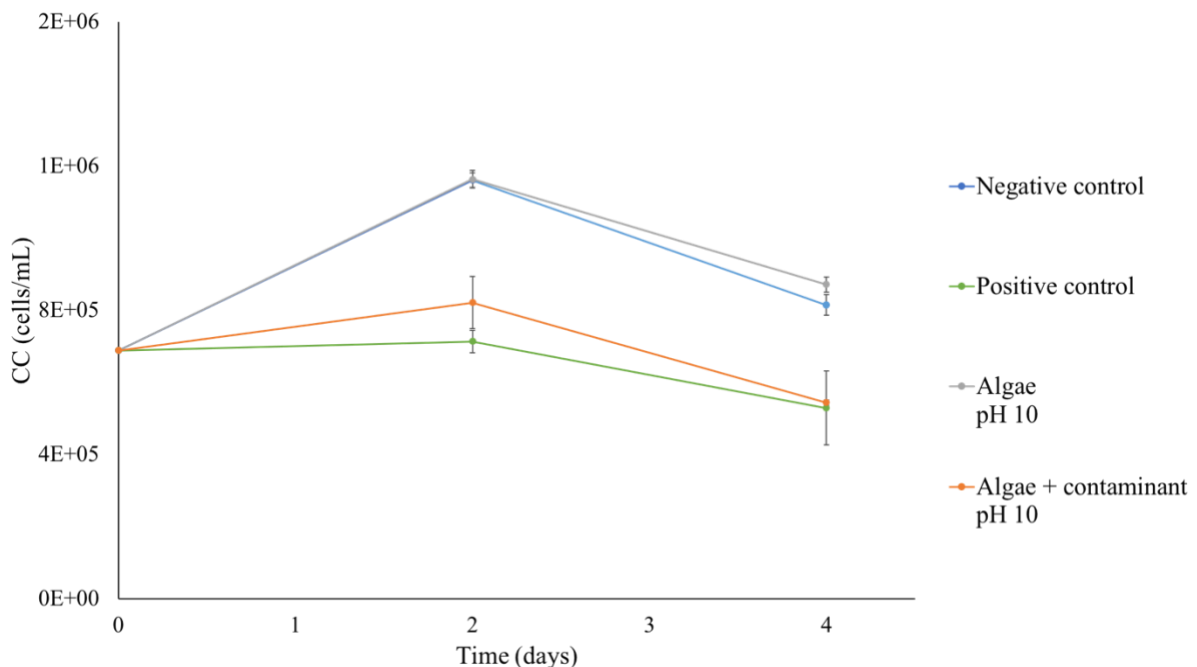


Figure 32: Growth curve of *P. tricornutum* cultures without (negative control) and with (Positive control) contaminant. Alkaline conditions, pH 10, were applied to the uncontaminated culture of *P. tricornutum* (Algae), and cultures with *P. tricornutum* with heterolobosean predator (Algae + contaminant). $n=3$, mean \pm SD.

4. Conclusion and future expectations

Two microalgal producing companies, namely Necton and Allmicroalgae, suffered high production costs due to the loss of biomass from culture collapse. Highly contaminated samples were taken and analysed using molecular methodologies in order to find out the eukaryotic contaminants responsible for the collapse of the microalgal cultures. The NGS results of *Tisochrysis lutea* contaminated samples obtained at the company Necton have led to the conclusion that this haptophyte was contaminated with a chrysophyte of the genus *Paraphysomonas*. One highly sensitive and specific primer pair was designed, and the PCR conditions were optimized to detect the 18S rDNA of this contaminant. Furthermore, two mitigation strategies were developed, namely salinity of 60 ppt and 1 mg/L of germanium dioxide in order to control the contaminant development up to one more week. Regarding *Phaeodactylum tricornutum*, the contaminated samples obtained at Allmicroalgae revealed that this diatom was contaminated with an Excavata microorganism belonging to the phylum Heterolobosea, most probably a novel species that is yet to be described. Three specific primers pairs were designed to detect the 18S rDNA of this contaminant. However, a sensitivity test is still required to test the limit of the detection of these primers. Furthermore, mitigation strategies need to be developed to control or eliminate this predator from *P. tricornutum* cultures.

For both microalgae, more samples need to be collected and analysed during the scale-up process, from the inoculum to the harvest process, in order to find out the scale-up step where the contaminants first appear. The mitigation strategies developed for the contaminant *Paraphysomonas*, of *T. lutea* cultures, still need to be implemented at large scale. Furthermore, the water and biomass of *T. lutea* cultures treated with GeO₂ need to be analysed, especially the concentrations of this compound still present in the microalgal samples and the changes on the biochemical composition of the microalgae, which is crucial for the company to provide consistent biomass. In addition, in the scope of the ALGAESOLUTIONS project, a kit is currently being developed for the detection of the chrysophyte *Paraphysomonas* in different microalgal cultures.

References

1. Tang DYY., Khoo KS., Chew KW., Tao Y., Ho SH., Show PL. Potential utilization of bioproducts from microalgae for the quality enhancement of natural products. *Bioresource Technology*. Elsevier Ltd; 2020. Available at: DOI:10.1016/j.biortech.2020.122997
2. Levasseur W., Perré P., Pozzobon V. A review of high value-added molecules production by microalgae in light of the classification. *Biotechnology Advances*. Elsevier Inc.; 2020. Available at: DOI:10.1016/j.biotechadv.2020.107545
3. Keeling PJ. The number, speed, and impact of plastid endosymbioses in eukaryotic evolution. *Annual Review of Plant Biology*. 2013. 583–607. Available at: DOI:10.1146/annurev-arplant-050312-120144
4. Chew KW., Chia SR., Show PL., Yap YJ., Ling TC., Chang JS. Effects of water culture medium, cultivation systems and growth modes for microalgae cultivation: A review. *Journal of the Taiwan Institute of Chemical Engineers*. Taiwan Institute of Chemical Engineers; 2018. 332–344. Available at: DOI:10.1016/j.jtice.2018.05.039
5. Javed F., Aslam M., Rashid N., Shamair Z., Khan AL., Yasin M., et al. Microalgae-based biofuels, resource recovery and wastewater treatment: A pathway towards sustainable biorefinery. *Fuel*. Elsevier Ltd; 2019; 255. Available at: DOI:10.1016/j.fuel.2019.115826
6. Day JG., Gong Y., Hu Q. Microzooplanktonic grazers – A potentially devastating threat to the commercial success of microalgal mass culture. *Algal Research*. Elsevier B.V.; 2017; **27**: 356–365. Available at: DOI:10.1016/j.algal.2017.08.024
7. Xue J., Balamurugan S., Li T., Cai JX., Chen TT., Wang X., et al. Biotechnological approaches to enhance biofuel producing potential of microalgae. *Fuel*. Elsevier Ltd; 2021; 302. Available at: DOI:10.1016/j.fuel.2021.121169
8. Spolaore P., Joannis-Cassan C., Duran E., Isambert A. Commercial applications of microalgae. *Journal of Bioscience and Bioengineering*. 2006; **101**: 87–96. Available at: DOI:10.1263/jbb.101.87
9. Torres-Tiji Y., Fields FJ., Mayfield SP. Microalgae as a future food source. *Biotechnology Advances*. Elsevier Inc.; 2020. Available at: DOI:10.1016/j.biotechadv.2020.107536
10. Farooq W., Suh WI., Park MS., Yang JW. Water use and its recycling in microalgae cultivation for biofuel application. *Bioresource Technology*. Elsevier Ltd; 2015. 73–81. Available at: DOI:10.1016/j.biortech.2014.10.140
11. Jankowska E., Sahu AK., Oleskowicz-Popiel P. Biogas from microalgae: Review on microalgae's cultivation, harvesting and pretreatment for anaerobic digestion. *Renewable and Sustainable Energy Reviews*. Elsevier Ltd; 2017. 692–709. Available at: DOI:10.1016/j.rser.2016.11.045
12. Lu W., Asraful Alam M., Liu S., Xu J., Parra Saldivar R. Critical processes and variables in microalgae biomass production coupled with bioremediation of nutrients and CO₂ from livestock farms: A review. *Science of the Total Environment*. Elsevier B.V.; 2020; 716. Available at: DOI:10.1016/j.scitotenv.2019.135247
13. Bacellar Mendes LB., Vermelho AB. Allelopathy as a potential strategy to improve microalgae cultivation. *Biotechnology for Biofuels*. 2013. Available at: DOI:10.1186/1754-6834-6-152
14. Verma R., Kumari KVLK., Srivastava A., Kumar A. Photoautotrophic, mixotrophic, and heterotrophic culture media optimization for enhanced microalgae production. *Journal*

- of *Environmental Chemical Engineering*. Elsevier Ltd; 2020; **8**. Available at: DOI:10.1016/j.jece.2020.104149
15. Molina D., de Carvalho JC., Júnior AIM., Faulds C., Bertrand E., Soccol CR. Biological contamination and its chemical control in microalgal mass cultures. *Applied Microbiology and Biotechnology*. Springer; 2019. 9345–9358. Available at: DOI:10.1007/s00253-019-10193-7
 16. Barceló-Villalobos M., Serrano CG., Zurano AS., García LA., Maldonado SE., Peña J., et al. Variations of culture parameters in a pilot-scale thin-layer reactor and their influence on the performance of *Scenedesmus almeriensis* culture. *Bioresource Technology Reports*. Elsevier Ltd; 2019; **6**: 190–197. Available at: DOI:10.1016/j.biteb.2019.03.007
 17. Hu J., Nagarajan D., Zhang Q., Chang JS., Lee DJ. Heterotrophic cultivation of microalgae for pigment production: A review. *Biotechnology Advances*. Elsevier Inc.; 2018. 54–67. Available at: DOI:10.1016/j.biotechadv.2017.09.009
 18. da Silva TL., Moniz P., Silva C., Reis A. The role of heterotrophic microalgae in waste conversion to biofuels and bioproducts. *Processes*. MDPI AG; 2021. Available at: DOI:10.3390/pr9071090
 19. Barros A., Pereira H., Campos J., Marques A., Varela J., Silva J. Heterotrophy as a tool to overcome the long and costly autotrophic scale-up process for large scale production of microalgae. *Scientific Reports*. Nature Publishing Group; 2019; **9**. Available at: DOI:10.1038/s41598-019-50206-z
 20. Siddiki SYA., Mofijur M., Kumar PS., Ahmed SF., Inayat A., Kusumo F., et al. Microalgae biomass as a sustainable source for biofuel, biochemical and biobased value-added products: An integrated biorefinery concept. *Fuel*. Elsevier Ltd; 2022; 307. Available at: DOI:10.1016/j.fuel.2021.121782
 21. Yuan D., Zhan X., Wang M., Wang X., Feng W., Gong Y., et al. Biodiversity and distribution of microzooplankton in *Spirulina (Arthrospira) platensis* mass cultures throughout China. *Algal Research*. Elsevier B.V.; 2018; **30**: 38–49. Available at: DOI:10.1016/j.algal.2017.12.009
 22. Cheregi O., Engelbrektsson J., Andersson MX., Strömberg N., Ekendahl S., Godhe A., et al. Marine microalgae for outdoor biomass production—A laboratory study simulating seasonal light and temperature for the west coast of Sweden. *Physiologia Plantarum*. John Wiley and Sons Inc; 2021; **173**: 543–554. Available at: DOI:10.1111/ppl.13412
 23. Loera-Quezada MM., Leyva-González MA., Velázquez-Juárez G., Sanchez-Calderón L., do Nascimento M., López-Arredondo D., et al. A novel genetic engineering platform for the effective management of biological contaminants for the production of microalgae. *Plant Biotechnology Journal*. Blackwell Publishing Ltd; 2016; **14**: 2066–2076. Available at: DOI:10.1111/pbi.12564
 24. di Caprio F. Methods to quantify biological contaminants in microalgae cultures. *Algal Research*. Elsevier B.V.; 2020. Available at: DOI:10.1016/j.algal.2020.101943
 25. Wang H., Zhang W., Chen L., Wang J., Liu T. The contamination and control of biological pollutants in mass cultivation of microalgae. *Bioresource Technology*. Elsevier Ltd; 2013. 745–750. Available at: DOI:10.1016/j.biortech.2012.10.158
 26. Lam TP., Lee TM., Chen CY., Chang JS. Strategies to control biological contaminants during microalgal cultivation in open ponds. *Bioresource Technology*. Elsevier Ltd; 2018. 180–187. Available at: DOI:10.1016/j.biortech.2017.12.088
 27. Conde TA., Couto D., Melo T., Costa M., Silva J., Domingues MR., et al. Polar lipidomic profile shows *Chlorococcum amblystomatis* as a promising source of value-added lipids. *Scientific Reports*. Nature Research; 2021; **11**. Available at: DOI:10.1038/s41598-021-83455-y

28. Mularczyk M., Michalak I., Marycz K. Astaxanthin and other nutrients from *Haematococcus pluvialis*—Multifunctional applications. *Marine Drugs*. MDPI AG; 2020. Available at: DOI:10.3390/md18090459
29. Benedetti M., Vecchi V., Barera S., Dall'Osto L. Biomass from microalgae: The potential of domestication towards sustainable biofactories. *Microbial Cell Factories*. BioMed Central Ltd.; 2018; **17**. Available at: DOI:10.1186/s12934-018-1019-3
30. Xin L., Hong-ying H., Yu-ping Z. Growth and lipid accumulation properties of a freshwater microalga *Scenedesmus* sp. under different cultivation temperature. *Bioresource Technology*. 2011; **102**: 3098–3102. Available at: DOI:10.1016/j.biortech.2010.10.055
31. Pourkarimi S., Hallajisani A., Nouralishahi A., Alizadehdakheel A., Golzary A. Factors affecting production of beta-carotene from *Dunaliella salina* microalgae. *Biocatalysis and Agricultural Biotechnology*. Elsevier Ltd; 2020. Available at: DOI:10.1016/j.bcab.2020.101771
32. Mantecón L., Moyano R., Cameán AM., Jos A. Safety assessment of a lyophilized biomass of *Tetraselmis chuii* (TetraSOD) in a 90 day feeding study. *Food and Chemical Toxicology*. Elsevier Ltd; 2019; 133. Available at: DOI:10.1016/j.fct.2019.110810
33. Mayer C., Richard L., Côme M., Ulmann L., Nazih H., Chénais B., et al. The marine microalga, *Tisochrysis lutea*, protects against metabolic disorders associated with metabolic syndrome and obesity. *Nutrients*. MDPI AG; 2021; **13**: 1–18. Available at: DOI:10.3390/nu13020430
34. Neumann U., Derwenskus F., Flister VF., Schmid-Staiger U., Hirth T., Bischoff SC. Fucoxanthin, a carotenoid derived from *Phaeodactylum tricorutum* exerts antiproliferative and antioxidant activities in vitro. *Antioxidants*. MDPI AG; 2019; **8**. Available at: DOI:10.3390/antiox8060183
35. El-Belely EF., Farag MMS., Said HA., Amin AS., Azab E., Gobouri AA., et al. Green synthesis of zinc oxide nanoparticles (ZnO-NPs) Using *Arthrospira platensis* (Class: Cyanophyceae) and evaluation of their biomedical activities. 2021; Available at: DOI:10.3390/nano
36. Tan J sen., Lee SY., Chew KW., Lam MK., Lim JW., Ho SH., et al. A review on microalgae cultivation and harvesting, and their biomass extraction processing using ionic liquids. *Bioengineered*. Taylor and Francis Inc.; 2020; **11**: 116–129. Available at: DOI:10.1080/21655979.2020.1711626
37. Kadir WNA., Lam MK., Uemura Y., Lim JW., Lee KT. Harvesting and pre-treatment of microalgae cultivated in wastewater for biodiesel production: A review. *Energy Conversion and Management*. Elsevier Ltd; 2018. 1416–1429. Available at: DOI:10.1016/j.enconman.2018.06.074
38. Méndez C., Uribe E. Environment and Resources of the South Pacific. *Latin American Journal of Aquatic Research* 553 *Lat. Am. J. Aquat. Res.* 2012.
39. Ma AT., Daniels EF., Gulizia N., Brahamsha B. Isolation of diverse amoebal grazers of freshwater cyanobacteria for the development of model systems to study predator-prey interactions. *Algal Research*. Elsevier B.V.; 2016; **13**: 85–93. Available at: DOI:10.1016/j.algal.2015.11.010
40. Troschl C., Fritz I., Sodnikar K., Drosig B. Contaminations in mass cultivation of cyanobacteria: Highly resilient *Colpoda steinii* leads to rapid crash of *Synechocystis* sp. cultures and is inhibited by partially anoxic conditions. *Algal Research*. Elsevier B.V.; 2017; **28**: 229–234. Available at: DOI:10.1016/j.algal.2017.11.002
41. Touloupakis E., Cicchi B., Benavides AMS., Torzillo G. Effect of high pH on growth of *Synechocystis* sp. PCC 6803 cultures and their contamination by golden algae

- (*Poterioochromonas* sp.). *Applied Microbiology and Biotechnology*. Springer Verlag; 2016; **100**: 1333–1341. Available at: DOI:10.1007/s00253-015-7024-0
42. Zhu Z., Luan G., Tan X., Zhang H., Lu X. Rescuing ethanol photosynthetic production of cyanobacteria in non-sterilized outdoor cultivations with a bicarbonate-based pH-rising strategy. *Biotechnology for Biofuels*. BioMed Central Ltd.; 2017; **10**. Available at: DOI:10.1186/s13068-017-0765-5
 43. Rasconi S., Jobard M., Jouve L., Sime-Ngando T. Use of calcofluor white for detection, identification, and quantification of phytoplanktonic fungal parasites. *Applied and Environmental Microbiology*. 2009; **75**: 2545–2553. Available at: DOI:10.1128/AEM.02211-08
 44. Pradeep V., van Ginkel SW., Park S., Igou T., Yi C., Fu H., et al. Use of copper to selectively inhibit *Brachionus calyciflorus* (predator) growth in *Chlorella kessleri* (prey) mass cultures for algae biodiesel production. *International Journal of Molecular Sciences*. MDPI AG; 2015; **16**: 20674–20684. Available at: DOI:10.3390/ijms160920674
 45. Steichen SA., Brown JK. Real-time quantitative detection of *Vampirovibrio chlorellavorus*, an obligate bacterial pathogen of *Chlorella sorokiniana*. *Journal of Applied Phycology*. Springer Netherlands; 2019; **31**: 1117–1129. Available at: DOI:10.1007/s10811-018-1659-z
 46. van Etten JL., Dunigan DD. Chloroviruses: Not your everyday plant virus. *Trends in Plant Science*. 2012. 1–8. Available at: DOI:10.1016/j.tplants.2011.10.005
 47. Ding Y., Peng X., Wang Z., Wen X., Geng Y., Zhang D., et al. Occurrence and characterization of an epibiotic parasite in cultures of oleaginous microalga *Graesiella* sp. WBG-1. *Journal of Applied Phycology*. Springer Netherlands; 2018; **30**: 819–830. Available at: DOI:10.1007/s10811-017-1302-4
 48. Dawidziuk A., Popiel D., Lubońska M., Grzebyk M., Wisniewski M., Koczyk G. Assessing contamination of microalgal astaxanthin producer *Haematococcus* cultures with high-resolution melting curve analysis. *Journal of Applied Genetics*. Springer Verlag; 2017; **58**: 277–285. Available at: DOI:10.1007/s13353-016-0378-x
 49. Gong Y., Patterson DJ., Li Y., Hu Z., Sommerfeld M., Chen Y., et al. *Vernalophrys algivore* gen. nov., sp. nov. (Rhizaria: Cercozoa: Vampyrellida), a new algal predator isolated from outdoor mass culture of *Scenedesmus dimorphus*. *Applied and Environmental Microbiology*. American Society for Microbiology; 2015; **81**: 3900–3913. Available at: DOI:10.1128/AEM.00160-15
 50. Letcher PM., Lopez S., Schmieder R., Lee PA., Behnke C., Powell MJ., et al. Characterization of *Amoebophilidium protococcarum*, an algal parasite new to the cryptomycota isolated from an outdoor algal pond used for the production of biofuel. *PLoS ONE*. 2013; **8**. Available at: DOI:10.1371/journal.pone.0056232
 51. Ni ZY., Li JY., Xiong ZZ., Cheng LH., Xu XH. Role of granular activated carbon in the microalgal cultivation from bacteria contamination. *Bioresource Technology*. Elsevier Ltd; 2018; **247**: 36–43. Available at: DOI:10.1016/j.biortech.2017.07.079
 52. Lam TP., Lee TM., Chen CY., Chang JS. Strategies to control biological contaminants during microalgal cultivation in open ponds. *Bioresource Technology*. Elsevier Ltd; 2018. 180–187. Available at: DOI:10.1016/j.biortech.2017.12.088
 53. Not F., Probert I., Ribeiro CG., Crenn K., Guillou L., Jeanthon C., et al. Photosymbiosis in marine pelagic environments. *The Marine Microbiome: An Untapped Source of Biodiversity and Biotechnological Potential*. Springer International Publishing; 2016. 305–332. Available at: DOI:10.1007/978-3-319-33000-6_11
 54. Hoffman Y., Aflalo C., Zarka A., Gutman J., James TY., Boussiba S. Isolation and characterization of a novel chytrid species (phylum Blastocladiomycota), parasitic on the

- green alga *Haematococcus*. *Mycological Research*. 2008; **112**: 70–81. Available at: DOI:10.1016/j.mycres.2007.09.002
55. Nagasaki K., Tarutani K., Yamaguchi M. Growth Characteristics of *Heterosigma akashiwo* virus and its possible use as a microbiological agent for red tide control. *Applied and environmental microbiology*. 1999. Available at: <https://journals.asm.org/journal/aem>
 56. Pereira H., Schulze PSC., Schüler LM., Santos T., Barreira L., Varela J. Fluorescence activated cell-sorting principles and applications in microalgal biotechnology. *Algal Research*. Elsevier B.V.; 2018. 113–120. Available at: DOI:10.1016/j.algal.2017.12.013
 57. Wang X., Li H., Zhan X., Ma M., Yuan D., Hu Q., et al. Development and application of quantitative real-time PCR based on the mitochondrial cytochrome oxidase subunit I gene for early detection of the grazer *Poteroochromonas malhamensis* contaminating *Chlorella* culture. *Algal Research*. Elsevier B.V.; 2021; **53**. Available at: DOI:10.1016/j.algal.2020.102133
 58. Holm ER., Stamper DM., Brizzolara RA., Barnes L., Deamer N., Burkholder JAM. Sonication of bacteria, phytoplankton and zooplankton: Application to treatment of ballast water. *Marine Pollution Bulletin*. 2008; **56**: 1201–1208. Available at: DOI:10.1016/j.marpolbul.2008.02.007
 59. Zahedi A., Greay TL., Papparini A., Linge KL., Joll CA., Ryan UM. Identification of eukaryotic microorganisms with 18S rRNA next-generation sequencing in wastewater treatment plants, with a more targeted NGS approach required for *Cryptosporidium* detection. *Water Research*. Elsevier Ltd; 2019; **158**: 301–312. Available at: DOI:10.1016/j.watres.2019.04.041
 60. Wheeler DL., Barrett T., Benson DA., Bryant SH., Canese K., Chetvernin V., et al. Database resources of the National Center for Biotechnology Information. *Nucleic Acids Research*. 2007; **35**. Available at: DOI:10.1093/nar/gkl1031
 61. Johnson M., Zaretskaya I., Raytselis Y., Merezuk Y., McGinnis S., Madden TL. NCBI BLAST: a better web interface. *Nucleic acids research*. 2008; **36**. Available at: DOI:10.1093/nar/gkn201
 62. Dereeper A., Guignon V., Blanc G., Audic S., Buffet S., Chevenet F., et al. Phylogeny.fr: robust phylogenetic analysis for the non-specialist. *Nucleic acids research*. 2008; **36**. Available at: DOI:10.1093/nar/gkn180
 63. Edgar RC. MUSCLE: A multiple sequence alignment method with reduced time and space complexity. *BMC Bioinformatics*. 2004; **5**. Available at: DOI:10.1186/1471-2105-5-113
 64. Guindon S., Lethiec F., Duroux P., Gascuel O. PHYML Online - A web server for fast maximum likelihood-based phylogenetic inference. *Nucleic Acids Research*. 2005; **33**. Available at: DOI:10.1093/nar/gki352
 65. Gascuel O. BIONJ: An improved version of the NJ algorithm based on a simple model of sequence data. Available at: <https://academic.oup.com/mbe/article/14/7/685/1119804>
 66. Ye J., Coulouris G., Zaretskaya I., Cutcutache I., Rozen S., Madden TL. Primer-BLAST: A tool to design target-specific primers for polymerase chain reaction. 2012. Available at: <http://www.biomedcentral.com/1471-2105/13/134>
 67. Biotium HCU. GelRed Nucleic Acid Gel Stain, 10,000X in Water. Product Information. 2009.
 68. Fabregas J., Abalde J., Herrero C., Cabezas B., Veiga M. Growth of the marine microalga *Tetraselmis suecica* in batch cultures with different salinities and nutrient concentrations. *Aquaculture*. 1984.

69. Schulze PSC., Carvalho CFM., Pereira H., Gangadhar KN., Schüler LM., Santos TF., et al. Urban wastewater treatment by *Tetraselmis* sp. CTP4 (Chlorophyta). *Bioresource Technology*. Elsevier Ltd; 2017; **223**: 175–183. Available at: DOI:10.1016/j.biortech.2016.10.027
70. Nicholls KH., Wujek DE. Chrysophycean algae. *Freshwater Algae of North America: Ecology and Classification*. Elsevier Inc.; 2003. 471–509. Available at: DOI:10.1016/B978-012741550-5/50013-1
71. Lewin J. Silicon metabolism in diatoms v. germanium dioxide, a specific inhibitor of diatom growth. *Phycologia*. 1966; **6**.
72. Wen X., Zhang A., Zhu X., Liang L., Huo Y., Wang K., et al. Controlling of two destructive zooplanktonic predators in *Chlorella* mass culture with surfactants. *Biotechnology for Biofuels*. BioMed Central Ltd; 2021; **14**. Available at: DOI:10.1186/s13068-021-01873-6
73. Witono JR., Novianty V., Arry Miryanti YIP., Kumalaputri AJ., Santoso H. H₂O₂ as a fungicide in the growth phase of green *Haematococcus pluvialis*. *IOP Conference Series: Materials Science and Engineering*. Institute of Physics Publishing; 2020. Available at: DOI:10.1088/1757-899X/823/1/012021
74. Keeling PJ., Burki F. Progress towards the tree of eukaryotes. *Current Biology*. Cell Press; 2019. 808–817. Available at: DOI:10.1016/j.cub.2019.07.031
75. Pawlowski J., Christen R., Lecroq B., Bachar D., Shahbazkia HR., Amaral-Zettler L., et al. Eukaryotic richness in the abyss: Insights from pyrotag sequencing. *PLoS ONE*. 2011; **6**. Available at: DOI:10.1371/journal.pone.0018169
76. Kounosu A., Murase K., Yoshida A., Maruyama H., Kikuchi T. Improved 18S and 28S rDNA primer sets for NGS-based parasite detection. *Scientific Reports*. Nature Publishing Group; 2019; **9**. Available at: DOI:10.1038/s41598-019-52422-z
77. Scoble JM., Cavalier-Smith T. Scale evolution in paraphysomonadida (Chrysophyceae): Sequence phylogeny and revised taxonomy of *Paraphysomonas*, new genus clathromonas, and 25 new species. *European Journal of Protistology*. Elsevier GmbH; 2014; **50**: 551–592. Available at: DOI:10.1016/j.ejop.2014.08.001
78. Davidson K., John EH. Grazing on phytoplankton prey by the heterotrophic microflagellate *Paraphysomonas vestita* in non-balanced growth conditions. *Protistology*. 2001.
79. Molina-Grima E., García-Camacho F., Acién-Fernández FG., Sánchez-Mirón A., Plouviez M., Shene C., et al. Pathogens and predators impacting commercial production of microalgae and cyanobacteria. *Biotechnology advances*. NLM (Medline); 2022. 107884. Available at: DOI:10.1016/j.biotechadv.2021.107884
80. Zhao L., Zhang Y., Geng X., Hu X., Zhang X., Xu H., et al. Potential to resist biological contamination in marine microalgae culture: Effect of extracellular substances of *Nannochloropsis oceanica* on population growth of *Euplotes vannus* and other protozoa. *Marine Pollution Bulletin*. Elsevier Ltd; 2021; 172. Available at: DOI:10.1016/j.marpolbul.2021.112868
81. Schnepf E. Light and electron microscopical observations in *Rhynchopus coscinodiscivorus* spec. nov., a colorless, phagotrophic euglenozoon with concealed flagella. *Archiv für Protistenkunde*. 1994; **144**: 63–74. Available at: DOI:10.1016/S0003-9365(11)80225-3
82. Kostygov AY., Karnkowska A., Votýpka J., Tashyreva D., Maciszewski K., Yurchenko V., et al. Euglenozoa: Taxonomy, diversity and ecology, symbioses and viruses. *Open Biology*. Royal Society Publishing; 2021. Available at: DOI:10.1098/rsob.200407

83. Geisen S., Vaultot D., Mahé F., Lara E., de Vargas C. A user guide to environmental protistology: 1 primers, metabarcoding, sequencing, and 2 analyses 3. Available at: DOI:10.1101/850610
84. Goldman JC., Caron'~" DA. Experimental studies on an omnivorous microflagellate: implications for grazing and nutrient regeneration in the marine microbial food chain. 1985.
85. Hernández-Becerril DU., Sampedro N., Garcés E. The chrysophyte genera *Clathromonas* and *Paraphysomonas* from the Catalan coast (NW Mediterranean Sea). *Nova Hedwigia, Beihefte*. Schweizerbart; 2019; **148**: 1–10. Available at: DOI:10.1127/nova-suppl/2019/015
86. Ishika T., Moheimani NR., Bahri PA., Laird DW., Blair S., Parlevliet D. Halo-adapted microalgae for fucoxanthin production: Effect of incremental increase in salinity. *Algal Research*. Elsevier B.V.; 2017; **28**: 66–73. Available at: DOI:10.1016/j.algal.2017.10.002
87. Leet RE. Formation of scales in *Paraphysomonas vestita* and the inhibition of growth by Germanium Dioxide. *J. Protozool.* 1978.
88. Pánek T., Ptáčková E., Čepička I. Survey on diversity of marine/saline anaerobic *Heterolobosea* (Excavata: Discoba) with description of seven new species. *International Journal of Systematic and Evolutionary Microbiology*. Society for General Microbiology; 2014; **64**: 2280–2304. Available at: DOI:10.1099/ijs.0.063487-0
89. Cavalier-Smith T., Lewis R., Chao EE., Oates B., Bass D. *Helkesimastix marina* n. sp. (Cercozoa: Sainouroidea superfam. n.) a gliding zooflagellate of novel ultrastructure and unusual ciliary behaviour. *Protist*. 2009; **160**: 452–479. Available at: DOI:10.1016/j.protis.2009.03.003
90. Aucher W., Delafont V., Ponlaitiac E., Alafaci A., Agogué H., Leboulanger C., et al. Morphology and ecology of two new amoebae, isolated from a thalassohaline Lake, Dziani Dzaha. *Protist*. Elsevier GmbH; 2020; **171**. Available at: DOI:10.1016/j.protis.2020.125770
91. Garstecki T., Brown S., de Jonckheere JF. Description of *Vahlkampfia signyensis* n. sp. (Heterolobosea), based on morphological, ultrastructural and molecular characteristics. *European Journal of Protistology*. Elsevier GmbH; 2005; **41**: 119–127. Available at: DOI:10.1016/j.ejop.2005.01.003
92. Park JS., Simpson AGB., Brown S., Cho BC. Ultrastructure and molecular phylogeny of two heterolobosean amoebae, *Euplaesiobystra hypersalinica* gen. et sp. nov. and *Tulamoeba peronaphora* gen. et sp. nov., isolated from an extremely hypersaline habitat. *Protist*. 2009; **160**: 265–283. Available at: DOI:10.1016/j.protis.2008.10.002

Annex

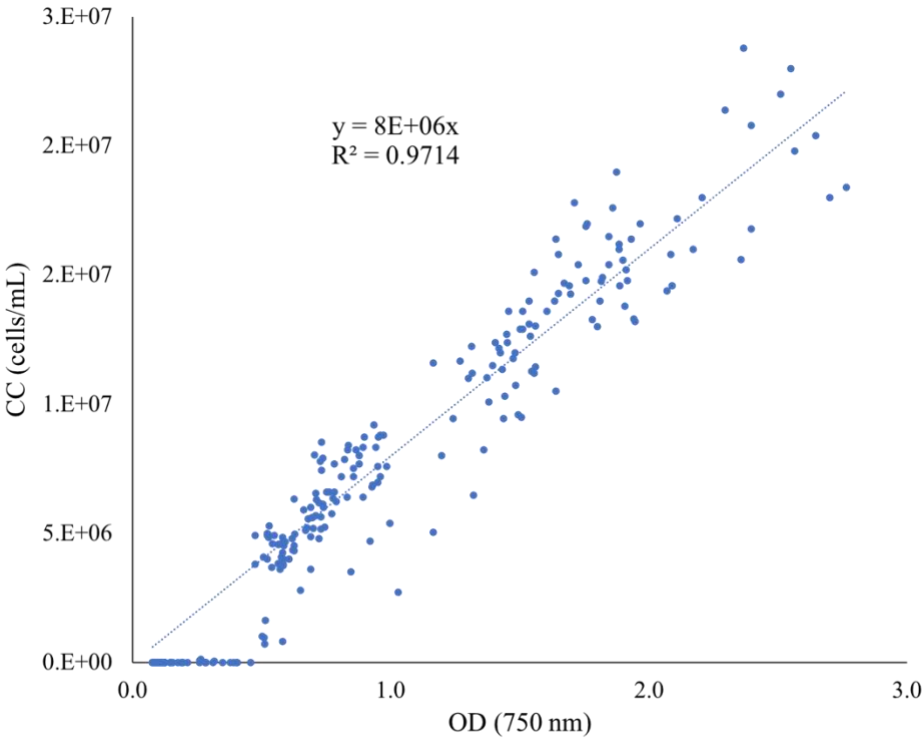


Figure A1: Correlation curve of *T. lutea* cell count. $y = 8E+06x$ and $R^2 = 0.9714$

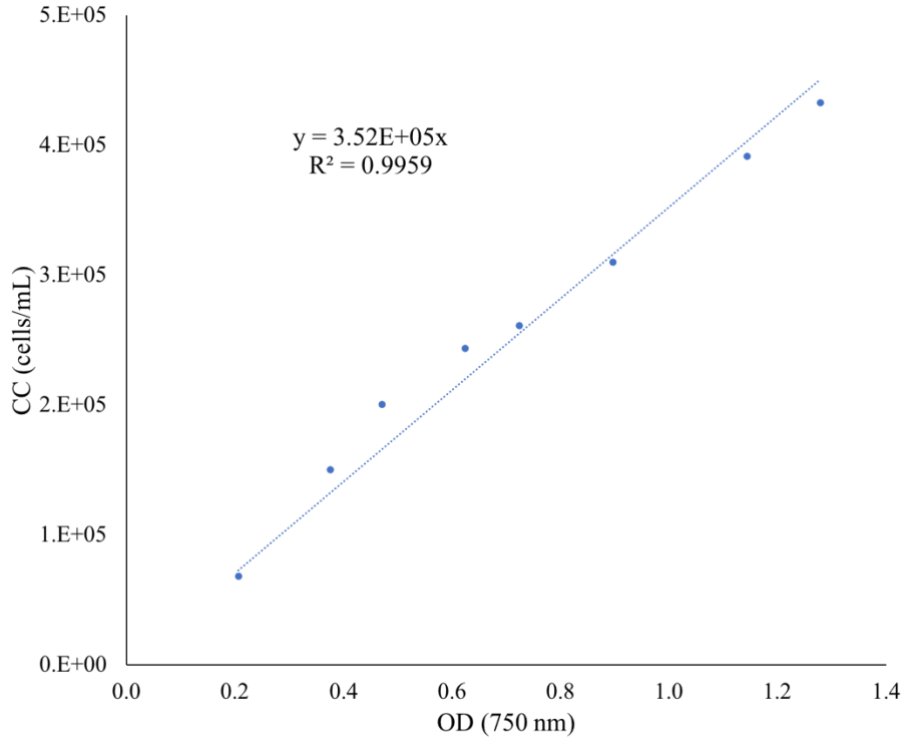


Figure A2: Correlation curve of *P. tricorutum* cell count. $y = 3.52E+05x$ and $R^2 = 0.9959$

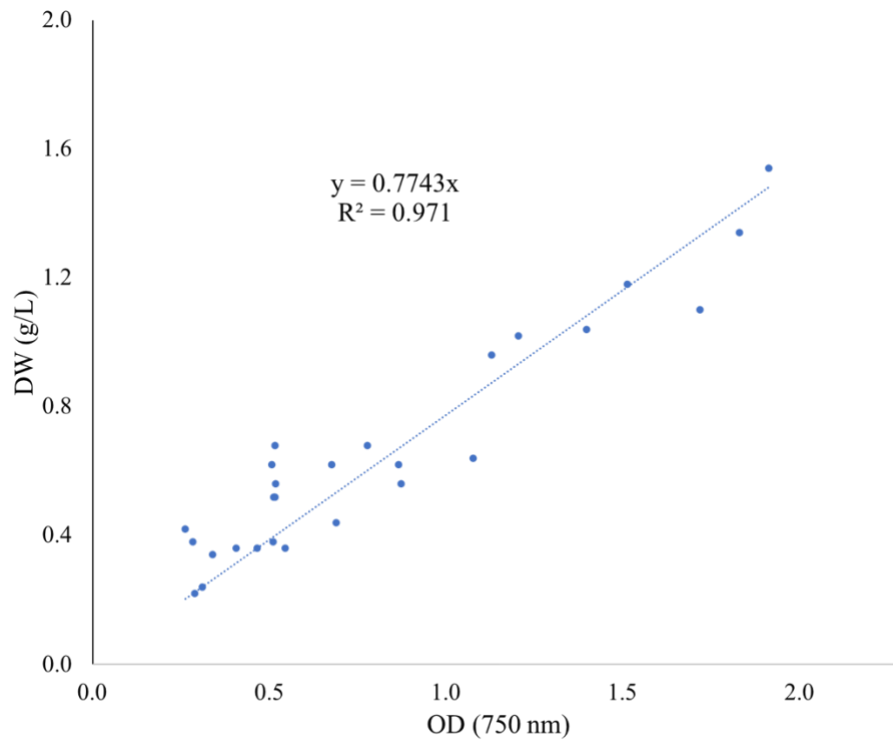


Figure A3: Correlation curve of *T. lutea* dry weight. $y = 0.7743x$ and $R^2 = 0.971$

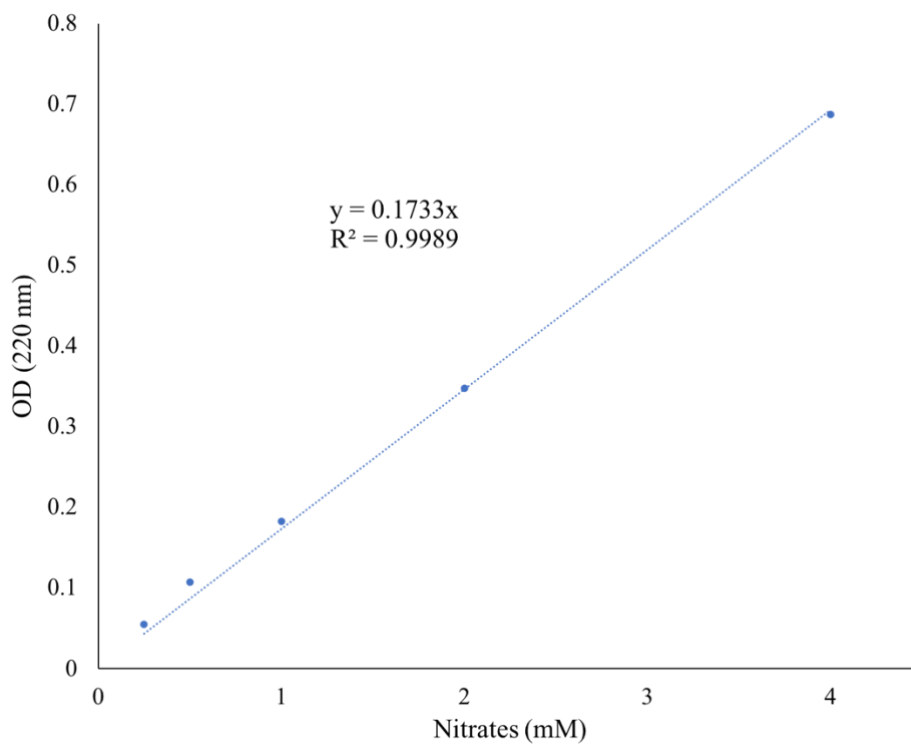


Figure A4: Correlation curve of dissolved nitrates. $y = 0.1733x$ and $R^2 = 0.9989$